PHILOSOPHICAL TRANSACTIONS OF THE ROYAL SOCIETY A MATHEMATICAL, PHYSICAL & ENGINEERING SCIENCES

On Simple Waves and Weak Shock Theory for the Equations of Alluvial River Hydraulics

D. D. L. Zanre and D. J. Needham

Phil. Trans. R. Soc. Lond. A 1996 **354**, 2993-3054
doi: 10.1098/rsta.1996.0137

On simple waves and weak shock theory for the equations of alluvial river hydraulics

By D. D. L. Zanré[1] and D. J. Needham[2]

[1]*School of Mathematics, University of East Anglia, Norwich NR4 7TJ, UK*
[2]*Department of Mathematics, University of Reading, Whiteknights, Reading RG6 6AF, UK*

Contents

This paper considers the hydraulic equations governing alluvial river dynamics. The shock-wave classes for this system were described and fully analysed by Needham & Hey (1991). The complementary expansion wave classes are determined in this paper. In addition, more general simple waves are considered and a weak-shock theory is established. This is used to consider several practical examples, including the dynamics of dredged river sections, the propagation of sediment slugs and the effects of sediment blocking and extraction.

Phil. Trans. R. Soc. Lond. A (1996) **354**, 2993–3054
Printed in Great Britain

1. Introduction

The mechanics of bed-load sediment transport in alluvial rivers and channels is of great interest to many scientists, including civil engineers, geologists, hydrologists, and more recently, ecologists. For example, the aggradation of a river bed due to sediment deposition upstream of dams can lead to serious structural damage, while the efficiency of reservoirs and irrigation channels is often reduced by the depositing of detritus. In extreme cases these may become useless, resulting in floods and droughts. Also, the dispersal of pollutants transported along a river bed attached to sediment can lead to environmental damage. Therefore, an understanding of the dynamics of the system of equations governing the flow in alluvial rivers is essential to the development of an understanding of all of these problems.

However, until very recently, a rational analytic approach has not been taken in determining solutions to the system of equations which governs the flow in an alluvial river or channel, namely the depth-averaged hydraulic equations augmented by a sediment transport function. Most of the solutions have been developed numerically (see, for example, Cunge *et al.* 1981; Bettes & White 1979; Peter 1981; Falconer & Owens 1984; Krishnappan 1985, 1986) for specific problems associated with particular rivers, the results of which usually cannot be generalized. On the other hand, the analytical approaches used by, for instance, Ribberink & Van der Sande (1985), Mehta *et al.* (1983), de Vries (1973), Gill (1983*a*, *b*, 1987) do not provide a fully comprehensive study of the dynamics of the flow because of the use of *ad hoc* approximations which result in what are known as the 'parabolic' or 'hyperbolic' models. The assumption of steady state conditions for the fluid mass continuity and the momentum equations, and then the linearization about the uniform flow, leads to the loss of two of the solutions for the characteristic wave speeds of the flow, one becoming infinite and thus physically unacceptable. Therefore, the so-called 'hyperbolic' model only exhibits a degenerate form of hyperbolic behaviour. Reynolds (1965) similarly attempted to solve a reduced nonlinear system of equations. However, his approximations led to a quasi-linear equation which contains a spurious singularity at $F = 1$, where F is the local Froude number of the flow. The occurrence of this singularity was not resolved by Reynolds. There would be a similar singularity in the nonlinear version of the 'hyperbolic' model used by Ribberink & Van der Sande (1985). The understanding and resolution of the defects in the above models is based on the development of a complete singular perturbation theory for the full nonlinear system of conservation laws. In the linearized regime, Needham (1988, 1990) returned to the full system of equations and, by the use of asymptotic techniques in conjunction with a wave hierarchy approach, showed that the system was formally hyperbolic. The resulting system was found to be a singular perturbation of the usual system governing linearized fixed bed hydraulics and this singular perturbation was examined fully. The differential form of the fully nonlinear system has also been shown to be formally hyperbolic (Zanré & Needham 1994) leading to the possibility of finite-time blow-up in the full nonlinear system, necessitating the inclusion of shock waves. Needham & Hey (1991, 1992) considered the possibility of weak (shock wave) solutions to the integral form of the conservation laws, requiring the introduction of a shock-depth function. Three shock wave families were found which were then analysed to establish stability via an energy dissipation criterion. In a recent paper, Zanré & Needham (1994) have generalized these three families of shock wave solutions and have established that the energy dissipation criterion

PHILOSOPHICAL TRANSACTIONS OF THE ROYAL SOCIETY A MATHEMATICAL, PHYSICAL & ENGINEERING SCIENCES

and the use of the Lax shock inequalities (see, for example, Lax 1957, 1973; Smoller 1983) provide equivalent conditions for determining regions of stability of such shock waves.

In this paper we examine the three simple wave families of the fully nonlinear equations, which are classical solutions to the differential form of the integral conservation laws. Each of these three families corresponds to a classical solution which propagates information along only one of the three characteristic families, $\lambda_i(\boldsymbol{u})$, $i = 1, 2, 3$, identified in Zanré & Needham (1994).

First, we construct the three families of expansion wave solutions, the counterparts of the three shock wave families discussed in Needham & Hey (1991, 1992) and in Zanré & Needham (1994). These exist in complimentary regions of the (H, F_0)-plane, where H and F_0 are as defined in Needham & Hey (1991, 1992). Then we examine the simple wave solutions for more general initial data. As may be expected, finite-time blow-up is exhibited in many cases (in $\|\boldsymbol{u}_x\|_\infty, \|\boldsymbol{u}_t\|_\infty$), after which the solution can only be continued in a piecewise-classical sense by the inclusion of a shock wave which satisfies the conditions derived by Needham & Hey (1991, 1992). Generally this is quite a lengthy and complicated procedure. However, for weak disturbances, we show that the insertion of a shock into a simple wave solution using the equal area rule of Whitham (1974) is equivalent (up to first nonlinear order in shock amplitude) to the fitting of a shock satisfying the full conditions of Needham & Hey (1991, 1992). In this case, we can readily follow the full evolution of the initial data. Examples of physically relevant problems are given, namely the evolution of a dredged channel, upstream and downstream sediment influx and starvation problems, and sediment slug passages.

2. Equations of motion

The integral conservation laws which govern the one-dimensional flow in an alluvial river or channel are the depth averaged hydraulic equations, augmented with a sediment transport function to allow closure of the system. These are

$$\frac{\mathrm{d}}{\mathrm{d}t}\int_{x_1}^{x_2} h\,\mathrm{d}x + [hv]_{x_1}^{x_2} = 0, \tag{2.1}$$

$$\frac{\mathrm{d}}{\mathrm{d}t}\int_{x_1}^{x_2} \xi\,\mathrm{d}x + [q]_{x_1}^{x_2} = 0, \tag{2.2}$$

$$\frac{\mathrm{d}}{\mathrm{d}t}\int_{x_1}^{x_2} hv\,\mathrm{d}x + [v^2h + \tfrac{1}{2}gh^2]_{x_1}^{x_2} + \int_{C_{\xi_{1,2}}} gh\,\mathrm{d}y = \int_{x_1}^{x_2} R(v,h,q)h\,\mathrm{d}x, \tag{2.3}$$

$$q = G(h,v). \tag{2.4}$$

The equations (2.1)–(2.3) are derived through conserving momentum and the fluid and sediment mass in a region of the flow between $x = x_1$ and $x = x_2$, where $x_2 > x_1$ and x is a measure of the horizontal distance from a fixed origin, 0 (see, for example, Stoker 1957). In these equations t represents time, v the depth-averaged fluid velocity in a horizontal direction and q the bed-load sediment flux per unit width transported across a vertical section of the flow. The bed level, ξ, is measured vertically downwards from the origin, with the flow depth being h, giving the distance of the free surface from the origin, η, as $\eta = h - \xi$. The coordinate system is illustrated in figure 1. $R(v,h,q)$ is a function which represents the resistance on the fluid flow

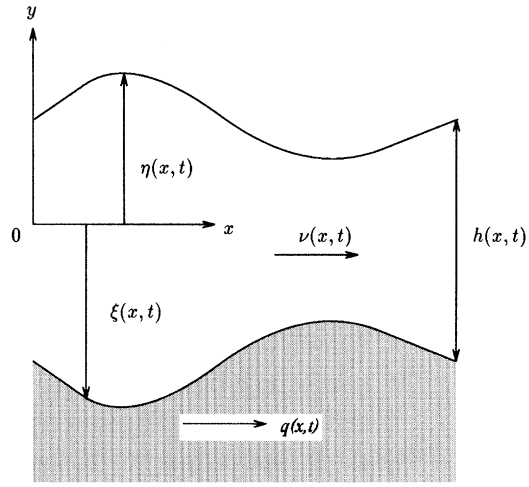

Figure 1. The coordinate system.

due to bed friction and $G(h, v)$ is the sediment transport function, the effects of specific forms of which are examined by Cunge *et al.* (1981). The final term on the left-hand side of equation (2.3) is a line integral with respect to y (the vertical coordinate measured in an upwards direction from 0) along $C_{\xi_{1,2}}$, an integral path denoting the part of the bed curve between $x = x_1$ and $x = x_2$. This arises from the normal reaction of hydrostatic pressure at the bed.

To continue with further analysis of the system (2.1)–(2.4), it is necessary to specify particular forms for R and G. Following Gibson (1934), we adopt the Chézy formula for a wide channel with a rectangular cross section as the functional form for R. This can be written as

$$R = -\tilde{C}_f(q)v^2/h, \tag{2.5}$$

where $\tilde{C}_f$ is the dimensionless Chézy coefficient, related to the usual Chézy coefficient, C_f through

$$\tilde{C}_f = C_f/(1 + C_g q). \tag{2.6}$$

Here C_g is a material constant which determines the extent to which the resistance of the flow would depend on sediment transport. From equations (2.5) and (2.6), we can see that the flow resistance becomes greater with increasing fluid velocity and decreases if the flow depth or the local bed-load sediment transport rate increases.

The chosen functional form for G is given by

$$G = mv^n, \tag{2.7}$$

as in Cunge *et al.* (1981). Here, m will generally be dependent on the properties of the flow and n a constant. Experiment has shown that in many cases if the flow is slowly varying in time then $1 \leqslant n \leqslant 2$, provided the bed is not dune covered where larger values for n may be obtained (Engelund & Hansen 1967). In this paper, we take m as a constant since this is a reasonable approximation to many of the sediment transport functions. Also, for simplicity, we take $n = 2$. However, in the following analysis the results will remain qualitatively similar for different functional forms for R and G provided R is monotone increasing with v and monotone decreasing with h, and G is a positive monotone increasing function of v.

The simplest solution of the conservation laws (2.1)–(2.4) is the uniform flow down an inclined plane of slope, S, with constant fluid discharge, Q_0, sediment discharge, q_0, bed-level, h_0, fluid velocity, v_0, and where $\xi = Sx$. Substituting into equations (2.1)–(2.7) gives the solution for the uniform flow as

$$v_0 = \left(\frac{q_0}{m}\right)^{1/2}, \quad h_0 = \left(\frac{Q_0^2 m}{q_0}\right)^{1/2}, \quad S = \frac{C_f}{gQ_0(1+C_g q_0)}\left(\frac{q_0}{m}\right)^{1/2}, \tag{2.8}$$

which is then used as a basis for the following dimensionless variables,

$$v = v_0 v', \quad h = h_0 h', \quad \xi = h_0 \xi', \quad q = q_0 q', \quad y = h_0 y', \quad x = l_0 x', \quad t = (l_0/v_0)t', \tag{2.9}$$

where l_0 is a typical horizontal length scale in the flow, with $l_0 \gg h_0$ in keeping with the hydraulic approximation. Substituting (2.9) into (2.1)–(2.4) and replacing G by (2.7) leads to the non-dimensional system,

$$\frac{\mathrm{d}}{\mathrm{d}t}\int_{x_1}^{x_2} h\,\mathrm{d}x + [hv]_{x_1}^{x_2} = 0, \tag{2.10}$$

$$\frac{\mathrm{d}}{\mathrm{d}t}\int_{x_1}^{x_2} \xi\,\mathrm{d}x - [\varepsilon v^2]_{x_1}^{x_2} = 0, \tag{2.11}$$

$$\frac{\mathrm{d}}{\mathrm{d}t}\int_{x_1}^{x_2} hv\,\mathrm{d}x + \left[v^2 h + \frac{1}{2F_0^2}h^2\right]_{x_1}^{x_2} + \frac{1}{F_0^2}\int_{C_{\xi_{1,2}}} h\,\mathrm{d}y = \frac{-C_f}{\sigma}\int_{x_1}^{x_2} \frac{v^2}{(1+\theta v^2)}\,\mathrm{d}x, \tag{2.12}$$

$$q = v^2, \tag{2.13}$$

where the primes have been dropped for convenience. Here, $F_0 = v_0/\sqrt{gh_0}$ is the Froude number of the uniform flow, $\varepsilon = q_0/Q_0$ ($\ll 1$) is the ratio of sediment to fluid discharge, $\sigma = h_0/l_0$, while $\theta = C_s q_0$ is a dimensionless measure of the influence of bedload sediment transport on flow resistance. When $\varepsilon, \theta \to 0$, the system (2.10)–(2.13) reduces formally to that associated with fixed bed hydraulics (see, for example, Stoker 1957). In terms of the dimensionless variables, the uniform flow can be written as

$$v = 1, \quad h = 1, \quad \xi = \frac{C_f F_0^2}{\sigma(1+\theta)}x, \quad q = 1. \tag{2.14}$$

To proceed, we will only consider classical solutions of the differential form of the integral conservation laws (2.10)–(2.12) given by

$$\frac{\partial h}{\partial t} + \frac{\partial}{\partial x}(hv) = 0, \tag{2.15}$$

$$\frac{\partial \xi}{\partial t} - \varepsilon\frac{\partial}{\partial x}(v^2) = 0, \tag{2.16}$$

$$\frac{\partial v}{\partial t} + v\frac{\partial v}{\partial x} + \frac{1}{F_0^2}\frac{\partial h}{\partial x} - \frac{1}{F_0^2}\frac{\partial \xi}{\partial x} = \frac{-C_f v^2}{\sigma h(1+\theta v^2)}, \tag{2.17}$$

subject to the additional admissibility conditions

$$-\infty < \xi(x,t) < \infty, \quad 0 < v(x,t) < \infty, \quad 0 < h(x,t) < \infty, \tag{2.18}$$

as defined in Zanré & Needham (1994). In their paper, Zanré & Needham established that the system (2.15)–(2.17) was formally hyperbolic, and that the canonical form

of the system can be written as

$$\left(\frac{\partial h}{\partial t}+\lambda_i(\boldsymbol{u})\frac{\partial h}{\partial x}\right)+\frac{(v-\lambda_i(\boldsymbol{u}))}{\lambda_i(\boldsymbol{u})}\left(\frac{\partial \xi}{\partial t}+\lambda_i(\boldsymbol{u})\frac{\partial \xi}{\partial x}\right)$$
$$-F_0^2(v-\lambda_i(\boldsymbol{u}))\left(\frac{\partial v}{\partial t}+\lambda_i(\boldsymbol{u})\frac{\partial v}{\partial x}\right)=\frac{F_0^2C_f(v-\lambda_i(\boldsymbol{u}))v^2}{\sigma h(1+\theta v^2)}, \tag{2.19}$$

for $i=1,2,3$. Here $\boldsymbol{u}=(h,v,\xi)^{\mathrm{T}}$ and $\lambda_i(\boldsymbol{u})$, $i=1,2,3$, are the eigenvalues of the system, (2.15)–(2.17), and represent the three characteristic families. These were found to be given by

$$\lambda_1(\boldsymbol{u})\sim\begin{cases}(v-\sqrt{h}/F_0)\left[1+\dfrac{\varepsilon v}{F_0^2(v-\sqrt{h}/F_0)^2}+O(\varepsilon^2)\right]; & \\ & 0<v<\sqrt{h}/F_0-O(\varepsilon^{1/2}),\\ \frac{1}{2}\varepsilon^{1/2}[\bar{v}-\sqrt{(\bar{v}^2+4\sqrt{h}/F_0^3)}]+O(\varepsilon); & v=\sqrt{h}/F_0\pm O(\varepsilon^{1/2}),\\ \dfrac{-2\varepsilon v^2}{F_0^2(v^2-h/F_0^2)}+O(\varepsilon^2); & v>\sqrt{h}/F_0+O(\varepsilon^{1/2}),\end{cases} \tag{2.20}$$

$$\lambda_2(\boldsymbol{u})\sim\begin{cases}\dfrac{2\varepsilon v^2}{F_0^2(h/F_0^2-v^2)}+O(\varepsilon^2); & 0<v<\sqrt{h}/F_0-O(\varepsilon^{1/2}),\\ \frac{1}{2}\varepsilon^{1/2}[\bar{v}+\sqrt{(\bar{v}^2+4\sqrt{h}/F_0^3)}]+O(\varepsilon); & v=\sqrt{h}/F_0\pm O(\varepsilon^{1/2}),\\ (v-\sqrt{h}/F_0)\left[1+\dfrac{\varepsilon v}{F_0^2(v-\sqrt{h}/F_0)^2}+O(\varepsilon^2)\right]; & \\ & v>\sqrt{h}/F_0+O(\varepsilon^{1/2}),\end{cases} \tag{2.21}$$

$$\lambda_3(\boldsymbol{u})\sim(v+\sqrt{h}/F_0)[1+\varepsilon vF_0^{-2}(v+\sqrt{h}/F_0)^{-2}+O(\varepsilon^2)];\quad v,h>0. \tag{2.22}$$

as $\varepsilon\to 0$, where $\bar{v}=(v-\sqrt{h}/F_0)\varepsilon^{-1/2}$.

The $\lambda_i(\boldsymbol{u})$ $(i=1,2,3)$ satisfy the ordering,

$$\lambda_1(\boldsymbol{u})<0<\lambda_2(\boldsymbol{u})<\lambda_3(\boldsymbol{u}), \tag{2.23}$$

for all admissible $\boldsymbol{u}$ satisfying (2.18). It can be seen from this ordering that the system (2.15)–(2.17) is indeed hyperbolic. Also, as $\varepsilon\to 0$, only the eigenvalues of $o(1)$ play the dominant role in the evolution of the bedform (Zanré & Needham 1994). Thus it can be seen from (2.22) that $\lambda_3(\boldsymbol{u})$ never becomes small enough to carry an $O(1)$ bedform structure. However, from (2.20) and (2.21), we can see that both the $\lambda_1(\boldsymbol{u})$ and $\lambda_2(\boldsymbol{u})$ eigenvalues have the necessary $O(\varepsilon)$ forms to allow an $O(1)$ bedform structure to evolve. When the local Froude number, $F\equiv(v/\sqrt{h})F_0$, is greater than unity, the $O(1)$ bedform development occurs predominantly on the $\lambda_1(\boldsymbol{u})$ characteristic. Conversely, when $F<1$, the $O(1)$ development in bedform is associated with the $\lambda_2(\boldsymbol{u})$ characteristic.

The canonical form (2.19), along with the definitions of the $\lambda_i(\boldsymbol{u})$, $i=1,2,3$, given by (2.20)–(2.22), will be used in the next section to find the three simple wave families s_1, s_2, s_3.

3. Simple waves

On taking the bedform, ξ, and the fluid velocity, v, to be functions of the flow depth, h, we make the substitutions

$$\xi = F(h), \qquad v = G(h) \tag{3.1}$$

into the canonical form (2.19), where F and G are differentiable functions to be determined. Dissipative effects are exhibited through the dimensionless parameter,

$$d_f = C_f/\sigma. \tag{3.2}$$

In a hydraulic flow both $\sigma \ll 1$ and $C_f \ll 1$ and so the effect of dissipation depends upon the relative smallness of the shallow water parameter σ and the flow resistance (Chézy) coefficient, C_f. In the present paper, we restrict attention to the case $d_f \ll 1$, which is usually the situation in most alluvial hydraulic flows. In particular, in what follows we let $d_f \to 0$. This, along with (3.1), reduces the canonical form, (2.19), to the three equations,

$$\left[\frac{\partial h}{\partial t} + \lambda_i(\boldsymbol{u})\frac{\partial h}{\partial x}\right]\left[1 + \frac{F'(h)(G(h) - \lambda_i(\boldsymbol{u}))}{\lambda_i(\boldsymbol{u})} - G'(h)F_0^2\,(G(h) - \lambda_i(\boldsymbol{u}))\right] = 0, \tag{3.3}$$

with $i = 1, 2, 3$ and where $'$ denotes differentiation with respect to h. The three equations (3.3) determine the three simple wave families s_i, $i = 1, 2, 3$ subject to the downstream condition that the flow is uniform, as given by (2.14), which requires $F(1) = 0$ and $G(1) = 1$.

(*a*) *The s_3-simple wave family*

Along the λ_3-characteristic, we have from (2.23) and (3.3) that

$$\frac{\partial h}{\partial t} + \lambda_3(\boldsymbol{u})\frac{\partial h}{\partial x} = 0, \tag{3.4}$$

$$1 + \frac{F'(h)(G(h) - \lambda_1(\boldsymbol{u}))}{\lambda_1(\boldsymbol{u})} - G'(h)F_0^2(G(h) - \lambda_1(\boldsymbol{u})) = 0, \tag{3.5}$$

$$1 + \frac{F'(h)(G(h) - \lambda_2(\boldsymbol{u}))}{\lambda_2(\boldsymbol{u})} - G'(h)F_0^2(G(h) - \lambda_2(\boldsymbol{u})) = 0. \tag{3.6}$$

On rearranging (3.6) we obtain an explicit form for $F'(h)$ as

$$F'(h) = \frac{\lambda_2(\boldsymbol{u})}{G(h) - \lambda_2(\boldsymbol{u})}[G'(h)F_0^2(G(h) - \lambda_2(\boldsymbol{u})) - 1], \tag{3.7}$$

to be solved in $h > 0$ subject to the condition

$$F(1) = 0. \tag{3.8}$$

Now substituting (3.7) into (3.5), we arrive at the following ordinary differential equation for $G(h)$,

$$1 + G'(h)F_0^2(G(h) - \lambda_1(\boldsymbol{u}))\left\{\frac{\lambda_2(\boldsymbol{u})}{\lambda_1(\boldsymbol{u})} - 1\right\} - \frac{(G(h) - \lambda_1(\boldsymbol{u}))\lambda_2(\boldsymbol{u})}{(G(h) - \lambda_2(\boldsymbol{u}))\lambda_1(\boldsymbol{u})} = 0, \tag{3.9}$$

to be solved in $h > 0$ subject to the condition

$$G(1) = 1. \tag{3.10}$$

The fluid velocity, $G(h)$, is determined by solution of (3.9), and this is substituted back into (3.7) to obtain the corresponding bedform, $F(h)$. The solution of (3.9) subject to (3.10) is now considered in the limit $\varepsilon \to 0$. This is complicated by the asymptotic structure of $\lambda_{1,2}(\boldsymbol{u})$ as $\varepsilon \to 0$, given by (2.20) and (2.21), which depends upon whether $G(h) < \sqrt{h}/F_0$ or $G(h) > \sqrt{h}/F_0$. For this reason we find it instructive to deal with the solution of (3.9), (3.10) separately in each of the cases $F_0 < 1 - O(\varepsilon^{1/2})$, $F_0 \sim 1 \pm O(\varepsilon^{1/2})$ and $F_0 > 1 + O(\varepsilon^{1/2})$.

(i) $F_0 < 1 - O(\varepsilon^{1/2})$

In this case, at $h = 1$, condition (3.10) establishes that $G(h) < \sqrt{h}/F_0$ and so, at least in some interval containing $h = 1$, we have from (2.20), (2.21),

$$\lambda_1(\boldsymbol{u}) \sim (G(h) - \sqrt{h}/F_0) + O(\varepsilon), \tag{3.11}$$

$$\lambda_2(\boldsymbol{u}) \sim \frac{2\varepsilon G(h)^2}{(h - F_0^2 G(h)^2)} + O(\varepsilon^2), \tag{3.12}$$

as $\varepsilon \to 0$. On substitution from (3.11), (3.12) into (3.9) we obtain the differential equation for $G(h)$ as,

$$G'(h) = 1/F_0\sqrt{h} + O(\varepsilon), \qquad G(1) = 1. \tag{3.13}$$

The solution of (3.13) is readily obtained as

$$G(h) = 1 + (2/F_0)(\sqrt{h} - 1) + O(\varepsilon), \quad (\tfrac{1}{2}(2 - F_0))^2 < h < (2 - F_0)^2 - O(\varepsilon^{1/2}). \tag{3.14}$$

The lower limit on h is obtained via the admissibility condition $v > 0$, while the upper limit occurs when $G(h) \sim \sqrt{h}/F_0$, and alternative asymptotic forms are required for $\lambda_{1,2}(\boldsymbol{u})$ to continue the solution of (3.9) into $h \geqslant (2 - F_0)^2 - O(\varepsilon^{1/2})$.

We next consider the form of $G(h)$ when $h = (2 - F_0)^2 \pm O(\varepsilon^{1/2})$. We introduce the scaled variables, $\bar{h}$ and $\bar{G}$, as

$$h = (2 - F_0)^2 + \varepsilon^{1/2}\bar{h}, \qquad G = (2 - F_0)/F_0 + \varepsilon^{1/2}\bar{G}, \tag{3.15}$$

being guided by (3.14), with $\bar{h}$, $\bar{G} = O(1)$ as $\varepsilon \to 0$ in this region. On substituting from (3.15) into (3.9) we obtain

$$\bar{G}'(\bar{h}) = \frac{1}{F_0(2 - F_0)} + O(\varepsilon^{1/2}), \quad -\infty < \bar{h} < \infty, \tag{3.16}$$

subject to matching with (3.14) as $\bar{h} \to -\infty$, which requires

$$\bar{G}(\bar{h}) = \frac{\bar{h}}{F_0(2 - F_0)} + O(1), \quad \text{as} \quad \bar{h} \to -\infty. \tag{3.17}$$

The solution of (3.17) and (3.16) is readily obtained as $\bar{G}(\bar{h}) = \bar{h}/F_0(2 - F_0)$, and so we have

$$G(h) = \frac{(2 - F_0)}{F_0} + \varepsilon^{1/2}\frac{\bar{h}}{F_0(2 - F_0)} + O(\varepsilon), \qquad h = (2 - F_0)^2 \pm O(\varepsilon^{1/2}) \tag{3.18}$$

as $\varepsilon \to 0$ with $\bar{h} = O(1)$.

For $\bar{h} \gg 1$, (3.18) moves into a domain where $G(h) > \sqrt{h}/F_0 + O(\varepsilon^{1/2})$ and a further region must be introduced to continue $G(h)$ into $h > (2 - F_0)^2 + O(\varepsilon^{1/2})$. Again we substitute into equation (3.9) for the appropriate forms of $\lambda_{1,2}(\boldsymbol{u})$ from

PHILOSOPHICAL TRANSACTIONS OF THE ROYAL SOCIETY A MATHEMATICAL, PHYSICAL & ENGINEERING SCIENCES

(2.20) and (2.21), after which we arrive at

$$G'(h) = \frac{1}{F_0\sqrt{h}} + O(\varepsilon), \qquad h > (2-F_0)^2 + O(\varepsilon^{1/2}),$$

which is to be solved subject to matching with (3.18) as $h \to (2-F_0)^2$, namely,

$$G(h) \to (2-F_0)/F_0 \quad \text{as} \quad h \to (2-F_0)^2.$$

The solution of this problem is readily obtained as

$$G(h) = 1 + \frac{2}{F_0}(\sqrt{h}-1) + O(\varepsilon), \qquad h > (2-F_0)^2 + O(\varepsilon^{1/2}). \tag{3.19}$$

The solution to (3.9), (3.10) is now complete, and we observe that as $\varepsilon \to 0$

$$G(h) \sim 1 + \frac{2}{F_0}(\sqrt{h}-1) + o(1), \quad \text{uniformly in} \quad h > \tfrac{1}{4}(2-F_0)^2, \tag{3.20}$$

via (3.14), (3.18) and (3.19). On substituting back from (3.20) into (3.7) and (2.22) we find that, as $\varepsilon \to 0$,

$$F(h) \sim \frac{4\varepsilon}{9F_0}\left\{(2-F_0)\log\left|\frac{F_0-2+3\sqrt{h}}{F_0+1}\right| + 6(1-\sqrt{h}) + O(\varepsilon)\right\}, \tag{3.21}$$

$$\lambda_3(h) \sim 1 + \frac{1}{F_0}(3\sqrt{h}-2) + O(\varepsilon), \tag{3.22}$$

uniformly in $h > \frac{1}{4}(2-F_0)^2$. We remark that the apparent singularity in (3.21) occurs outside the admissible domain of h, namely in $h < \frac{1}{4}(2-F_0)^2$.

(ii) $F_0 > 1 + O(\varepsilon^{1/2})$

In this case at $h = 1$, condition (3.10) establishes that $G(h) > \sqrt{h}/F_0$, and so, at least in some interval containing $h = 1$, we have, from (2.20), (2.21),

$$\lambda_1(\boldsymbol{u}) \sim O(\varepsilon), \qquad \lambda_2(\boldsymbol{u}) \sim (G(h) - \sqrt{h}/F_0) + O(\varepsilon) \tag{3.23}$$

as $\varepsilon \to 0$. After substituting from (3.23) into (3.9) we obtain the differential equation for $G(h)$ as (3.13) and so again we have

$$G(h) = 1 + \frac{2}{F_0}(\sqrt{h}-1) + O(\varepsilon), \quad h > H^*(2-F_0)[(2-F_0)^2 + O(\varepsilon^{1/2})] \tag{3.24}$$

with $H^*(\cdot)$ being the Heaviside function, defined as

$$H^*(x) = \begin{cases} 1, & \text{if } x \geqslant 0, \\ 0, & \text{if } x < 0. \end{cases}$$

As in case § 3 *a* (i), two further regions are necessary when $F_0 \leqslant 2$, to continue $G(h)$ into $h \sim (2-F_0)^2 \pm O(\varepsilon^{1/2})$ and $(\frac{1}{2}(2-F_0))^2 < h < (2-F_0)^2 - O(\varepsilon^{1/2})$. The details are as in case § 3 *a* (i) and we finally arrive at the forms (3.20)–(3.22) for $G(h)$, $F(h)$ and $\lambda_3(h)$ as $\varepsilon \to 0$, uniformly in $h > \frac{1}{4}H^*(2-F_0)(2-F_0)^2$.

(iii) $F_0 \sim 1 \pm O(\varepsilon^{1/2})$

In this case we readily establish that as $\varepsilon \to 0$

$$G(h) \sim 2\sqrt{h} - 1 + O(\varepsilon^{1/2}), \tag{3.25}$$

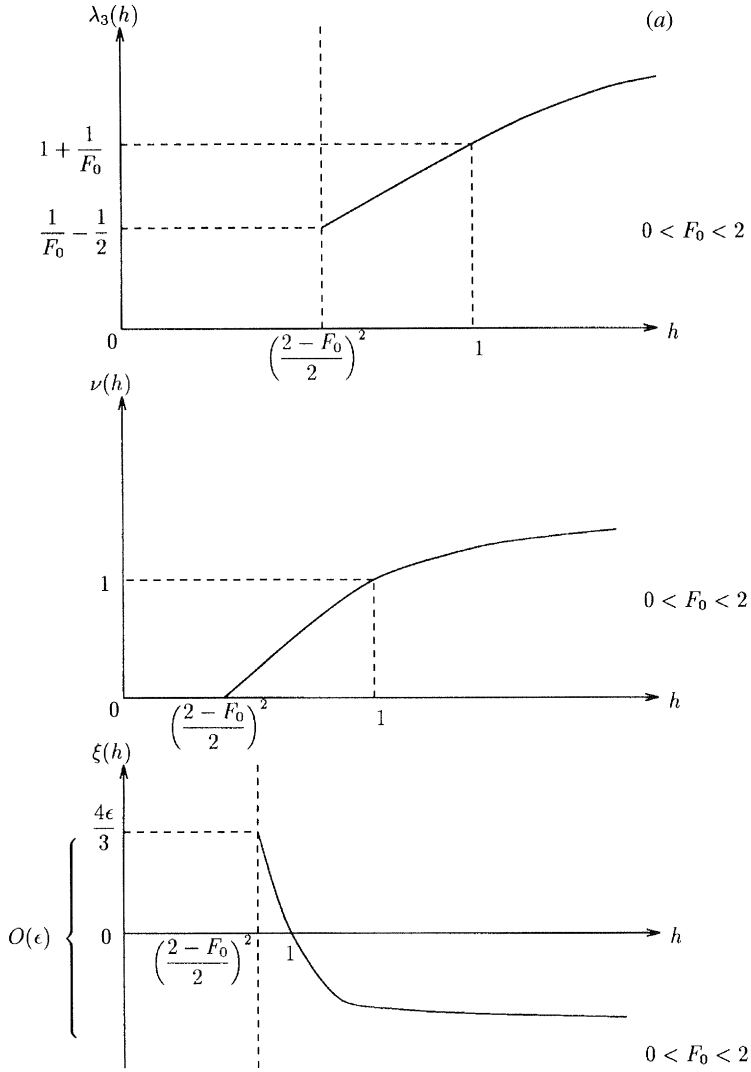

Figure 2. (*a*) Graph of $\lambda_3(h)$, $\nu(h)$, $\xi(h)$ when $0 < F_0 < 2$.

$$F(h) \sim \tfrac{4}{9}\varepsilon\{\log|\tfrac{3}{2}\sqrt{h}-\tfrac{1}{2}|+6(1-\sqrt{h})\}+O(\varepsilon^{3/2}), \tag{3.26}$$

$$\lambda_3(h) \sim 3\sqrt{h}-1+O(\varepsilon^{1/2}), \tag{3.27}$$

uniformly for $h > \frac{1}{4}$.

Therefore, via (3.20)–(3.27) we have established that the s_3-simple wave has, as $\varepsilon \to 0$

$$\lambda_3(h) \sim 1+\frac{1}{F_0}(3\sqrt{h}-2)+O(\varepsilon), \tag{3.28}$$

$$v(h) = G(h) \sim 1-\frac{2}{F_0}+2\frac{\sqrt{h}}{F_0}+O(\varepsilon), \tag{3.29}$$

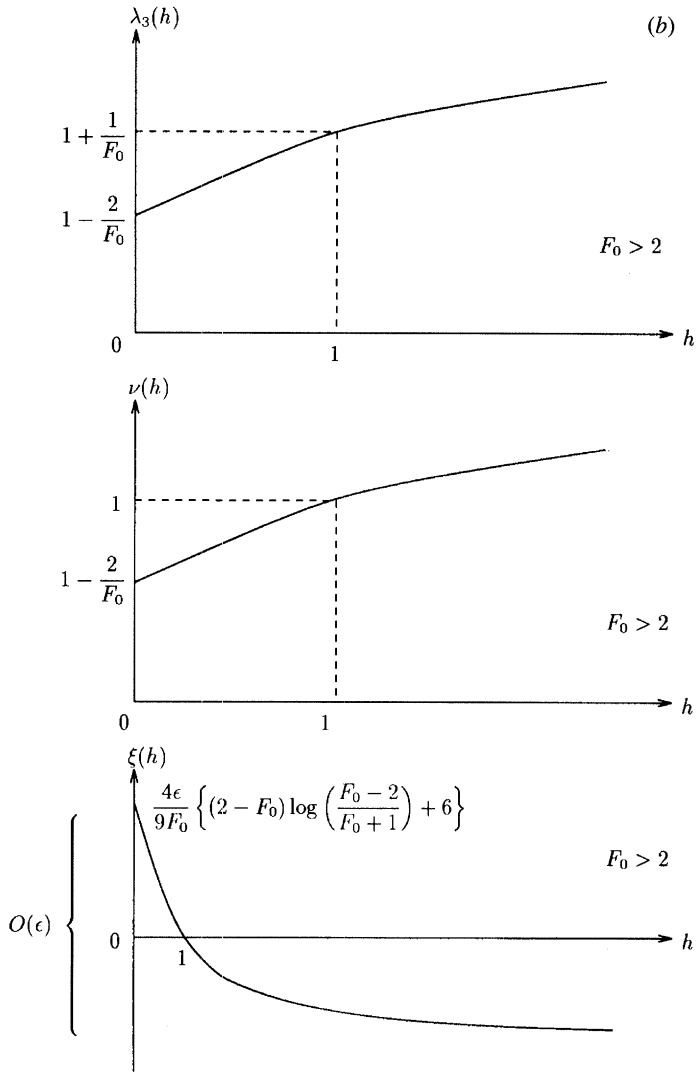

Figure 2. (*b*) Graph of $\lambda_3(h)$, $\nu(h)$, $\xi(h)$ when $F_0 > 2$ for s_3-simple wave.

$$\xi(h) = F(h) \sim \frac{4\varepsilon}{9F_0}\left\{(2-F_0)\log\left|\frac{F_0-2+3\sqrt{h}}{F_0+1}\right| + 6(1-\sqrt{h})\right\} + O(\varepsilon^2), \quad (3.30)$$

uniformly in $F_0 > 0$, $h > \frac{1}{4}H^*(2-F_0)(2-F_0)^2$, with $h(x,t)$ satisfying the partial differential equation

$$\frac{\partial h}{\partial t} + \lambda_3(h)\frac{\partial h}{\partial x} = 0. \quad (3.31)$$

Sketches of $\lambda_3(h)$, $v(h)$ and $\xi(h)$ are given in figure 2 for the cases $F_0 < 2$ and $F_0 > 2$. We notice that there is a cut-off point in the region $F_0 < 2$ at $h = \frac{1}{4}(2-F_0)^2$, below which the velocity, $v(h)$ becomes negative. As can be seen from the graphs, the characteristic wave speed, $\lambda_3(h)$, is always positive and $O(1)$. As expected, the resulting bedform, $\xi(h)$, is never of a significant order to be of any great interest in sediment transport problems, being always of $O(\varepsilon)$.

(*b*) *The s_2- and s_1-simple wave families*

In a similar manner to that of § 3 *a*, we can establish via (3.3) that along the $\lambda_2(\boldsymbol{u})$-characteristic, the properties of the s_2-simple wave family can be determined from the equations,

$$\frac{\partial h}{\partial t} + \lambda_2(\boldsymbol{u})\frac{\partial h}{\partial x} = 0, \tag{3.32}$$

$$1 + \frac{F'(h)(G(h) - \lambda_1(\boldsymbol{u}))}{\lambda_1(\boldsymbol{u})} - G'(h)F_0^2(G(h) - \lambda_1(\boldsymbol{u})) = 0, \tag{3.33}$$

$$1 + \frac{F'(h)(G(h) - \lambda_3(\boldsymbol{u}))}{\lambda_3(\boldsymbol{u})} - G'(h)F_0^2(G(h) - \lambda_3(\boldsymbol{u})) = 0, \tag{3.34}$$

whereas, along the $\lambda_1(\boldsymbol{u})$-characteristic, we have for the s_1-simple wave that

$$\frac{\partial h}{\partial t} + \lambda_1(\boldsymbol{u})\frac{\partial h}{\partial x} = 0, \tag{3.35}$$

$$1 + \frac{F'(h)(G(h) - \lambda_2(\boldsymbol{u}))}{\lambda_2(\boldsymbol{u})} - G'(h)F_0^2(G(h) - \lambda_2(\boldsymbol{u})) = 0, \tag{3.36}$$

$$1 + \frac{F'(h)(G(h) - \lambda_3(\boldsymbol{u}))}{\lambda_3(\boldsymbol{u})} - G'(h)F_0^2(G(h) - \lambda_3(\boldsymbol{u})) = 0. \tag{3.37}$$

Again we can in both cases, respectively, rearrange equation (3.33) or (3.36) to provide an explicit expression for $F'(h)$, after which substitution into equation (3.34) or (3.37) leaves a single first order ordinary differential equation to be solved for $G(h)$, subject to the conditions $G(1) = 1$ and $F(1) = 0$. As in § 3 *a* we consider the solution of this problem as $\varepsilon \to 0$. Again this is complicated by the asymptotic structure of each $\lambda_i(\boldsymbol{u})$ $(i = 1, 2, 3)$ as $\varepsilon \to 0$, which depends upon whether $G(h) < \sqrt{h}/F_0$ or $G(h) > \sqrt{h}/F_0$. As before it is therefore instructive to consider the cases $F_0 < 1 - O(\varepsilon^{1/2})$, $F_0 \sim 1 \pm O(\varepsilon^{1/2})$ and $F_0 > 1 + O(\varepsilon^{1/2})$ separately.

Omitting details, the properties of the s_2-simple wave family are obtained as the following.

In $F_0 < 1 - O(\varepsilon^{1/2})$:

$$\lambda_2(h) \sim \begin{cases} (3/F_0)(F_0^{1/3} - \sqrt{h}) + O(\varepsilon), & 0 < h < F_0^{2/3} - O(\varepsilon^{1/2}), \\ \dfrac{\varepsilon^{1/2}}{2}\left[\dfrac{-3\bar{h}}{2F_0^{4/3}} + \left(\dfrac{9\bar{h}^2}{4F_0^{8/3}} + \dfrac{4}{F_0^{8/3}}\right)^{1/2}\right] + O(\varepsilon), & h = F_0^{2/3} \pm O(\varepsilon^{1/2}), \\ 2\varepsilon/(h^3 - F_0^2) + O(\varepsilon^2), & h > F_0^{2/3} + O(\varepsilon^{1/2}), \end{cases} \tag{3.38}$$

$$v(h) = G(h) \sim \begin{cases} (2/F_0)(\tfrac{3}{2}F_0^{1/3} - \sqrt{h}) + O(\varepsilon), & 0 < h < F_0^{2/3} - O(\varepsilon^{1/2}), \\ F_0^{-2/3} - \varepsilon^{1/2}\bar{h}/4F_0^{4/3} + O(\varepsilon), & h = F_0^{2/3} \pm O(\varepsilon^{1/2}), \\ 1/h + O(\varepsilon), & h > F_0^{2/3} + O(\varepsilon^{1/2}), \end{cases} \tag{3.39}$$

$$\xi(h) = F(h) \sim \begin{cases} (\frac{3}{2}F_0^{2/3} - \frac{1}{2}F_0^2 - 1) + O(\varepsilon), & 0 < h < F_0^{2/3} - O(\varepsilon^{1/2}), \\ (\frac{3}{2}F_0^{2/3} - \frac{1}{2}F_0^2 - 1) + O(\varepsilon^{1/2}), & h = F_0^{2/3} \pm O(\varepsilon^{1/2}), \\ (h + F_0^2/2h^2 - 1 - \frac{1}{2}F_0^2) + O(\varepsilon), & h > F_0^{2/3} + O(\varepsilon^{1/2}), \end{cases} \tag{3.40}$$

where $\bar{h} = (h - F_0^{2/3})\varepsilon^{-1/2}$ and the depth, h, satisfies the partial differential equation

$$\frac{\partial h}{\partial t} + \lambda_2(h)\frac{\partial h}{\partial x} = 0, \tag{3.41}$$

with $\lambda_2(h)$ given by (3.38). Sketches of $\lambda_2(h)$, $v(h)$ and $\xi(h)$ are given in figure 3. We observe that the $\lambda_2(h)$-characteristic speed is always positive and that the bedform structure $\xi(h)$ is always $O(1)$.

In $F_0 > 1 + O(\varepsilon^{1/2})$:

$$\lambda_2(h) \sim \begin{cases} (-3\sqrt{h}/F_0 + 2/F_0 + 1) + O(\varepsilon), & 0 < h < (\frac{1}{3}(2+F_0))^2 - O(\varepsilon^{1/2}), \\ \dfrac{\varepsilon^{1/2}}{2}\left[\dfrac{-9\hat{h}}{2F_0(2+F_0)} + \left(\dfrac{81\hat{h}^2}{4F_0^2(2+F_0)^2} + \dfrac{4}{3F_0^3}(2+F_0)\right)^{1/2}\right] + O(\varepsilon), & \\ \qquad\qquad h = (\frac{1}{3}(2+F_0))^2 \pm O(\varepsilon^{1/2}), & \\ \dfrac{-2\varepsilon(2+F_0)^6}{F_0^2[(2+F_0)^6 - 3^6h^3]} + O(\varepsilon^2), & h > (\frac{1}{3}(2+F_0))^2 + O(\varepsilon^{1/2}), \end{cases} \tag{3.42}$$

$$v(h) = G(h) \sim \begin{cases} (-2\sqrt{h}/F_0 + 1 + 2/F_0) + O(\varepsilon), & 0 < h < (\frac{1}{3}(2+F_0))^2 - O(\varepsilon^{1/2}), \\ (2+F_0)/3F_0 + O(\varepsilon^{1/2}), & h = (\frac{1}{3}(2+F_0))^2 \pm O(\varepsilon^{1/2}), \\ (2+F_0)^3/27F_0h + O(\varepsilon), & h > (\frac{1}{3}(2+F_0))^2 + O(\varepsilon^{1/2}), \end{cases} \tag{3.43}$$

$$\xi(h) = F(h) \sim \begin{cases} \dfrac{-4\varepsilon}{3F_0}\left[\dfrac{(2+F_0)}{3}\log\left|\dfrac{3\sqrt{h} - 2 - F_0}{1 - F_0}\right| + 2(1 - \sqrt{h})\right] + O(\varepsilon^2), & \\ \qquad\qquad 0 < h < (\frac{1}{3}(2+F_0))^2 - O(\varepsilon^{1/2}), & \\ O(\varepsilon^{1/2}), \qquad h = (\frac{1}{3}(2+F_0)) \pm O(\varepsilon^{1/2}), & \\ h + (2+F_0)^6/2\cdot 3^6h^2 - \frac{3}{2}(\frac{1}{3}(2+F_0))^2 + O(\varepsilon), & \\ \qquad\qquad h > (\frac{1}{3}(2+F_0))^2 + O(\varepsilon^{1/2}), & \end{cases} \tag{3.44}$$

with $\hat{h} = (h - (\frac{1}{3}(2+F_0))^2)\varepsilon^{-1/2}$ and h also satisfying (3.41), where in this case $\lambda_2(h)$ is as given in (3.42). Figure 3 contains the sketches of $\lambda_2(h)$, $v(h)$ and $\xi(h)$ for this region, where again we can see that the characteristics wavespeed is always positive. There is a transition region through $h = (\frac{1}{3}(2+F_0))^2$, where the bedform development evolves from $O(\varepsilon)$ to $O(1)$, when $\lambda_2(h)$ is $O(1)$ and $O(\varepsilon)$ respectively.

We observe that (3.38)–(3.40) continue into (3.42)–(3.44) when $F_0 = 1 \pm O(\varepsilon^{1/2})$. Therefore we have the following.

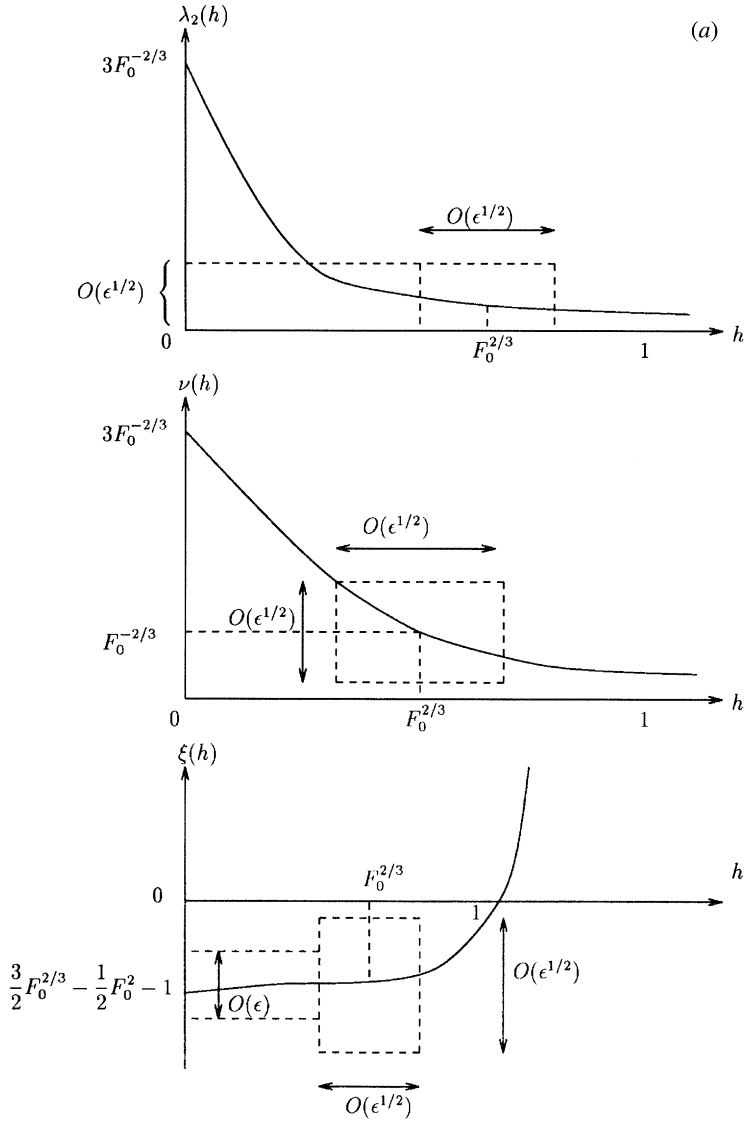

Figure 3. (*a*) Graph of $\lambda_2(h)$, $\nu(h)$, $\xi(h)$ when $F_0 < 1 - O(\varepsilon^{1/2})$.

In $F_0 = 1 \pm 0(\varepsilon^{1/2})$:

$$\lambda_2(h) \sim \begin{cases} 3(1-\sqrt{h}) + O(\varepsilon), & 0 < h < 1 - O(\varepsilon^{1/2}), \\ \frac{1}{2}\varepsilon^{1/2}[-\frac{3}{2}\tilde{h} + (\frac{9}{4}\tilde{h}^2 + 4)^{1/2}] + O(\varepsilon), & h = 1 \pm O(\varepsilon^{1/2}), \\ 2\varepsilon/(h^3 - 1) + O(\varepsilon^2), & h > 1 + O(\varepsilon^{1/2}), \end{cases} \tag{3.45}$$

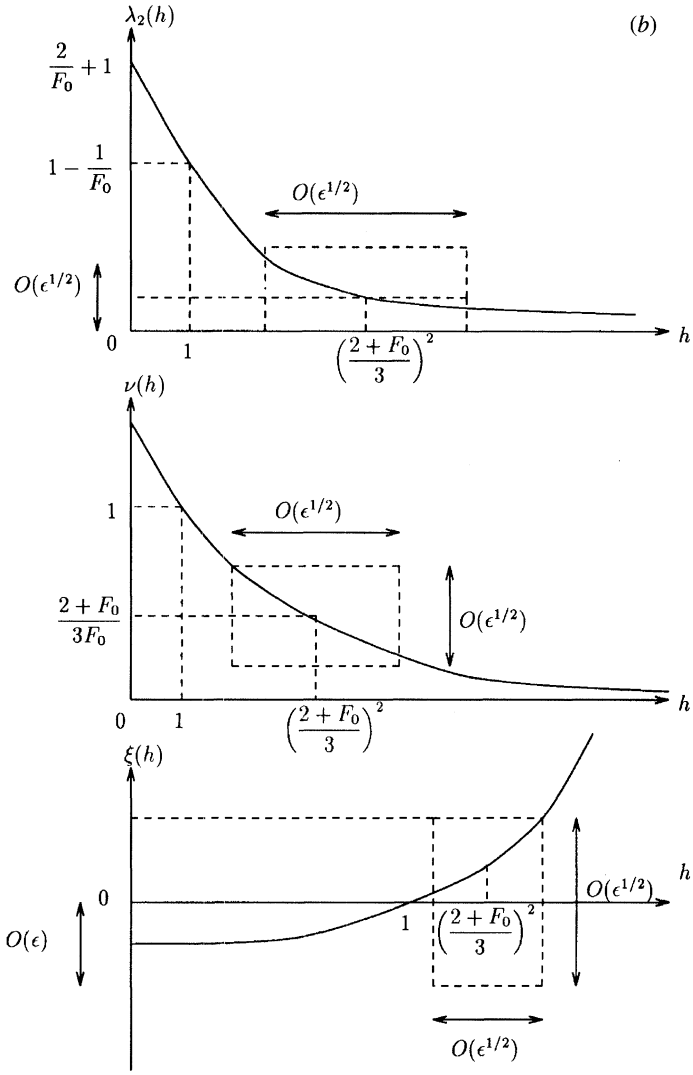

Figure 3. (*b*) Graph of $\lambda_2(h)$, $\nu(h)$, $\xi(h)$ when $F_0 > 1 + O(\varepsilon^{1/2})$ for s_2-simple wave.

$$v(h) = G(h) \sim \begin{cases} (3 - 2\sqrt{h}) + O(\varepsilon), & 0 < h < 1 - O(\varepsilon^{1/2}), \\ 1 - \frac{1}{4}\varepsilon^{1/2}\tilde{h} + O(\varepsilon), & h = 1 \pm O(\varepsilon^{1/2}), \\ 1/h + O(\varepsilon), & h > 1 + O(\varepsilon^{1/2}), \end{cases} \tag{3.46}$$

$$\xi(h) = F(h) \sim \begin{cases} \frac{4}{3}\varepsilon(2(\sqrt{h} - 1) - \log|1 - \sqrt{h}|) + O(\varepsilon), & 0 < h < 1 - O(\varepsilon^{1/2}), \\ O(\varepsilon^{1/2}), & h = 1 \pm O(\varepsilon^{1/2}), \\ (h + 1/2h^2 - \frac{3}{2}) + O(\varepsilon), & h > 1 + O(\varepsilon^{1/2}), \end{cases} \tag{3.47}$$

where $\tilde{h} = (h - 1)\varepsilon^{-1/2}$.

Finally, from (3.35)–(3.37), we find that the s_1-simple wave family is given by the following.

In $F_0 < 1 - O(\varepsilon^{1/2})$:

$$\lambda_1(h) \sim \begin{cases} \dfrac{-2\varepsilon(2+F_0)^6}{F_0^2[(2+F_0)^6 - 3^6h^3]} + O(\varepsilon^2), & 0 < h < (\tfrac{1}{3}(2+F_0))^2 - O(\varepsilon^{1/2}), \\ \dfrac{\varepsilon^{1/2}}{2}\left[\dfrac{-9\hat{h}}{2F_0(2+F_0)} + \left(\dfrac{81\hat{h}^2}{4F_0^2(2+F_0)^2} + \dfrac{4}{3F_0^3}(2+F_0)\right)^{1/2}\right] + O(\varepsilon), & \\ \qquad h = (\tfrac{1}{3}(2+F_0))^2 \pm O(\varepsilon^{1/2}), & \\ (-3\sqrt{h}/F_0 + 2/F_0 + 1) + O(\varepsilon), & \\ \qquad (\tfrac{1}{3}(2+F_0))^2 + O(\varepsilon^{1/2}) < h < (\tfrac{1}{2}(2+F_0))^2, & \end{cases} \tag{3.48}$$

$$v(h) = G(h) \sim \begin{cases} \dfrac{(2+F_0)^3}{27F_0h} + O(\varepsilon), & 0 < h < (\tfrac{1}{3}(2+F_0))^2 - O(\varepsilon^{1/2}), \\ \dfrac{2+F_0}{3F_0} + O(\varepsilon^{1/2}), & h = (\tfrac{1}{3}(2+F_0))^2 \pm O(\varepsilon^{1/2}), \\ (-2\sqrt{h}/F_0 + 1 + 2/F_0) + O(\varepsilon), & \\ \qquad (\tfrac{1}{3}(2+F_0))^2 + O(\varepsilon^{1/2}) < h < (\tfrac{1}{2}(2+F_0))^2, & \end{cases} \tag{3.49}$$

$$\xi(h) = F(h) \sim \begin{cases} h + \dfrac{(2+F_0)^6}{2\cdot 3^6h^2} - \dfrac{3}{2}\left(\dfrac{2+F_0}{3}\right)^2 + O(\varepsilon), & \\ \qquad 0 < h < (\tfrac{1}{3}(2+F_0))^2 - O(\varepsilon^{1/2}), & \\ O(\varepsilon^{1/2}), \qquad h = (\tfrac{1}{3}(2+F_0))^2 \pm O(\varepsilon^{1/2}), & \\ \dfrac{-4\varepsilon}{3F_0}\left[\dfrac{(2+F_0)}{3}\log\left|\dfrac{3\sqrt{h}-2-F_0}{1-F_0}\right| + 2(1-\sqrt{h})\right] + O(\varepsilon^2), & \\ \qquad (\tfrac{1}{3}(2+F_0))^2 + O(\varepsilon^{1/2}) < h < (\tfrac{1}{2}(2+F_0))^2, & \end{cases} \tag{3.50}$$

where $\hat{h} = (h - (\frac{1}{3}(2+F_0))^2)\varepsilon^{-1/2}$ and h satisfies the equation

$$\frac{\partial h}{\partial t} + \lambda_1(h)\frac{\partial h}{\partial x} = 0, \tag{3.51}$$

with $\lambda_1(h)$ as given by (3.48). The $\lambda_1(h)$, $v(h)$ and $\xi(h)$ are illustrated in figure 4. As can be seen from the graphs, the characteristics wavespeed is always negative. There is a transition region around $h \sim (\frac{1}{3}(2+F_0))^2$, after which the bedform has diminished in size from $O(1)$ to $O(\tilde{\varepsilon})$ and, as expected $\lambda_1(h)$ has increased to become $O(1)$.

In $F_0 > 1 + O(\varepsilon^{1/2})$:

$$\lambda_1(h) \sim \begin{cases} \dfrac{-2\varepsilon}{F_0^2 - h^3} + O(\varepsilon^2), & 0 < h < F_0^{2/3} - O(\varepsilon^{1/2}), \\ \dfrac{\varepsilon^{1/2}}{2}\left[\dfrac{-3\bar{h}}{2F_0^{4/3}} + \left(\dfrac{9\bar{h}^2}{4F_0^{8/3}} + \dfrac{4}{F_0^{8/3}}\right)^{1/2}\right] + O(\varepsilon), & h = F_0^{2/3} \pm O(\varepsilon^{1/2}), \\ 3(1/F_0^{2/3} - \sqrt{h}/F_0) + O(\varepsilon), & F_0^{2/3} + O(\varepsilon^{1/2}) < h < \frac{9}{4}F_0^{2/3}, \end{cases} \tag{3.52}$$

$$v(h) = G(h) \sim \begin{cases} 1/h + O(\varepsilon), & 0 < h < F_0^{2/3} - O(\varepsilon^{1/2}), \\ F_0^{-2/3} + O(\varepsilon^{1/2}), & h = F_0^{2/3} \pm O(\varepsilon^{1/2}), \\ (-2\sqrt{h}/F_0 + 3F_0^{-2/3}) + O(\varepsilon), & F_0^{2/3} + O(\varepsilon^{1/2}) < h < \frac{9}{4}F_0^{2/3}, \end{cases} \tag{3.53}$$

$$\xi(h) = F(h) \sim \begin{cases} (h + F_0^2/2h^2 - 1 - \frac{1}{2}F_0^2) + O(\varepsilon), & 0 < h < F_0^{2/3} - O(\varepsilon^{1/2}), \\ (\frac{3}{2}F_0^{2/3} - \frac{1}{2}F_0^2 - 1) + O(\varepsilon^{1/2}), & h = F_0^{2/3} \pm O(\varepsilon^{1/2}), \\ (\frac{3}{2}F_0^{2/3} - \frac{1}{2}F_0^2 - 1) + O(\varepsilon), & F_0^{2/3} + O(\varepsilon^{1/2}) < h < \frac{9}{4}F_0^{2/3}, \end{cases} \tag{3.54}$$

with $\bar{h} = (h - F_0^{2/3})\varepsilon^{-1/2}$ and h satisfying (3.51), where $\lambda_1(h)$ is as given in (3.52). Figure 4 illustrates $\lambda_1(h)$, $v(h)$ and $\xi(h)$ for the region $F_0 > 1 + O(\varepsilon^{1/2})$. The bedform disturbance produced is always $O(1)$, and $\lambda_1(h)$ is, as expected, always negative. Also the forms of $\lambda_1(h)$, $v(h)$ and $\xi(h)$ given by (3.48)–(3.50) and (3.52)–(3.54) are continuous across $F_0 = 1$. Therefore, we have the following.

In $F_0 = 1 \pm O(\varepsilon^{1/2})$:

$$\lambda_1(h) \sim \begin{cases} -2\varepsilon/(1 - h^3) + O(\varepsilon^2), & 0 < h < 1 - O(\varepsilon^{1/2}), \\ \frac{1}{2}\varepsilon^{1/2}[-\frac{3}{2}\tilde{h} + (\frac{9}{4}\tilde{h}^2 + 4)^{1/2}] + O(\varepsilon), & h = 1 \pm O(\varepsilon^{1/2}), \\ 3(1 - \sqrt{h}) + O(\varepsilon), & 1 + O(\varepsilon^{1/2}) < h < \frac{9}{4}, \end{cases} \tag{3.55}$$

$$v(h) = G(h) \sim \begin{cases} 1/h + O(\varepsilon), & 0 < h < 1 - O(\varepsilon^{1/2}), \\ 1 - \frac{1}{4}\varepsilon^{1/2}\tilde{h} + O(\varepsilon), & h = 1 \pm O(\varepsilon^{1/2}), \\ (-2\sqrt{h} + 3) + O(\varepsilon), & 1 + O(\varepsilon^{1/2}) < h < \frac{9}{4}, \end{cases} \tag{3.56}$$

$$\xi(h) = F(h) \sim \begin{cases} (h + 1/2h^2 - \frac{3}{2}) + O(\varepsilon), & 0 < h < 1 - O(\varepsilon^{1/2}), \\ O(\varepsilon^{1/2}), & h = 1 \pm O(\varepsilon^{1/2}), \\ \frac{4}{3}\varepsilon(2(\sqrt{h} - 1) - \log|1 - \sqrt{h}|) + O(\varepsilon^2), & 1 + O(\varepsilon^{1/2}) < h < \frac{9}{4}, \end{cases} \tag{3.57}$$

where $\tilde{h} = (h - 1)\varepsilon^{-1/2}$.

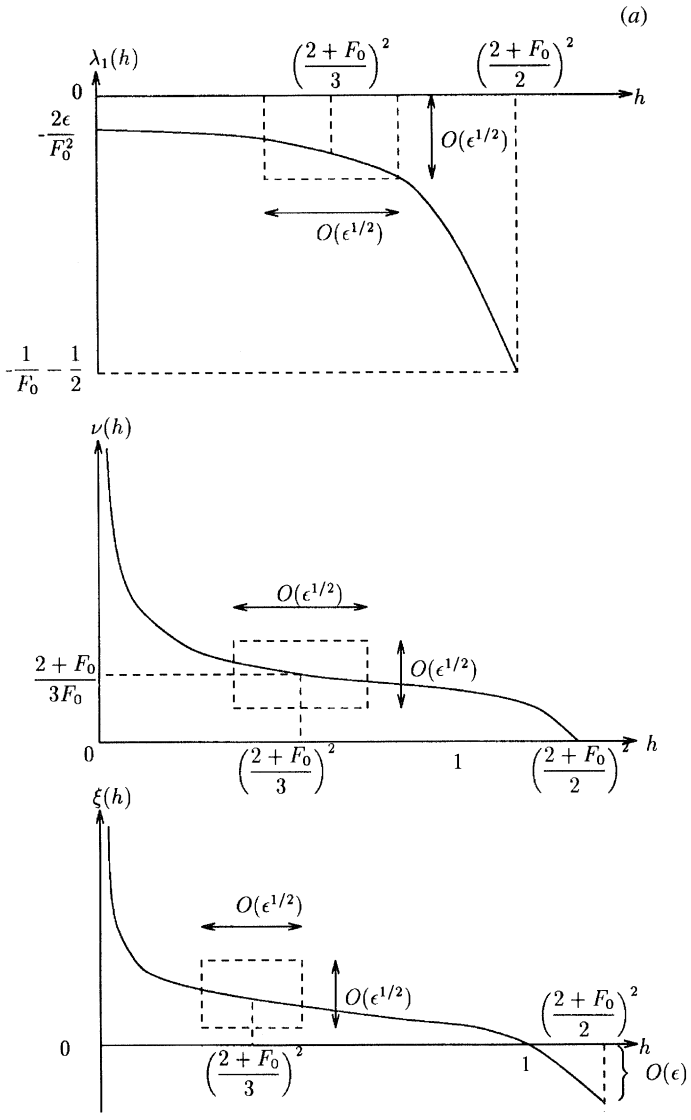

Figure 4. (*a*) Graph of $\lambda_1(h)$, $\nu(h)$, $\xi(h)$ when $F_0 < 1 - O(\varepsilon^{1/2})$.

As noted earlier, we observe that the bedform associated with the s_3-simple wave is only an $O(\varepsilon)$ disturbance, under all conditions. However, under appropriate conditions, both of the s_2- and s_1-simple waves may propagate $O(1)$ bedform disturbances. We now examine these in more detail, beginning with the construction of the three expansion wave solutions.

4. Expansion waves

The expansion wave solutions associated with the hyperbolic system (2.15)–(2.17) are those simple wave solutions to (2.15)–(2.17) which remain continuous for all

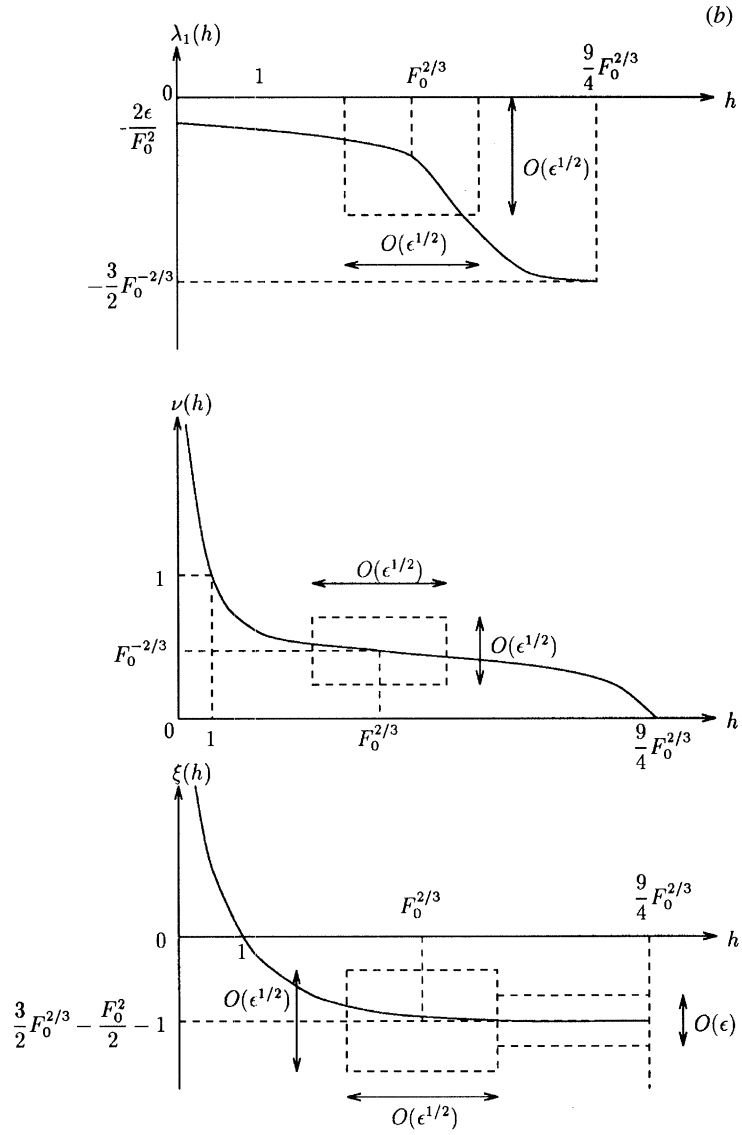

Figure 4. (*b*) Graph of $\lambda_1(h)$, $\nu(h)$, $\xi(h)$ when $F_0 > 1 + O(\varepsilon^{1/2})$ for s_1-simple wave.

$t > 0$, and satisfy the initial conditions,

$$\left.\begin{aligned} h(x,0) &= \begin{cases} H, & x < 0, \\ 1, & x \geqslant 0, \end{cases} \equiv h_0(x), \\ v(x,0) &= G(h_0(x)), \qquad -\infty < x < \infty, \\ \xi(x,0) &= F(h_0(x)), \end{aligned}\right\} \tag{4.1}$$

with $F(\cdot)$, $G(\cdot)$ as defined in § 3, and $H > 0$ being the depth at the rear of the expansion wave. In general there will be three distinct expansion waves associated with each of the s_1-, s_2-, s_3-simple wave families.

An expansion wave in the s_i-simple wave family is a solution of equations,

$$\frac{\partial h}{\partial t} + \lambda_i(h)\frac{\partial h}{\partial x} = 0, \qquad -\infty < x < \infty, \quad t > 0, \tag{4.2a}$$

$$v = G(h), \qquad \xi = F(h), \tag{4.2b}$$

subject to initial conditions (4.1). For the solution to remain continuous, we require, from (4.2 *a*), that

$$\lambda_i(H) < \lambda_i(1). \tag{4.3}$$

The corresponding expansion wave then has the similarity form,

$$h(x,t) = \begin{cases} 1, & x \geqslant \lambda_i(1)t, \\ \chi(x/t), & \lambda_i(H)t \leqslant x < \lambda_i(1)t, \\ H, & x \leqslant \lambda_i(H)t, \end{cases} \tag{4.4}$$

where $\chi(\cdot)$ is the inverse function of $\lambda_i(h)$ for $m \leqslant h \leqslant M$, with $m = \min(1, H)$ and $M = \max(1, H)$.

We can now give the details of the expansion wave solutions e_1, e_2 and e_3 associated with the simple wave families s_1, s_2 and s_3 respectively.

(*a*) *The e_3-expansion wave solution*

Along the λ_3-characteristic, we have via (3.28) and (3.31) that

$$\frac{\partial h}{\partial t} + \left(1 + \frac{3\sqrt{h}}{F_0} - \frac{2}{F_0}\right)\frac{\partial h}{\partial x} = 0 \tag{4.5}$$

at leading order as $\varepsilon \to 0$, uniformly in $h > 0$. Since $\lambda_3(h)$ is a monotone increasing function of h (see figure 2), we then require $H < 1$ for an expansion wave solution to exist, via (4.3). In addition we also require, for admissibility that

$$H > \tfrac{1}{4}H^*(2 - F_0)(2 - F_0)^2.$$

Therefore, an expansion wave exists for each H in the range,

$$\tfrac{1}{4}H^*(2 - F_0)(2 - F_0)^2 < H < 1, \tag{4.6}$$

after which its details are obtained from (3.28) and (4.4) as

$$h_e(x,t) \sim \begin{cases} 1, & x \geqslant (1 + 1/F_0)t, \\ \dfrac{1}{9}\left(2 - F_0 + \left(\dfrac{x}{t}F_0\right)\right)^2, & \left(1 + \dfrac{3\sqrt{H}}{F_0} - \dfrac{2}{F_0}\right)t \leqslant x \leqslant \left(1 + \dfrac{1}{F_0}\right)t, \\ H, & x \leqslant (1 + 3\sqrt{H}/F_0 - 2/F_0)t. \end{cases} \tag{4.7}$$

as $\varepsilon \to 0$ uniformly in H, F_0.

After substitution of (4.7) into (3.29) and (3.30), we find that the e_3-expansion

wave solution is given by (4.7) and

$$\xi_e(x,t) \sim \begin{cases} \dfrac{4\varepsilon}{3F_0}\left(\tfrac{1}{3}(2-F_0)\log\left|\dfrac{3\sqrt{H}-2+F_0}{F_0+1}\right| + 2(1-\sqrt{H})\right), \\ \qquad x \leqslant \left(1+\dfrac{3\sqrt{H}}{F_0}-\dfrac{2}{F_0}\right)t, \\ \dfrac{4\varepsilon}{3F_0}\left(\tfrac{1}{3}(2-F_0)\log\left|\dfrac{(x/t)F_0}{F_0+1}\right| + 2(1+F_0-(x/t)F_0)\right), \\ \qquad \left(1+\dfrac{3\sqrt{H}}{F_0}-\dfrac{2}{F_0}\right)t \leqslant x \leqslant \left(1+\dfrac{1}{F_0}\right)t, \\ 0, \qquad x \geqslant (1+1/F_0)t, \end{cases} \tag{4.8}$$

$$v_e(x,t) \sim \begin{cases} 1-\dfrac{2}{F_0}+\dfrac{2\sqrt{H}}{F_0}, & x \leqslant \left(1+\dfrac{3\sqrt{H}}{F_0}-\dfrac{2}{F_0}\right)t, \\ \dfrac{1}{3}-\dfrac{2}{3F_0}+\dfrac{2}{3}\dfrac{x}{t}, & \left(1+\dfrac{3\sqrt{H}}{F_0}-\dfrac{2}{F_0}\right)t \leqslant x \leqslant \left(1+\dfrac{1}{F_0}\right)t, \\ 1, & x \geqslant (1+1/F_0)t. \end{cases} \tag{4.9}$$

The free surface (given by $\eta = h - \xi$) and bedform profiles are given in figure 5, along with a graph of the fluid velocity. As can be seen from the graphs, whereas $-\xi_e$ is monotone increasing with x, the free surface is monotone decreasing. The bedform never attains an $O(1)$ structure, always being of $O(\varepsilon)$, and as expected, the e_3-expansion wave solution does not play a significant role in bedform evolution. From the graph of the fluid velocity (related to the sediment flux via (2.13)), we also observe that there is a reduction in the upstream transport of bedload sediment for this expansion wave solution.

(*b*) *The e_2-expansion wave solution*

For the e_2-expansion wave, the form of $\lambda_2(h)$ suggests that we consider the cases $F_0 < 1 - O(\varepsilon^{1/2})$ and $F_0 > 1 + O(\varepsilon^{1/2})$ separately. However, since the s_2-simple wave family is continuous across $F_0 \sim 1$, the expansion wave solution will also be continuous across this region, and the case $F_0 = 1 \pm O(\varepsilon^{1/2})$ follows directly.

(i) *In $F_0 < 1 - O(\varepsilon^{1/2})$*

Along the λ_2-characteristic we have, via (3.38) and (3.41), that

$$\left.\begin{array}{ll} \dfrac{\partial h}{\partial t} + 3\left(F_0^{-2/3} - \dfrac{\sqrt{h}}{F_0}\right)\dfrac{\partial h}{\partial x}, & 0 < h < F_0^{2/3} - O(\varepsilon^{1/2}), \\ \dfrac{\partial h}{\partial t} + \tfrac{1}{2}\varepsilon^{1/2}\{-\tfrac{3}{2}F_0^{-4/3}\bar{h} + (\tfrac{9}{4}F_0^{8/3}\bar{h}^2 + 4F_0^{-8/3})^{1/2}\}\dfrac{\partial h}{\partial x}, & \\ & h = F_0^{2/3} \pm O(\varepsilon^{1/2}), \\ \dfrac{\partial h}{\partial t} - \dfrac{2\varepsilon}{F_0^2 - h^3}\dfrac{\partial h}{\partial x}, & h > F_0^{2/3} + O(\varepsilon^{1/2}), \end{array}\right\} = 0, \tag{4.10}$$

at leading order as $\varepsilon \to 0$, uniformly in $h > 0$. Since $\lambda_2(h)$ is a monotone decreasing function of h (see figure 3*a*), we then require $H > 1$ for an expansion wave solution

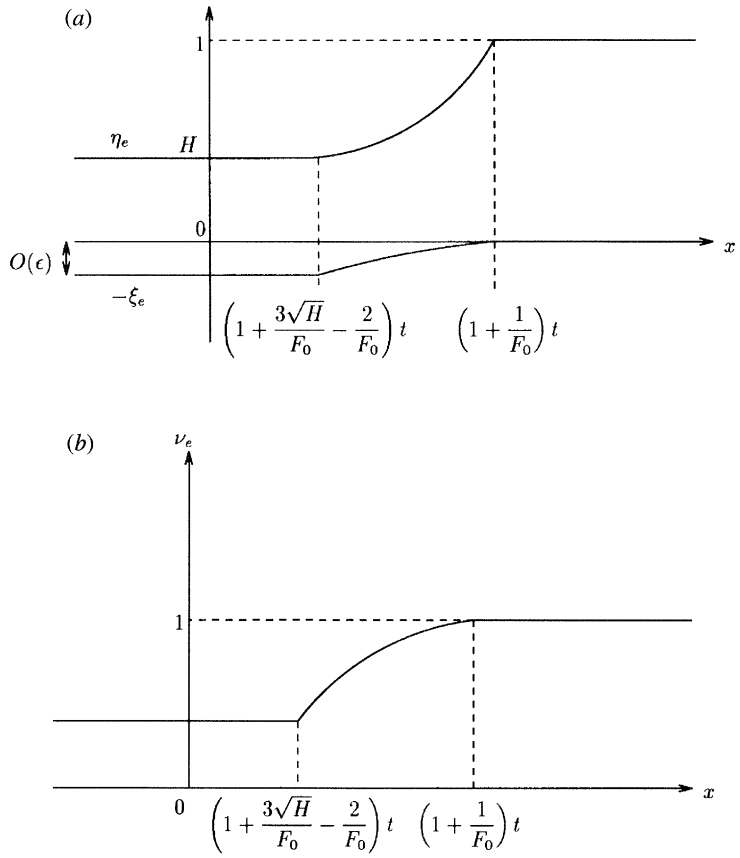

Figure 5. (*a*) The e_3-expansion wave profiles. (*b*) The corresponding fluid velocity profile.

to exist, via (4.3), while admissibility requires only that $H > 0$. Thus, in this case, an expansion wave exists for each H in the range,

$$H > 1. \tag{4.11}$$

To obtain the details of the expansion wave, we first note that in this case $h = 1$ lies in the region $h > F_0^{2/3} + O(\varepsilon^{1/2})$ as does $h = H$, via (4.11). Hence we have from (3.38) that

$$\lambda_2(1) \sim \frac{2\varepsilon}{(1-F_0^2)} > 0, \qquad \lambda_2(H) \sim \frac{2\varepsilon}{(H^3-F_0^2)} > 0. \tag{4.12}$$

Therefore, using (3.42) and (4.4), we arrive at

$$h_e(x,t) \sim \begin{cases} 1, & x \geqslant \dfrac{2\varepsilon t}{1-F_0^2}, \\ \left(F_0^2 + \dfrac{2\varepsilon t}{x}\right)^{1/3}, & \dfrac{2\varepsilon t}{H^3-F_0^2} \leqslant x \leqslant \dfrac{2\varepsilon t}{1-F_0^2}, \\ H, & x \leqslant \dfrac{2\varepsilon t}{H^3-F_0^2} \end{cases} \tag{4.13}$$

as $\varepsilon \to 0$ uniformly in H, F_0.

On substitution of (4.13) into the appropriate forms for the fluid velocity and bedform in the domain $h > F_0^{2/3} + O(\varepsilon^{1/2})$, given in (3.39)–(3.40), we obtain the remaining details for the e_2-expansion wave as

$$\xi_e(x,t) \sim \begin{cases} H + \dfrac{F_0^2}{2H^2} - 1 - \dfrac{F_0^2}{2}, & x \leqslant \dfrac{2\varepsilon t}{H^3 - F_0^2}, \\ \left(F_0^2 + \dfrac{2\varepsilon t}{x}\right)^{-2/3} \left(\frac{3}{2}F_0^2 + \dfrac{2\varepsilon t}{x} - \frac{1}{2}(2+F_0^2)\left(F_0^2 + \dfrac{2\varepsilon t}{x}\right)^{2/3}\right), & \dfrac{2\varepsilon t}{H^3 - F_0^2} \leqslant x \leqslant \dfrac{2\varepsilon t}{1 - F_0^2}, \\ 0, & x < \dfrac{2\varepsilon t}{1 - F_0^2}, \end{cases} \tag{4.14}$$

$$v_e(x,t) \sim \begin{cases} \dfrac{1}{H}, & x \leqslant \dfrac{2\varepsilon t}{H^3 - F_0^2}, \\ \left(F_0^2 + \dfrac{2\varepsilon t}{x}\right)^{-1/3}, & \dfrac{2\varepsilon t}{H^3 - F_0^2} \leqslant x \leqslant \dfrac{2\varepsilon t}{1 - F_0^2}, \\ 1, & x \geqslant \dfrac{2\varepsilon t}{1 - F_0^2}. \end{cases} \tag{4.15}$$

It should be noted that in this case there is a constant fluid flux, $Q_e = h_e v_e$ throughout the expansion wave. The free surface, bedform and velocity profiles are given in figure 6. Again, it can be seen that there is a reduction in the upstream sediment flux and the bedform structure is of $O(1)$ throughout. A significant bedform disturbance is carried in this expansion wave.

(ii) *In* $F_0 > 1 + O(\varepsilon^{1/2})$

Along the λ_2-characteristic we have, via (3.41) and (3.42), that

$$\left.\begin{array}{ll} \dfrac{\partial h}{\partial t} + \left(1 + \dfrac{2 - 3\sqrt{h}}{F_0}\right)\dfrac{\partial h}{\partial x}, & 0 < h < (\frac{1}{3}(2+F_0))^2 - O(\varepsilon^{1/2}), \\ \dfrac{\partial h}{\partial t} + \dfrac{\varepsilon^{1/2}}{2}\left\{\dfrac{-9\hat{h}}{2F_0(2+F_0)} + \left(\dfrac{81\hat{h}^2}{4F_0^2(2+F_0)^2} + \dfrac{4}{3F_0^3}(2+F_0)\right)^{1/2}\right\}\dfrac{\partial h}{\partial x}, & \\ \qquad h = (\frac{1}{3}(2+F_0))^2 \pm O(\varepsilon^{1/2}), & \\ \dfrac{\partial h}{\partial t} - \dfrac{2\varepsilon(2+F_0)^6}{F_0^2[(2+F_0)^6 - (9h)^3]}\dfrac{\partial h}{\partial x}, & h > (\frac{1}{3}(2+F_0))^2 + O(\varepsilon^{1/2}), \end{array}\right\} = 0, \tag{4.16}$$

with $\hat{h} = (h - (\frac{1}{3}(2+F_0))^2)\varepsilon^{-1/2}$, at leading order as $\varepsilon \to 0$, uniformly in $h > 0$. Again $\lambda_2(h)$ is a monotone decreasing function of h (see figure 3*b*), and we require $H > 1$ for an expansion wave solution to exist, via (4.3), while admissibility requires only that $H > 0$. In this case we again have that an expansion wave exists for each

$$H > 1. \tag{4.17}$$

To obtain the details of the expansion waves, we first observe that in this case $h = 1$ lies in the interval $0 < h < (\frac{1}{3}(2+F_0))^2 - O(\varepsilon^{1/2})$. Hence, from (3.42), we have

$$\lambda_2(1) \sim 1 - 1/F_0. \tag{4.18}$$

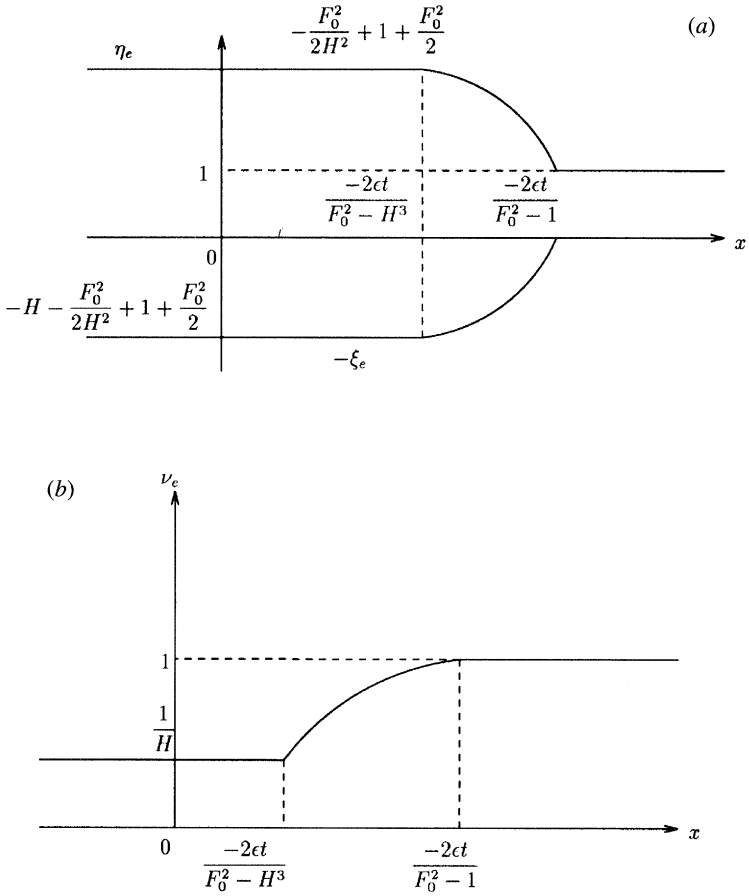

Figure 6. $F_0 < 1 - O(\varepsilon^{1/2})$. (*a*) The e_2-expansion wave profiles. (*b*) The corresponding fluid velocity profile.

In addition, at $h = H$, we find that

$$\lambda_2(H) \sim \begin{cases} 1 + (2 - 3\sqrt{H})/F_0, & 1 < H < (\frac{1}{3}(2+F_0))^2 - O(\varepsilon^{1/2}), \\ O(\varepsilon^{1/2}), & H = (\frac{1}{3}(2+F_0))^2 \pm O(\varepsilon^{1/2}), \\ \dfrac{2\varepsilon(2+F_0)^6}{F_0^2((9H)^3 - (2+F_0)^6)}, & H > (\frac{1}{3}(2+F_0))^2 + O(\varepsilon^{1/2}), \end{cases} \tag{4.19}$$

via (3.42). Clearly the structure of the expansion wave depends upon whether $H < (\frac{1}{3}(2+F_0))^2 - O(\varepsilon^{1/2})$ or $H > (\frac{1}{3}(2+F_0))^2 + O(\varepsilon^{1/2})$.

We consider first the case when $1 < H < (\frac{1}{3}(2+F_0))^2 - O(\varepsilon^{1/2})$. On using (3.42) and (4.4) we obtain the expansion wave as

$$h_e(x,t) \sim \begin{cases} H, & x \leqslant (1 + (2 - 3\sqrt{H})/F_0)t, \\ \frac{1}{9}(2 + F_0 - (x/t)F_0)^2, & (1 + (2 - 3\sqrt{H})/F_0)t \leqslant x \leqslant (1 - 1/F_0)t, \\ 1, & x \geqslant (1 - 1/F_0)t, \end{cases} \tag{4.20}$$

$$\xi_e(x,t) \sim \begin{cases} \dfrac{-4\varepsilon}{9F_0}\left\{(2+F_0)\log\left|\dfrac{3\sqrt{H}-2-F_0}{1-F_0}\right|+6(1-\sqrt{H})\right\}, \\ \qquad x \leqslant (1+(2-3\sqrt{H})/F_0)t, \\ \dfrac{-4\varepsilon}{9F_0}\left\{(2+F_0)\log\left|\dfrac{(x/t)F_0}{F_0-1}\right|+2\left(1-F_0+\dfrac{x}{t}F_0\right)\right\}, \\ \qquad (1+(2-3\sqrt{H})/F_0)t \leqslant x \leqslant (1-1/F_0)t, \\ 0, \qquad x \geqslant (1-1/F_0)t, \end{cases} \tag{4.21}$$

$$v_e(x,t) \sim \begin{cases} 1+(2-2\sqrt{H})/F_0, & x \leqslant (1+(2-3\sqrt{H})/F_0)t, \\ \dfrac{1}{3}\left(1+\dfrac{2}{F_0}+\dfrac{2x}{t}\right), & \left(1+\dfrac{2-3\sqrt{H}}{F_0}\right)t \leqslant x \leqslant \left(1-\dfrac{1}{F_0}\right)t, \\ 1, & x \geqslant (1-1/F_0)t. \end{cases} \tag{4.22}$$

From the above, it can be seen that the wave never carries an $O(1)$ bedform. However, it should be noted that there is still a reduction in upstream sediment transport, q, and there is also a decrease in the fluid flux. The η, $-\xi$ and v profiles are illustrated in figure 7.

We now consider the situation when $H > (\frac{1}{3}(2+F_0))^2 + O(\varepsilon^{1/2})$. In this case, via (3.42), there are three distinct regions in the structure of the expansion wave.

For $1 \leqslant h \leqslant (\frac{1}{3}(2+F_0))^2 - O(\varepsilon^{1/2})$, the propagation speed is $O(1)$. However, this drops to $O(\varepsilon^{1/2})$ when

$$(\tfrac{1}{3}(2+F_0))^2 - O(\varepsilon^{1/2}) < h < (\tfrac{1}{3}(2+F_0))^2 + O(\varepsilon^{1/2})$$

and finally the propagation speed becomes $O(\varepsilon)$ when $(\frac{1}{3}(2+F_0))^2 + O(\varepsilon^{1/2}) < h \leqslant H$. It is convenient to define transition points associated with the above structure changes in the expansion wave. We denote these by $x = x_L^c(t)$ and $x = x_R^c(t)$, where $x_{L,R}^c(t)$ are defined implicitly by

$$h_e(x_L^c,t) = (\tfrac{1}{3}(2+F_0))^2 + \varepsilon^{1/2}, \qquad h_e(x_R^c,t) = (\tfrac{1}{3}(2+F_0))^2 - \varepsilon^{1/2}.$$

On using (3.42), we obtain estimates as

$$x_L^c(t) \sim \frac{2(2+F_0)^6}{27}\varepsilon^{1/2}t, \qquad x_R^c(t) \sim \frac{9}{2F_0(2+F_0)}\varepsilon^{1/2}t. \tag{4.23}$$

We can now use (3.42) and (4.4) to construct the expansion wave as

$$h_e(x,t) \sim \begin{cases} H, & x \leqslant \lambda_2(H)t, \\ \left[\dfrac{(2+F_0)^6\{2\varepsilon+(x/t)F_0^2\}}{(27F_0)^2 x/t}\right]^{1/3}, & \lambda_2(H)t \leqslant x \leqslant x_L^c, \\ O(1), & x_L^c \leqslant x \leqslant x_R^c, \\ \frac{1}{9}(2+F_0-(x/t)F_0)^2, & x_R^c \leqslant x \leqslant \lambda_2(1)t, \\ 1, & x \geqslant \lambda_2(1)t, \end{cases} \tag{4.24}$$

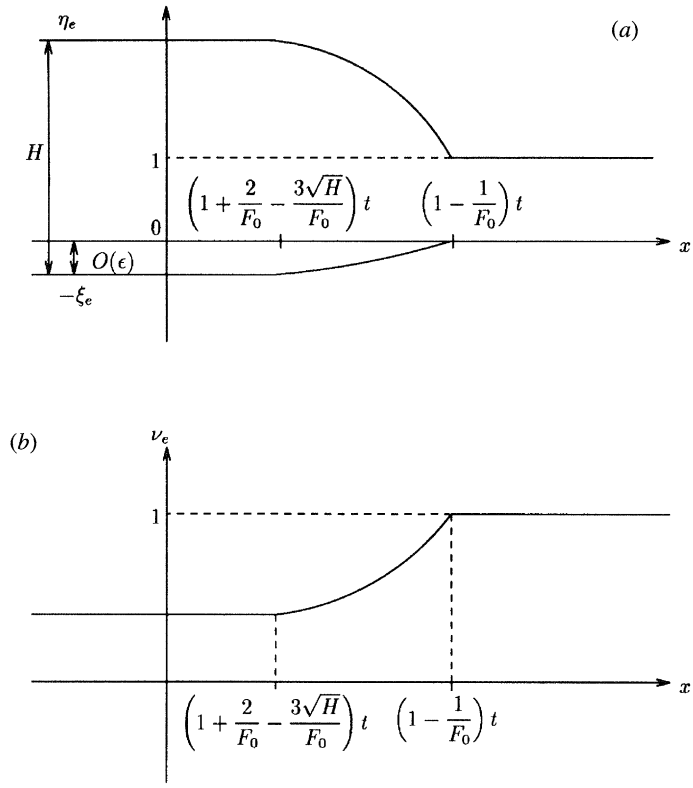

Figure 7. $F_0 > 1 + O(\varepsilon^{1/2})$, $H < (\frac{1}{3}(2+F_0))^2 - O(\varepsilon^{1/2})$. (*a*) The e_2-expansion wave profiles. (*b*) The corresponding fluid velocity profile.

$$\xi_e(x,t) \sim \begin{cases} H + \dfrac{(2+F_0)^6}{2\cdot 3^6 H^2} - \dfrac{3}{2}\left(\dfrac{2+F_0}{3}\right)^2, & x \leqslant \lambda_2(H)t, \\ \left[\dfrac{(2+F_0)^6(2\varepsilon+(x/t)F_0^2)}{(27F_0)^2 x/t}\right]^{1/3} \\ \quad + \dfrac{(2+F_0)^6((x/t)F_0^2)^{1/3}}{18((2+F_0)^5[2\varepsilon+(x/t)F_0^2])^{1/3}} - \dfrac{3}{2}\left(\dfrac{2+F_0}{3}\right)^2, \\ \qquad \lambda_2(H)t \leqslant x \leqslant x_L^c, \\ O(\varepsilon^{1/2}), \qquad x_L^c \leqslant x \leqslant x_R^c, \\ \dfrac{-4\varepsilon}{9F_0}\left\{(2+F_0)\log\left|\dfrac{(x/t)F_0}{F_0-1}\right| + 2\left(1-F_0+\dfrac{x}{t}F_0\right)\right\}, \\ \qquad x_R^c \leqslant x \leqslant \lambda_2(1)t, \\ 0, \qquad x \geqslant \lambda_2(1)t, \end{cases} \tag{4.25}$$

$$v_e(x,t) \sim \begin{cases} \dfrac{(2+F_0)^3}{27F_0H}, & x \leqslant \lambda_2(H)t, \\ \dfrac{(2+F_0)^3}{27F_0}\left[\dfrac{(27F_0^2)^2 x/t}{(2+F_0)^6\{2\varepsilon+(x/t)F_0^2\}}\right]^{1/3}, & \lambda_2(H)t \leqslant x \leqslant x_L^c, \\ O(1), & x_L^c \leqslant x \leqslant x_R^c, \\ \frac{1}{3}(1+2/F_0+2x/t), & x_R^c \leqslant x \leqslant \lambda_2(1)t, \\ 1, & x \geqslant \lambda_2(1)t, \end{cases} \tag{4.26}$$

where

$$\lambda_2(H) = \frac{-2\varepsilon(2+F_0)^6}{F_0^2[(2+F_0)^6-(9H)^3]}$$

and $\lambda_2(1) = (1-1//F_0)$, with x_R^c and x_L^c as given by (4.23). The case when $H \sim (\frac{1}{3}(2+F_0))^2 \pm O(\varepsilon^{1/2})$ can be treated in a similar manner. No new features arise and so the details are not pursued here.

We observe that there is still a decrease in fluid flux and reduction in upstream sediment transport. With $H > (\frac{1}{3}(2+F_0))^2 + O(\varepsilon^{1/2})$, an $O(1)$ bedform is present, while for $1 < H < (\frac{1}{3}(2+F_0))^2 - O(\varepsilon^{1/2})$, the bedform is uniformly of $O(\varepsilon)$. The profiles for η, $-\xi$ and v are given in figure 8.

(*c*) *The e_1-expansion wave solution*

As in the previous section, we shall consider the solution for the e_1-expansion wave in both the regions $0 < F_0 < 1 - O(\varepsilon^{1/2})$ and $F_0 > 1 + O(\varepsilon^{1/2})$ due to the complicated structure of the s_1-simple wave family. Again, since the s_1-simple wave family is continuous across $F_0 \sim 1$, it follows that the e_1-expansion wave solution will also be continuous across this region, and the region $F_0 \sim 1 \pm O(\varepsilon^{1/2})$ need not be considered independently.

(i) $F_0 < 1 - O(\varepsilon^{1/2})$

Along the λ_1-characteristic we have, via (3.48) and (3.51), that

$$\left.\begin{aligned} &\frac{\partial h}{\partial t} - \frac{2\varepsilon(2+F_0)^6}{F_0^2[(2+F_0)^6-(9h)^3]}\frac{\partial h}{\partial x}, && 0 < h < (\tfrac{1}{3}(2+F_0))^2 - O(\varepsilon^{1/2}), \\ &\frac{\partial h}{\partial t} + \frac{\varepsilon^{1/2}}{2}\left\{\frac{-9\hat{h}}{2F_0(2+F_0)} + \left(\frac{81\hat{h}^2}{4F_0^2(2+F_0)^2} + \frac{4}{3F_0^3}(2+F_0)\right)^{1/2}\right\}\frac{\partial h}{\partial x}, \\ &\qquad\qquad h = (\tfrac{1}{3}(2+F_0))^2 \pm O(\varepsilon^{1/2}), \\ &\frac{\partial h}{\partial t} + \left(1 + \frac{2-3\sqrt{h}}{F_0}\right)\frac{\partial h}{\partial x}, && (\tfrac{1}{3}(2+F_0))^2 + O(\varepsilon^{1/2}) < h < (\tfrac{1}{2}(2+F_0))^2, \end{aligned}\right\} = 0 \tag{4.27}$$

to leading order as $\varepsilon \to 0$, uniformly in $h > 0$, with $\hat{h} = [h - \frac{1}{9}(2+F_0)^2]\varepsilon^{-1/2}$. Since $\lambda_1(h)$ is a monotone decreasing function of h (see figure 4*a*), we then require $H > 1$ for an expansion wave solution to exist, via (4.3), while admissibility requires that $H < \frac{1}{4}(2+F_0)^2$. Thus, in this case, an expansion wave exists for each H in the range,

$$1 < H < (\tfrac{1}{2}(2+F_0))^2. \tag{4.28}$$

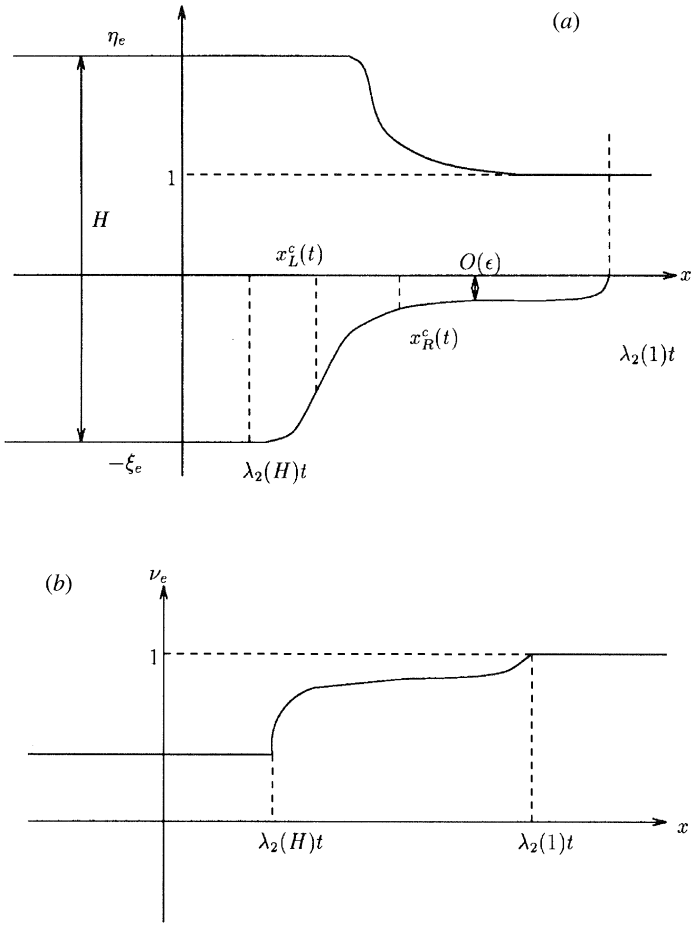

Figure 8. $F_0 > 1 + O(\varepsilon^{1/2})$, $H > (\frac{1}{3}(2+F_0))^2 + O(\varepsilon^{1/2})$. (*a*) The e_2-expansion wave profiles. (*b*) The corresponding fluid velocity profile.

To obtain details of the expansion wave, we first note that in this case $h = 1$ lies in the region $h > \frac{1}{9}(2+F_0)^2 + O(\varepsilon^{1/2})$, as does $h = H$, via (4.28). Therefore we have from (3.48) that

$$\lambda_1(1) \sim 1 - \frac{1}{F_0} < 0, \qquad \lambda_1(H) \sim 1 + \frac{2 - 3\sqrt{H}}{F_0} < 0. \tag{4.29}$$

Therefore, using (3.52) and (4.4), we arrive at

$$h_e(x,t) \sim \begin{cases} H, & x \leqslant \left(1 + \dfrac{2-3\sqrt{H}}{F_0}\right)t, \\ \dfrac{1}{9}\left(2 + F_0 - \dfrac{x}{t}F_0\right)^2, & \left(1 + \dfrac{2-3\sqrt{H}}{F_0}\right)t \leqslant x \leqslant \left(1 - \dfrac{1}{F_0}\right)t, \\ 1, & x \geqslant \left(1 - \dfrac{1}{F_0}\right)t, \end{cases} \tag{4.30}$$

as $\varepsilon \to 0$ uniformly in H, F_0. On substitution of (4.30) into the appropriate forms for the fluid velocity and bedform in the domain $h > \frac{1}{9}(2+F_0)^2 + O(\varepsilon^{1/2})$, given in

(3.49) and (3.50), we obtain the remaining details of the e_1-expansion wave as

$$\xi_e(x,t) \sim \begin{cases} \dfrac{-4\varepsilon}{9F_0}\left\{(2+F_0)\log\left|\dfrac{3\sqrt{H}-2-F_0}{1-F_0}\right|+6(1-\sqrt{H})\right\}, \\ \qquad x \leqslant (1+(2-3\sqrt{H})/F_0)t, \\ \dfrac{-4\varepsilon}{9F_0}\left\{(2+F_0)\log\left|\dfrac{(x/t)F_0}{F_0-1}\right|+2(1-F_0+(x/t)F_0)\right\}, \\ \qquad (1+(2-3\sqrt{H})/F_0)t \leqslant x \leqslant (1-1/F_0)t, \\ 0, \qquad x \geqslant (1-1/F_0)t, \end{cases} \tag{4.31}$$

$$v_e(x,t) \sim \begin{cases} 1+(2-2\sqrt{H})/F_0, & x \leqslant (1+(2-3\sqrt{H})/F_0)t, \\ \dfrac{1}{3}\left(1+\dfrac{2}{F_0}+\dfrac{2x}{t}\right), & \left(1+\dfrac{2-3\sqrt{H}}{F_0}\right)t \leqslant x \leqslant \left(1-\dfrac{1}{F_0}\right)t, \\ 1, & x \geqslant (1-1/F_0). \end{cases} \tag{4.32}$$

We note the similarity in the profiles with those associated with the e_1-expansion wave as given in figure 7*a*. It is clear in this case that the bedform is always of $O(\varepsilon)$, and this solution is insignificant in sediment transport problems. However, note that a reduction in the upstream sediment flux is again required in this expansion wave.

(ii) $F_0 > 1 + O(\varepsilon^{1/2})$

Along the λ_1-characteristic we now have, from (3.51) and (3.52) that

$$\left.\begin{array}{ll} \dfrac{\partial h}{\partial t} - \dfrac{2\varepsilon}{F_0^2-h^3}\dfrac{\partial h}{\partial x}, & 0 < h < F_0^{2/3} - O(\varepsilon^{1/2}), \\ \dfrac{\partial h}{\partial t} + \frac{1}{2}\varepsilon^{1/2}\{-\frac{3}{2}F_0^{-4/3}\bar{h} + (\frac{9}{4}F_0^{-8/3}\bar{h}^2 + 4F_0^{-8/3})^{1/2}\}\dfrac{\partial h}{\partial x}, & \\ & h = F_0^{2/3} \pm O(\varepsilon^{1/2}), \\ \dfrac{\partial h}{\partial t} + 3(F_0^{-2/3} - \sqrt{h}/F_0)\dfrac{\partial h}{\partial x}, & F_0^{2/3} + O(\varepsilon^{1/2}) < h < \frac{9}{4}F_0^{2/3}, \end{array}\right\} = 0 \tag{4.33}$$

at leading order as $\varepsilon \to 0$, uniformly in $h > 0$, with $\bar{h} = (h - F_0^{2/3})\varepsilon^{-1/2}$. As before, $\lambda_1(h)$ is a monotone decreasing function of h (see figure 4*b*) and we require $H > 1$ for an expansion wave solution to exist, via (4.3), while admissibility requires that $H < \frac{9}{4}F_0^{2/3}$. The condition for the existence of an expansion wave, in this case, is thus

$$1 < H < \tfrac{9}{4}F_0^{2/3}. \tag{4.34}$$

To obtain the details of the expansion wave, we first observe that, in this case, $h = 1$ lies in the interval $0 < h < F_0^{2/3} - O(\varepsilon^{1/2})$. Hence, from (3.52) we have

$$\lambda_1(1) \sim \frac{-2\varepsilon}{F_0^2 - 1} \tag{4.35}$$

while, at $h = H$, we find that

$$\lambda_1(H) \sim \begin{cases} -2\varepsilon/(F_0^2 - H^3), & 0 < H < F_0^{2/3} - O(\varepsilon^{1/2}), \\ O(\varepsilon^{1/2}), & H = F_0^{2/3} \pm O(\varepsilon^{1/2}), \\ 3(F_0^{-2/3} - \sqrt{H}/F_0), & F_0^{2/3} + O(\varepsilon^{1/2}) < H < \frac{9}{4}F_0^{2/3}, \end{cases} \tag{4.36}$$

via (3.52). It is clear from (4.36) that the structure of the expansion wave depends upon whether $H < F_0^{2/3} - O(\varepsilon^{1/2})$, or $H > F_0^{2/3} + O(\varepsilon^{1/2})$.

We begin with the case when $1 < H < F_0^{2/3} - O(\varepsilon^{1/2})$. On using (3.52) and (4.4) we obtain the expansion wave as

$$h_e(x,t) \sim \begin{cases} H, & x \leqslant \dfrac{-2\varepsilon t}{F_0^2 - H^3}, \\ \left(F_0^2 + \dfrac{2\varepsilon t}{x}\right)^{1/3}, & \dfrac{-2\varepsilon t}{F_0^2 - H^3} \leqslant x \leqslant \dfrac{-2\varepsilon t}{F_0^2 - 1}, \\ 1, & x \geqslant \dfrac{-2\varepsilon t}{F_0^2 - 1}, \end{cases} \tag{4.37}$$

$$\xi_e(x,t) \sim \begin{cases} H + \dfrac{F_0^2}{2H^2} - 1 - \frac{1}{2}F_0^2, & x \leqslant \dfrac{2\varepsilon t}{H^3 - F_0^2}, \\ \left(F_0^2 + \dfrac{2\varepsilon t}{x}\right)^{-2/3}\left(\dfrac{3F_0^2}{2} + \dfrac{2\varepsilon t}{x} - \left(\dfrac{2 + F_0^2}{2}\right)\left(F_0^2 + \dfrac{2\varepsilon t}{x}\right)^{2/3}\right), & \\ & \dfrac{2\varepsilon t}{H^3 - F_0^2} \leqslant x \leqslant \dfrac{2\varepsilon t}{1 - F_0^2}, \\ 0, & x \geqslant \dfrac{2\varepsilon t}{1 - F_0^2}, \end{cases}$$

$$v_e(x,t) \sim \begin{cases} \dfrac{1}{H}, & x \leqslant \dfrac{2\varepsilon t}{H^3 - F_0^2}, \\ \left(F_0^2 + \dfrac{2\varepsilon t}{x}\right)^{-1/3}, & \dfrac{2\varepsilon t}{H^3 - F_0^2} \leqslant x \leqslant \dfrac{2\varepsilon t}{1 - F_0^2}, \\ 1, & x \geqslant \dfrac{2\varepsilon t}{1 - F_0^2}. \end{cases}$$

We observe that in this case the expansion wave carries an $O(1)$ bedform structure, and again requires a reduction in the upstream sediment transport rate.

We now consider the situation when $H > F_0^{2/3} + O(\varepsilon^{1/2})$. In this case, via (3.52), there are three distinct regions in the structure of the expansion wave. For

$$1 < h \leqslant F_0^{2/3} - O(\varepsilon^{1/2}),$$

the propagation speed is $O(\varepsilon)$. This increases to $O(\varepsilon^{1/2})$ when

$$F_0^{2/3} - O(\varepsilon^{1/2}) < h < F_0^{2/3} + O(\varepsilon^{1/2})$$

and finally the propagation speed becomes $O(1)$ when $F_0^{2/3} + O(\varepsilon^{1/2}) \leqslant h \leqslant H$. It is convenient to define transition points associated with the above structure changes in the expansion wave. We denote these by $x_L^c(t)$ and $x_R^c(t)$, which are implicitly

defined by

$$h_e(x_L^c, t) = F_0^{2/3} + \varepsilon^{1/2}, \qquad h_e(x_R^c, t) = F_0^{2/3} - \varepsilon^{1/2}.$$

On using (3.52), we obtain estimates as

$$x_L^c \sim (-\tfrac{3}{2}\varepsilon^{1/2} F_0^{-2/3})t, \qquad x_R^c \sim (-2\varepsilon^{1/2}/3F_0^2)t. \tag{4.38}$$

Finally, the solution for the e_1-expansion wave, in this case is

$$h_e(x,t) \sim \begin{cases} H, & x \leqslant \lambda_1(H)t, \\ \frac{1}{9}(3F_0^{1/3} - (x/t)F_0)^2, & \lambda_1(H)t \leqslant x \leqslant x_L^c, \\ O(1), & x_L^c \leqslant x \leqslant x_R^c, \\ (F_0^2 + 2\varepsilon t/x)^{1/3}, & x_R^c \leqslant x \leqslant \lambda_1(1)t, \\ 1, & x \geqslant \lambda_1(1)t, \end{cases} \tag{4.39}$$

$$\xi_e(x,t) \sim \begin{cases} \frac{3}{2}F_0^{2/3} - \frac{1}{2}F_0^2 - 1, & x \leqslant \lambda_1(H)t, \\ \frac{3}{2}F_0^{2/3} - \frac{1}{2}F_0^2 - 1, & \lambda_1(H)t \leqslant x \leqslant x_L^c, \\ \frac{3}{2}F_0^{2/3} - \frac{1}{2}F_0^2 - 1, & x_L^c \leqslant x \leqslant x_R^c, \\ \left(F_0^2 + \dfrac{2\varepsilon t}{x}\right)^{-2/3} \left\{ \dfrac{3F_0^2}{2} + \dfrac{2\varepsilon t}{x} \right. & \\ \qquad \left. - \left(\dfrac{2+F_0}{2}\right)^2 \left(F_0^2 + \dfrac{2\varepsilon t}{x}\right)^{2/3} \right\}, & x_R^c \leqslant x \leqslant \lambda_1(1)t, \\ 0, & x \geqslant \lambda_1(1)t, \end{cases} \tag{4.40}$$

$$v_e(x,t) \sim \begin{cases} 3F_0^{-2/3} - 2\sqrt{H/F_0}, & x \leqslant \lambda_1(H)t, \\ 3F_0^{-2/3} - \frac{2}{3}(3F_0^{-2/3} - x/t), & \lambda_1(H)t \leqslant x \leqslant x_L^c, \\ O(1), & x_L^c \leqslant x \leqslant x_R^c, \\ (F_0^2 + 2\varepsilon t/x)^{-1/3}, & x_R^c \leqslant x \leqslant \lambda_1(1)t, \\ 1, & x \geqslant \lambda_1(1)t, \end{cases} \tag{4.41}$$

with $\lambda_1(H) \sim 3(F_0^{-2/3} - \sqrt{H/F_0})$, $\lambda_1(1) \sim -2\varepsilon/(F_0^2 - 1)$ and x_R^c and x_L^c given by (4.38). The distributions of the free surface, bedform and velocity are given in figure 9. As before, we notice the upstream reduction in the sediment transport rate. We can also see that there is an $O(1)$ bedform structure, suggesting that this would be the dominant expansion wave solution in $F_0 > 1 + O(\varepsilon^{1/2})$. We note that $H = F_0^{2/3} \pm O(\varepsilon^{1/2})$ is a reduced version of this final case.

We observe from the three expansion wave solutions, e_i, $i = 1, 2, 3$, that the e_3-expansion wave, (4.7)–(4.9), never attains an $O(1)$ bedform, and so is never a significant solution for sediment transport problems. When $F_0 < 1$, we can see that the dominant role in bedform evolution of a significant order is played by the e_2-expansion

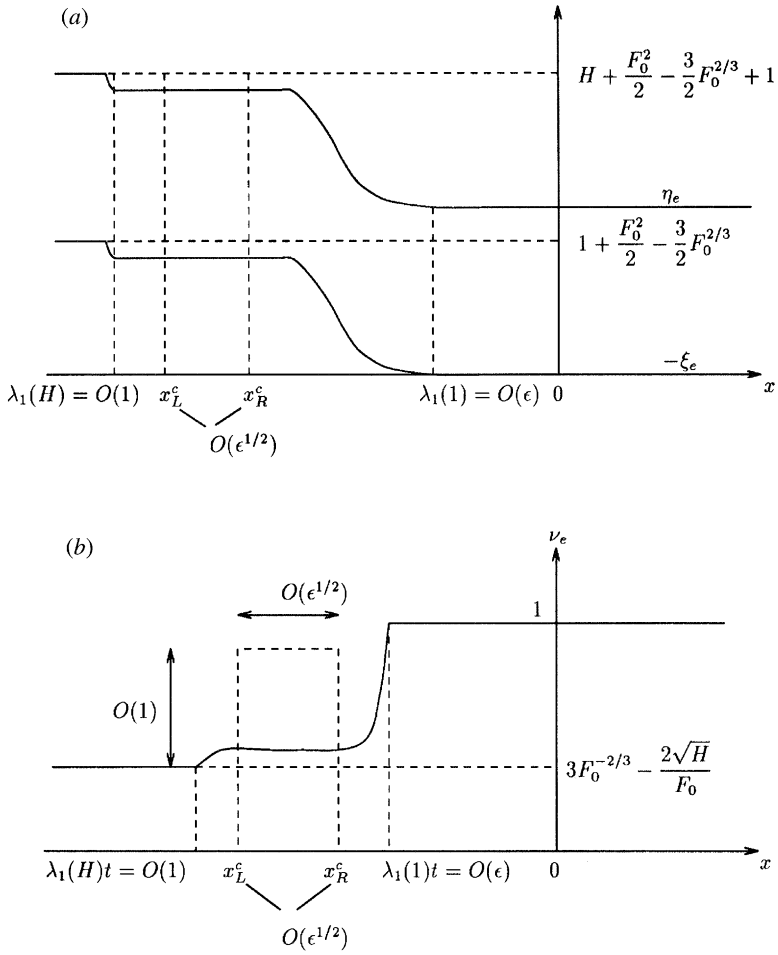

Figure 9. $F_0 > 1 + O(\varepsilon^{1/2})$, $H > F_0^{2/3} + O(\varepsilon^{1/2})$. (*a*) The e_1-expansion wave profiles. (*b*) The corresponding fluid velocity profile.

wave solution. When $F_0 > 1$, the e_1-expansion wave solution will dominate the bedform evolution. Also, we observe that in all cases there is a reduction in upstream sediment transport rate, associated with an expansion wave solution. It should be noted that

an e_1-expansion wave solution exists provided $H > 1$, $F_0 > 0$,
an e_2-expansion wave solution exists provided $H > 1$, $F_0 > 0$,
an e_3-expansion wave solution exists provided $0 < H < 1$, $F_0 > 0$,

which are the regions complementary to those established for the C_i-shock wave families, $i = 1, 2, 3$, by Zanré & Needham (1994), and is consistent with the theory that a shock wave and expansion wave solution determined from the same $\lambda_i(\boldsymbol{u})$ characteristics ($i = 1, 2, 3$), given by (2.20)–(2.22), cannot exist in the same regions of the (H, F_0)-plane.

(*d*) *The sediment expansion wave*

As shown in Needham & Hey (1991) the increase of sediment transport rate upstream of an otherwise uniform alluvial river flow leads to the generation of a down-

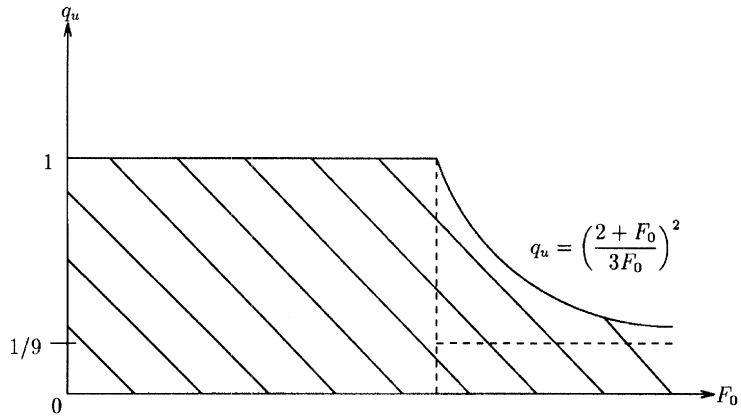

Figure 10. The (q_u, F_0) plane. The shaded region represents parameter values where downstream sediment expansion wave propagation occurs.

stream, slowly propagating step in bedform, referred to as a sediment bore. This was found to be associated with a C_2-shock wave propagation, Needham & Hey (1991). Observations show that the decrease of upstream sediment transport rate in an otherwise uniform alluvial river flow leads to the downstream, slow propagation of an expanding step in bedform. This can be associated with e_2-expansion wave propagation, and we refer to this as a sediment expansion wave.

With the upstream sediment transport rate being $q_u = v_u^2 < 1$ (v_u is the upstream fluid velocity) we now examine § 4 *b* to decide under which conditions the downstream propagation of a sediment expansion wave may occur. From § 4 *b* we readily find that when $F_0 \leqslant 1$ a sediment expansion wave will propagate downstream for any $q_u < 1$. However, for $F_0 > 1$, a sediment expansion wave is generated only if the reduction in q is sufficiently large, namely when

$$q_u \leqslant \left(\frac{2+F_0}{3F_0}\right)^2 < 1.$$

For small reductions with $(2+F_0)^2/9F_0^2 < q_u < 1$, the sediment expansion wave is 'washed-out'. An illustration of the accessible regions for downstream sediment expansion wave propagation is given in the (q_u, F_0)-plane in figure 10.

5. General simple waves

In this section we consider more general structures which can propagate in the system as either s_1-, s_2- or s_3-simple waves, as derived in § 3. However, it is instructive first to note that simple waves generated from a broader class of initial data than that associated with the expansion wave families of § 4, will not always be global solutions of the partial differential equations (2.15)–(2.17). In general, finite-time blow-up will occur in $|u_x|$ and $|u_t|$. Solutions can be continued beyond this point by the insertion of suitable shock waves as described in Needham & Hey (1991).

First we consider global simple waves associated with monotone bedforms, after which we consider simple waves associated with hump and depression bedforms. From (3.31), (3.41) and (3.51), we observe that the s_i-simple wave families ($i = 1, 2, 3$) all

satisfy the hyperbolic conservation law

$$\frac{\partial h}{\partial t} + \lambda_i(h)\frac{\partial h}{\partial x} = 0, \qquad i = 1, 2, 3. \tag{5.1}$$

Following Whitham (1974), we consider the curve, C, in the (x, t)-plane which satisfies

$$\frac{\mathrm{d}x}{\mathrm{d}t} = \lambda_i(h), \qquad i = 1, 2, 3. \tag{5.2}$$

From (5.1) and (5.2) we deduce that

$$\frac{\mathrm{d}h}{\mathrm{d}t} = 0 \tag{5.3}$$

on C, from which we observe that h remains constant along the curve C. Therefore, from (5.2), since the quantities, $\lambda_i(h)$, $i = 1, 2, 3$ are now constant, C must be a family of straight line curves in the (x, t)-plane with slope $\lambda_i(h)$, $i = 1, 2, 3$. If at $t = 0$ one of the lines satisfies $x = \zeta$, then $h = h_0(\zeta)$ along that curve, which has a slope of

$$\lambda_i(h_0(\zeta)) \equiv \Gamma_i(\zeta), \qquad i = 1, 2, 3. \tag{5.4}$$

The equation of the curve is then

$$x = \zeta + \Gamma_i(\zeta)t, \qquad i = 1, 2, 3, \tag{5.5}$$

and allowing ζ to vary, we obtain the solution, with $h = h_0(x)$ at $t = 0$, as

$$h = h_0(\zeta), \quad \text{on} \quad x = \zeta + \Gamma_i(\zeta)t, \tag{5.6}$$

for $i = 1, 2, 3$. This solution holds provided the relation $x = \zeta + \Gamma_i(\zeta)t$ remains as a single-valued relation between x and ζ. For times beyond which this no longer holds, then h becomes multiple valued. We note that, if $\lambda_i'(h) > 0$, higher values of h propagate faster than lower values, while if $\lambda_i'(h) < 0$, higher values of h propagate slower than lower values.

When h becomes multivalued, (5.6) no longer provides a solution of (2.15)–(2.17). However, up to that point (5.6) does provide a solution. We, then, need to determine the breaking time, t_{B}, where two neighbouring characteristics first intersect. This occurs for two characteristic curves cutting the x-axis at $x = \zeta$ and $x = \zeta + \mathrm{d}\zeta$, when

$$\Gamma_i(\zeta)t + \zeta = \Gamma_i(\zeta + \mathrm{d}\zeta)t + \zeta + \mathrm{d}\zeta$$

from (5.6). Therefore, by rearranging and allowing $\mathrm{d}\zeta$ to approach 0, we find that

$$t = -\frac{1}{\Gamma_i'(\zeta)} = -\frac{1}{(\mathrm{d}\lambda_i/\mathrm{d}h)h_0'(\zeta)}, \qquad i = 1, 2, 3. \tag{5.7}$$

Breaking occurs at $t = t_{\mathrm{B}}$, when characteristic intersection first arises, so that

$$t_{\mathrm{B}}^{-1} = \{-\Gamma_i'(\zeta)_{\max}; \quad -\infty < \zeta < \infty\} \tag{5.8}$$

for $i = 1, 2, 3$.

Using the above method of characteristics, we now proceed to analyse steps, humps and depressions, after a brief qualitative discussion of these situations. In all the following cases, the initial downstream conditions are the uniform flow conditions, namely

$$h = 1, \qquad \xi = 0, \qquad q = 1. \tag{5.9}$$

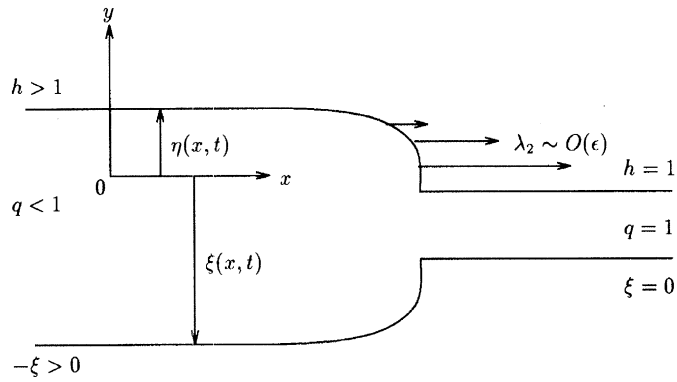

Figure 11. The bedform and flow depth configuration for the s_2-simple wave with step down initial data in $F_0 < 1 - O(\varepsilon^{1/2})$.

Since we are only interested in $O(1)$ bedform development, we must consider the cases when $F_0 < 1$ and $F_0 > 1$ separately, where significant bedforms are carried by the $\lambda_2(h)$- and $\lambda_1(h)$-characteristic wavespeeds, respectively.

(*a*) *Monotone bedforms when* $F_0 < 1$

In this case we need the s_2-simple wave properties, (3.38)–(3.41), when $F_0 < 1$, in order to generate an $O(1)$ monotone bedform disturbance. We consider both the cases of a step down and a step up in bedform.

(i) *Step down in bedform*

From figure 3*a* we observe that as the initial bedform steps down, with ξ becoming increasingly positive, h also increases from unity, and so the characteristic wavespeed, $\lambda_2(h)$, is $O(\varepsilon)$ and is monotone decreasing with larger h. The initial situation is as illustrated in figure 11. It is readily seen that, as time progresses, an expansion wave develops propagating in the downstream direction, and associated with it the usual decrease in upstream sediment flux.

If we examine this situation using the initial condition for the flow depth as

$$h_0(x) = \begin{cases} H, & x \leqslant 0, \\ H - (H-1)x^2, & 0 \leqslant x \leqslant 1, \\ 1, & x \geqslant 1, \end{cases} \tag{5.10}$$

with $H > 1$, then we find from (3.41) and (5.2)–(5.6), that the solution for h is global and is given by

$$h = h(\zeta) = \begin{cases} H, & \zeta \leqslant 0, \\ H - (H-1)\zeta^2, & 0 < \zeta < 1, \\ 1, & \zeta \geqslant 1, \end{cases} \tag{5.11}$$

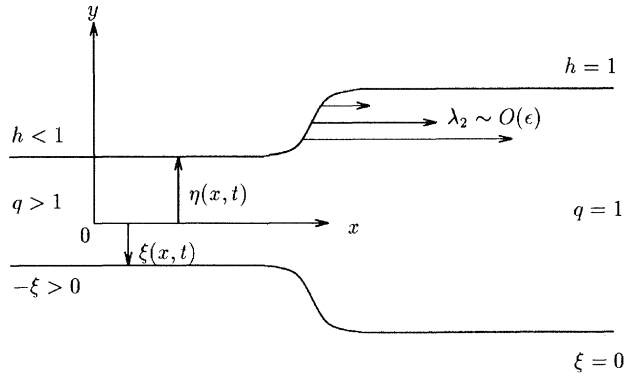

Figure 12. The bedform and flow depth configuration for the s_2-simple wave with step up initial data in $F_0 < 1 - O(\varepsilon^{1/2})$.

$$\lambda_2(h(\zeta)) = \Gamma_2(\zeta) \sim \begin{cases} \dfrac{-2\varepsilon}{F_0^2 - H^3}, & \zeta \leqslant 0, \\ \dfrac{-2\varepsilon}{F_0^2 - [H - (H-1)\zeta^2]^3}, & 0 \leqslant \zeta \leqslant 1, \\ \dfrac{-2\varepsilon}{F_0^2 - 1}, & \zeta \geqslant 1, \end{cases} \tag{5.12}$$

on $x = \zeta + \Gamma_2(\zeta)t$. It is easily established that $\lambda_2'(h) < 0$, which results in a decrease in propagation speed with increase in h giving an expansion wave structure. The associated bedform ξ can be obtained from (3.40) via (5.11).

(ii) *Step up in bedform*

In this situation, from figure 3*a*, we see that as initially ξ becomes increasingly negative, resulting in a step up in bedform, there is a decrease in the flow depth. Since $h < 1$, the depth height can fall into any of the three regions of validity for $\lambda_2(h)$, and the characteristic wavespeed may not necessarily be $O(\varepsilon)$ for all h. If h does not decrease from unity to the extent that it no longer lies in the region $h > F_0^{2/3} + O(\varepsilon^{1/2})$, then $\lambda_2(h)$ is uniformly $O(\varepsilon)$, and increases monotonically with decreasing h. Therefore, from figure 12, we can see that in increasing time, the profile will eventually fold and a shock wave, propagating downstream with speed $O(\varepsilon)$, is formed in a timescale $t = O(\varepsilon^{-1})$. However, we note that if the flow depth decreases greatly from unity, then h will be in the region $0 < h < F_0^{2/3} - O(\varepsilon^{1/2})$, and the characteristic wavespeed $\lambda_2(h)$ is now $O(1)$ at the tail of the wave. This leads to a shock occurring in an $O(1)$ timescale at the tail, propagating with an $O(1)$ speed initially. This decelerates to a speed of $O(\varepsilon)$ over a timescale of $O(\varepsilon^{-1})$ and the previous situation is recovered in the long time evolution. In either case, for a step up in bedform, there is always an increase in the upstream sediment transport rate, and the waves propagate in the downstream direction, eventually requiring a shock, and thus generating a sediment bore.

For analysis, we only consider the case with $h > F_0^{2/3} + O(\varepsilon^{1/2})$. Therefore, from

(3.41) and (5.2)–(5.6), we find that if initially h satisfies the condition

$$h_0(x) = \begin{cases} H, & x \leqslant -1, \\ 1-(1-H)x^2, & -1 < x < 0, \\ 1, & x \geqslant 0, \end{cases} \tag{5.13}$$

with $F_0^{2/3} + O(\varepsilon^{1/2}) < H < 1$, then the solution for h, until the breaking time where the shock wave begins, is given by the family

$$h = h(\zeta) = \begin{cases} H, & \zeta \leqslant -1, \\ 1-(1-H)\zeta^2, & -1 < \zeta < 0, \\ 1, & \zeta \geqslant 0, \end{cases} \tag{5.14}$$

$$\lambda_2(h(\zeta)) = \Gamma_2(\zeta) \sim \begin{cases} \dfrac{-2\varepsilon}{F_0^2 - H^3}, & \zeta \leqslant -1, \\ \dfrac{-2\varepsilon}{F_0^2 - [1-(1-H)\zeta^2]^3}, & -1 < \zeta < 0, \\ \dfrac{-2\varepsilon}{F_0^2 - 1}, & \zeta \geqslant 0, \end{cases} \tag{5.15}$$

on $x = \zeta + \Gamma_2(\zeta)t$. It is readily established that a shock is formed since $\lambda_2'(h) < 0$, which implies that higher values of h propagate slower than lower values. Therefore, it is necessary to find the breaking time. However, if we attempt to determine t_{B} from (5.8), we have to solve a polynomial of degree 10 in ζ, and so we look for an upper bound on t_{B}, by finding a bound on $\Gamma_2'(\zeta)_{\max}$. We know that

$$\Gamma_2'(\zeta) \sim \begin{cases} 0, & \zeta \leqslant -1, \\ \dfrac{12\varepsilon(1-H)\zeta(1-(1-H)\zeta^2)^2}{\{F_0^2 - [1-(1-H)\xi^2]^2\}^2}, & -1 < \zeta < 0, \\ 0, & \zeta \geqslant 0, \end{cases} \tag{5.16}$$

is zero when $\zeta(1-(1-H)\zeta^2)^2 = 0$. It is readily seen that $\Gamma_2'(\zeta) < 0$ between $-1 < \zeta < 0$ and non-negative between $0 < \zeta < 1$. Hence the wave has to break in $\zeta \geqslant -1$, and we find that

$$0 \leqslant t_{\mathrm{B}} \leqslant \frac{[F_0^2 - H^3]^2}{12\varepsilon(1-H)H^2}, \tag{5.17}$$

which is $O(1/\varepsilon)$ as anticipated.

Thus we have seen that both step up and step down bedforms, when $F_0 < 1$, develop on the s_2-simple wave. In the step down case, a sediment expansion wave is generated in the long-time which propagates downstream with an $O(\varepsilon)$ propagation speed. However, in the step up case, the formation of a sediment bore occurs over a timescale of $O(\varepsilon^{-1})$, propagating downstream with speed of $O(\varepsilon)$.

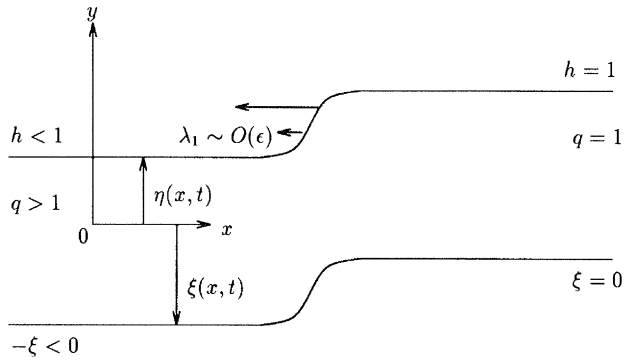

Figure 13. The bedform and flow depth configuration for the s_1-simple wave with step down initial data in $F_0 > 1 + O(\varepsilon^{1/2})$.

(*b*) *Monotone bedforms when* $F_0 > 1$

When $F_0 > 1$, the s_1-simple wave carries an $O(1)$ step in bedform. We use the properties of the s_1-simple wave family in $F_0 > 1 + O(\varepsilon^{1/2})$, as given by (3.52)–(3.54) in conjunction with (3.51), to examine the evolution of steps both up and down in bedform. We note that since $\lambda_1(h) < 0$, bedforms in this case will propagate upstream.

(i) *Step down in bedform*

From figure 4*b* we can see that as ξ steps down, becoming more positive, h decreases. Therefore, upstream $h < 1$ and $\lambda_1(h)$, given by (3.52) in

$$0 < h < F_0^{2/3} - O(\varepsilon^{1/2}),$$

is always $O(\varepsilon)$ and monotonically decreasing in magnitude with decreasing h. Hence, the top part of the wave propagates faster than the lower part, eventually resulting in a shock wave as shown in figure 13. Due to the negative characteristic wavespeed, the wave propagates upstream, where there is an increase in the sediment transport rate. As before, we consider the situation with the initial depth height profile given by (5.13) with $H < 1$, then solving (3.51) through (5.2)–(5.6), we find that up to the breaking time the solution is given by

$$h = h(\zeta) = \begin{cases} H, & \zeta \leqslant -1, \\ 1 - (1-H)\zeta^2, & -1 < \zeta < 0, \\ 1, & \zeta \geqslant 0, \end{cases} \tag{5.18}$$

$$\lambda_1(h(\zeta)) = \Gamma_1(\zeta) \sim \begin{cases} \dfrac{-2\varepsilon}{F_0^2 - H^3}, & \xi \leqslant -1, \\ \dfrac{-2\varepsilon}{F_0^2 - [1-(1-H)\zeta^2]^3}, & -1 < \zeta < 0, \\ \dfrac{-2\varepsilon}{F_0^2 - 1}, & \zeta \geqslant 0, \end{cases} \tag{5.19}$$

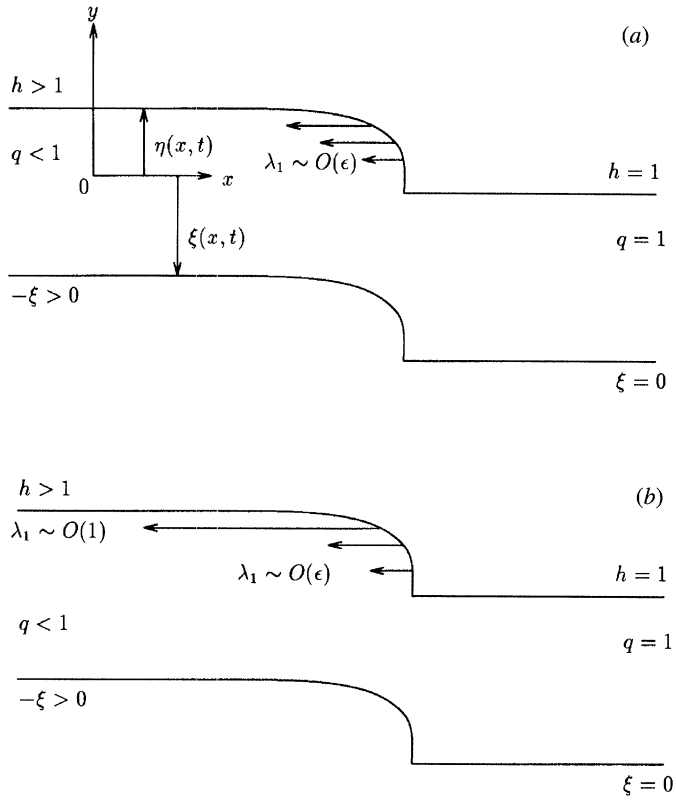

Figure 14. The bedform and flow depth configuration for the s_1-simple wave with step up initial data in $F_0 > 1 + O(\varepsilon^{1/2})$. (*a*) $H < F_0^{2/3} - O(\varepsilon^{1/2})$. (*b*) $H > F_0^{2/3} + O(\varepsilon^{1/2})$.

on $x = \Gamma_1(\zeta)t + \zeta$. It is easily seen that $\lambda_1'(h) < 0$, confirming that a shock wave is formed. In a similar way to that for a step up in bedform when $F_0 < 1$, we find that a bound on the breaking time t_B is given by (5.17). Thus, in this case, the formation of an upstream sediment bore occurs in finite t, with propagation speed of $O(\varepsilon)$ and step height of $O(1)$.

(ii) *Step up in bedform*

In this case, as the bedform steps up, becoming more negative, h increases. Since upstream $h > 1$, then provided h remains less than $9F_0^{2/3}/4$, the flow depth could increase by a sufficient quantity to enable an $O(1)$ characteristic wavespeed to develop. As h increases $|\lambda_1(h)|$ also increases. If $\lambda_1(h)$ is always $O(\varepsilon)$, then the situation is as illustrated in figure 14*a*, and an expansion wave develops, with the expected reduction in the upstream sediment transport flux. However, if $\lambda_1(h)$ becomes $O(1)$, an $O(\varepsilon)$ 'lip' develops in the bedform, which travels at a faster rate than the part of the bedform carried by the $O(\varepsilon)$ characteristic wavespeed, forming an expansion wave which travels on two timescales, with the upper 'lip' part of the bedwave moving at an $(O(1))$ speed and lower main part at the $O(\varepsilon)$ speed. However, the major part of the bedform propagates with speed $O(\varepsilon)$, figure 14*b*.

To continue the analysis, we only consider the case when $\lambda_1(h)$ remains $O(\varepsilon)$. With initial conditions given by (5.10) with $1 < H < F_0^{2/3} - O(\varepsilon^{1/2})$, we find from

(5.2)–(5.6) that the solution is

$$h = h(\zeta) = \begin{cases} H, & \zeta \leqslant 0, \\ H - (H-1)\zeta^2, & 0 < \zeta < 1, \\ 1, & \zeta \geqslant 1, \end{cases} \tag{5.20}$$

$$\lambda_1(h(\zeta)) = \Gamma_1(\zeta) \sim \begin{cases} \dfrac{-2\varepsilon}{F_0^2 - H^3}, & \zeta \leqslant 0, \\ \dfrac{-2\varepsilon}{F_0^2 - [H-(H-1)\zeta^2]^3}, & 0 < \zeta < 1, \\ \dfrac{-2\varepsilon}{F_0^2 - 1}, & \zeta \geqslant 1, \end{cases} \tag{5.21}$$

on $x = \zeta + \Gamma_1(\zeta)t$. Here, $\lambda_1'(h) < 0$ and an expansion wave develops. Therefore, (5.20)–(5.21) is the solution for h for all time. Thus, in this case, an upstream propagating sediment expansion wave develops, propagating with a speed of $O(\varepsilon)$.

The results of §§ 5 *a* and 5 *b* are summarized in table 1.

(*c*) *Non-monotone bedforms when* $F_0 < 1$

As before, to accommodate an $O(1)$ bedform development the characteristic wave-speed is given by the s_2-simple wave family defined in (3.38)–(3.41). In this section we consider depressions and humps in bedform in a similar manner to the previous sections on monotone bedforms.

(i) *Depression in bedform*

The depression in the bedform is equivalent to a step down followed by a step up in bedform, with both upstream and downstream conditions of uniform flow. Again, from figure 3*a*, we observe that as h increases $\lambda_2(h)$ decreases and vice versa, resulting in an expansion at the front (facing downstream) and eventually a shock at the back, as illustrated in figure 15*a*. The time for evolution is of $O(\varepsilon^{-1})$ with the shock and expansion wave propagating with speed of $O(\varepsilon)$. The sediment transport rate decreases upstream from $q = 1$ to $q < 1$, followed by an increase back to $q = 1$, as is expected, and the system propagates in the downstream direction. Therefore, in finite time, we anticipate that a dredged section of bedform will be filled by an advancing sediment bore, preceded by an advancing sediment expansion wave. If we initially have the flow depth given by

$$h_0(x) = \begin{cases} 1, & x \leqslant -1, \\ H - (H-1)x^2, & -1 < x < 1, \\ 1, & x \geqslant 1, \end{cases} \tag{5.22}$$

Table 1. *Summary for steps up and down in bedform, denoted by u and d, respectively, for* $F_0 < 1$ *and* $F_0 > 1$

('+' indicates a disturbance past the critical value $h = F_0^{2/3}$, while '−' indicates no disturbance past this value. Upstream conditions are to the left and the uniform conditions are downstream.)

F_0	u^+	d^+	u^-	d^-
$F_0 < 1$				
(λ_2-wave gives $O(1)$ step in bedform, propagating downstream.)	Shock develops on $O(1)$ timescale with amplitude $O(\varepsilon)$. Develops into a sediment bore on $O(1/\varepsilon)$ timescale with $O(\varepsilon)$ propagation speed and $O(1)$ amplitude. Increase in sediment flux, q.	Situation always as in d^-.	Shock develops on $O(1/\varepsilon)$ timescale. This is a sediment bore propagating with $O(\varepsilon)$ speed and amplitude of $O(1)$. Increase in sediment flux, q.	Sediment expansion wave evolves in $O(1/\varepsilon)$ timescale. Decrease in sediment flux, q.
$F_0 > 1$				
(λ_1-wave gives $O(1)$ step in bedform, propagating upstream.)	Sediment expansion wave develops on $O(1)$ timescale with amplitude $O(\varepsilon)$. Eventually develops on $O(1/\varepsilon)$ timescale to $O(\varepsilon)$ propagation speed and $O(1)$ amplitude. Decrease in sediment flux, q.	Situation always as in d^-.	Sediment expansion wave develops on $O(1/\varepsilon)$ timescale with $O(1)$ amplitude. Decrease in sediment flux, q.	Shock develops on $O(1/\varepsilon)$ timescale. This is a sediment bore propagating with $O(\varepsilon)$ speed and amplitude of $O(1)$. Increase in sediment flux, q.

with $H > 1$, then the solution of (3.41) from (4.41)–(5.4) is given by

$$h = h(\zeta) = \begin{cases} 1, & \zeta \leqslant -1, \\ H - (H-1)\zeta^2, & -1 < \zeta < 1, \\ 1, & \zeta \geqslant 1, \end{cases} \tag{5.23}$$

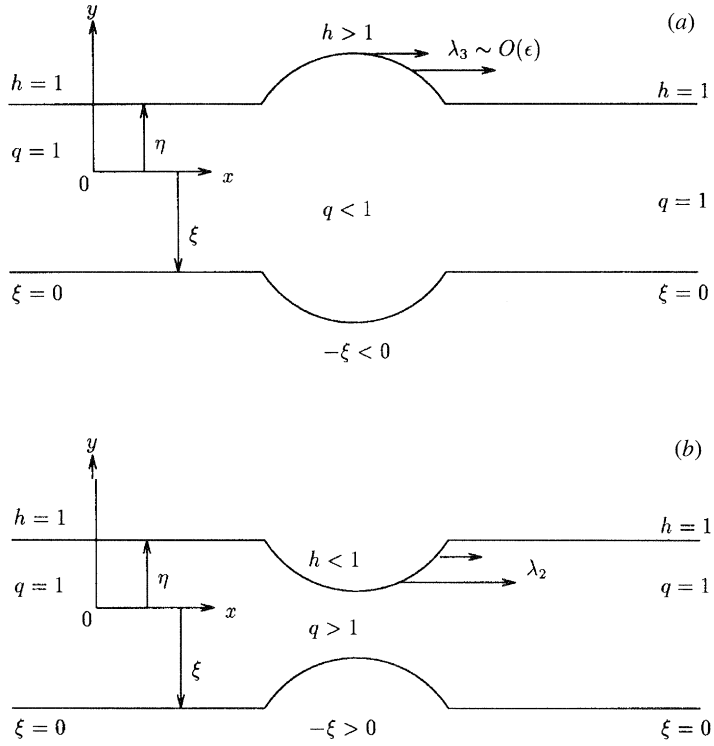

Figure 15. The bedform and flow depth configuration for the s_2-simple wave in $F_0 < 1$ with (a) depression and (b) hump initial data.

$$\lambda_2(h(\zeta)) = \Gamma_2(\zeta) \sim \begin{cases} \dfrac{-2\varepsilon}{F_0^2 - 1} + O(\varepsilon^2), & \zeta \leqslant -1, \\ \dfrac{-2\varepsilon}{F_0^2 - [H - (H-1)\zeta^2]^3} + O(\varepsilon^2), & -1 < \zeta < 1, \\ \dfrac{-2\varepsilon}{F_0^2 - 1} + O(\varepsilon^2), & \zeta \geqslant -1, \end{cases} \tag{5.24}$$

on $x = \zeta + \Gamma_2(\zeta)t$. We find that $\lambda_2'(h) < 0$, confirming an expansion wave at the front and a shock at the back. Therefore, the solution (5.23)–(5.24) is only applicable until the breaking time, t_{B}. As before, by differentiating (5.24) and noting that the solution will become multivalued in $\zeta \leqslant -1$, we find that a bound on t_{B} is

$$0 \leqslant t_{\mathrm{B}} \leqslant [F_0^2 - 1]^2 / 12\varepsilon(H - 1). \tag{5.25}$$

Thus we would expect the dredged section to be filled in a time of $O(1/\varepsilon)$.

(ii) *Hump in bedform*

This situation can be viewed as a step up in bedform, followed by a step down. Again, $\lambda_2(h)$ increases as h decreases. However, if h decreases past $h = F_0^{2/3}$, the characteristic wavespeed becomes $O(1)$. First, if h does not fall below the critical value, then λ_2 remains $O(\varepsilon)$ and the bedform is always $O(1)$, with a shock at the front and an expansion at the back. If h falls below the critical value, then the $O(\varepsilon)$ 'lip' forms on the riverbed, and the system proceeds on the fast timescale, $O(1)$, followed by the slower moving part on the timescale $O(1/\varepsilon)$. The situation is

illustrated in figure 15*b*. In both cases, the sediment transport rate first increases from unity and then returns to unity. On taking the analysis further, we consider only the case where $\lambda_2(h)$ remains $O(\varepsilon)$. With the initial condition

$$h_0(x) = \begin{cases} 1, & x \leqslant -1, \\ H + (1-H)x^2, & -1 < x < 1, \\ 1, & x \geqslant 1, \end{cases} \tag{5.26}$$

with $F_0^{2/3} + O(\varepsilon^{1/2}) < H < 1$, the solution of (3.41), using (5.2)–(5.6), gives

$$h = h(\zeta) = \begin{cases} 1, & \zeta \leqslant -1, \\ H + (1-H)\zeta^2, & -1 < \zeta < 1, \\ 1, & \xi \geqslant 1, \end{cases} \tag{5.27}$$

$$\lambda_2(h(\zeta)) = \Gamma_2(\zeta) \sim \begin{cases} \dfrac{-2\varepsilon}{F_0^2 - 1}, & \zeta \leqslant -1, \\ \dfrac{-2\varepsilon}{F_0^2 - [H + (1-H)\zeta^2]^3}, & -1 < \zeta < 1, \\ \dfrac{-2\varepsilon}{F_0^2 - 1}, & \zeta \geqslant -1, \end{cases} \tag{5.28}$$

on $x = \zeta + \Gamma(\zeta)t$. Again, it is readily seen that $\lambda_2'(h) < 0$ yields the anticipated shock wave at the front and expansion wave at the back, with the breaking time, as before, occurring within the bounds given in (5.25). Thus, in this case a sediment bore develops at the head of the hump, with a sediment expansion wave at the rear.

(*d*) *Non-monotone bedforms when* $F_0 > 1$

To accommodate $O(1)$ bedforms when $F_0 > 1$, we must use the properties of the s_1-simple family, (3.51)–(3.53). As h increases, we observe from figure 4*b* that the magnitude of the characteristic wavespeed also increases.

(i) *Depression in bedform*

This is equivalent to a step down in bedform, followed by a step up. As can be seen from figure 16*a*, there is an expansion at the back (facing upstream) and a shock wave forms at the front. There is initially an increase in the upstream sediment transport rate, followed by a decrease and the system propagates in the upstream direction. The analysis is similar to that for a hump on the riverbed when $F_0 < 1$, where the initial data is given by (5.26), and the solution is as in (5.27)–(5.28), with λ_1 and Γ_1 replacing λ_2 and Γ_2, respectively. The bound on the breaking time is given by (5.25), and again we would expect a dredged section upstream to be filled in a time $O(1/\varepsilon)$.

(ii) *Hump in bedform*

This is similar to a step up in bedform, followed by a step down, but with $h > 1$, enabling the characteristic wavespeed to become $O(1)$ if h increases past the critical value of $h = F_0^{2/3}$. If the flow depth does not become larger than the critical value

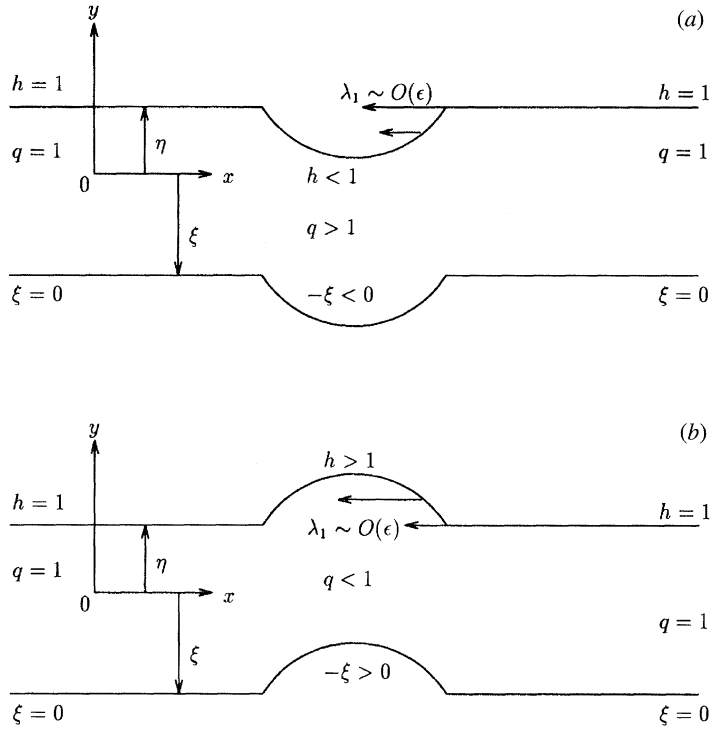

Figure 16. The bedform and flow depth configuration for the s_1-simple wave in $F_0 > 1$ with (a) depression and (b) hump initial data.

then the situation is as in figure 16b. There is a shock at the front and an expansion at the back, with the system propagating upstream. The sediment flux first decreases and then increases, as expected. If h increases beyond the critical value, then the situation is similar, but the $O(\varepsilon)$ 'lip' forms on the riverbed profile travelling on the fast $O(1)$ timescale. The analysis is again continued for the simpler case and, due to the symmetry of the problem, is found to be similar to that for a depression in bedform when $F_0 < 1$. Thus, using the initial data from (5.22) and solving (3.51) via (5.2)–(5.6), we find that the solution is the same as that in (5.23)–(5.24), with λ_2 and Γ_2 replaced by their respective counterparts in this region. Again the breaking time, t_{B}, lies within the bounds of (5.25).

A summary of the results for non-monotone bedforms when $F_0 < 1$ and $F_0 > 1$ is given in table 2.

(e) *Sediment transport rate increase and reduction*

We use the method of characteristics to determine whether the bedform will develop expansion or shock waves for an increase and reduction in upstream sediment flux. If a shock wave develops, then we say that the bedform shocks, and if an expansion wave is formed, we say that the bedform expands. The problem can be regarded as a boundary-value problem, where along $t = 0$, $q = 1$ and along $x = 0$, $q > 1$ for an increase in the sediment transport rate, and $q < 1$ for a reduction. Since the sediment is injected upstream, the resulting bedform can only propagate downstream. Thus, the problem can only involve either the λ_2 or λ_3-characteristic wavespeeds,

Table 2. *Summary for humps and depressions in bedform, denoted by H and D, respectively, for $F_0 < 1$ and $F_0 > 1$*

('+' indicates a disturbance past the critical value $h = F_0^{2/3}$, while '−' indicates no disturbance past this value. Upstream conditions are to the left and the uniform conditions are downstream, with the back of the system facing upstream.)

F_0	H^+	D^+	H^-	D^-
$F_0 < 1$				
(λ_2-wave gives $O(1)$ structure in bedform, propagating downstream.)	Back evolves a sediment expansion wave in timescales $O(1)$, $O(1/\varepsilon)$. Front develops shock in timescales $O(1)$, $O(1/\varepsilon)$ and propagates as sediment bore. Sediment flux, q, increases from $q = 1$ to $q > 1$ and then decreases to $q = 1$.	See D^-.	Back evolves as sediment expansion wave in time $O(1/\varepsilon)$. Front develops shock, which propagates as sediment bore in timescale $O(1/\varepsilon)$. Sediment flux, q, increases from $q = 1$ to $q > 1$ and then decreases to $q = 1$.	Back develops sediment bore in timescale $O(1/\varepsilon)$. Front evolves as sediment expansion wave in timescale $O(1/\varepsilon)$. Sediment flux, q, decreases from $q = 1$ to $q < 1$ and then increases to $q = 1$.
$F_0 > 1$				
(λ_1-wave gives $O(1)$ structure in bedform, propagating upstream.)	Back develops a sediment bore in timescales $O(1)$, $O(1/\varepsilon)$. Front evolves as sediment expansion wave in timescales $O(1)$, $O(1/\varepsilon)$. Sediment flux, q, decreases from $q = 1$ to $q < 1$ and then increases to $q = 1$.	See D^-.	Back develops shock, propagating as a sediment bore, in $O(1/\varepsilon)$. Front evolves as a sediment expansion wave in timescale $O(1/\varepsilon)$. Sediment flux, q, decreases from $q = 1$ to $q < 1$ and then increases to $q = 1$. $O(1/\varepsilon)$ timescale with $O(1)$ amplitude. Decrease in sediment flux, q.	Back evolves as a sediment expansion wave in timescale $O(1/\varepsilon)$. Front develops a sediment bore in timescale $O(1/\varepsilon)$. Sediment flux, q, increases from $q = 1$ to $q > 1$ and then decreases to $q = 1$.

since $\lambda_1 < 0$. If the situation involves λ_2, we have to consider the cases when the Froude number of the uniform flow is either less than or greater than unity.

The λ_2-wave. First we consider the case when $F_0 < 1$, where an $O(1)$ bedform develops. From figure 3*a* we know that v and $\lambda_2(h)$ are both monotone increasing

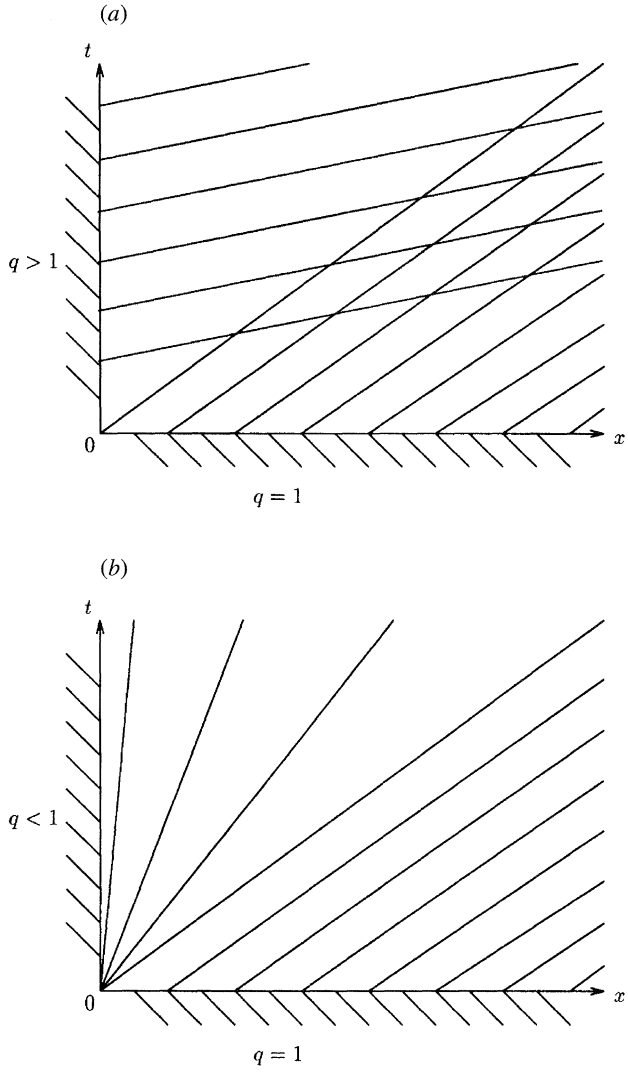

Figure 17. The λ_2-characteristic curves, when $F_0 < 1$, for upstream (a) increase and (b) decrease in sediment flux.

with decreasing h. Since $q = v^2$, there is an increase in characteristic slope as more sediment is injected. This results in the intersection of neighbouring characteristics and a shock wave is formed immediately, as shown in figure 17a. Conversely, when there is a reduction in the sediment flux, there is a decrease in the slopes of the characteristic lines, and an expansion wave is formed, as in figure 17b. When $F_0 > 1$, an $O(\varepsilon)$ bedform is generated, and from figure 3b we see that, again, v and $\lambda_2(h)$ are monotone increasing with decreasing h. Thus, we have a shock wave for an increase in sediment flux, and an expansion wave for a decrease, as before. Thus, significant bedforms only develop when $F_0 < 1$, being a sediment bore for $q > 1$ and a sediment expansion wave when $q < 1$. These are 'washed-out' when $F_0 > 1$.

The λ_3-wave. From figure 2a, b, we observe that v and $\lambda_3(h)$ are both monotone increasing with increasing h, and the bedform always remains $O(\varepsilon)$. Hence, if more

Table 3. *Summary of sediment injection and reduction upstream in an otherwise uniform alluvial river flow*

q	λ_2-wave $F_0 < 1$	λ_2-wave $F_0 > 1$	λ_3-wave
$q > 1$: increase in sediment flux	$O(1)$ step in bedform, evolves as sediment bore. Results in a shock wave immediately.	'wash-out: $O(\varepsilon)$ step in bedform, evolves. Results in a shock wave immediately.	'wash-out': $O(\varepsilon)$ step in bedform. Results in a shock wave immediately.
$q < 1$: decrease in sediment flux	$O(1)$ step in bedform. Results in a sediment expansion wave.	'wash-out': $O(\varepsilon)$ step in bedform. Results in an expansion wave.	'wash-out': $O(\varepsilon)$ step in bedform. Results in an expansion wave.

sediment is injected into the system, there is an increase in the slope of the characteristic curves, resulting in a shock wave, and similarly a decrease in sediment flux results in an expansion wave.

The results are summarized in table 3.

6. Weak shock theory

When there is finite-time blow-up in $|u_t|$ and $|u_x|$, we continue the solution by the insertion of shock waves. Using the non-dimensional integral conservation laws (2.10)–(2.12), in conjunction with the shock depth function of Needham & Hey (1991), we can extend the solution in situations (such as those discussed in the previous section), where the solution becomes multivalued, by allowing piecewise-classical solutions, resulting in the introduction of shock waves. Usually, these shock waves have to satisfy the full conditions given in Needham & Hey (1991), which are in general difficult to apply. In this section, however, we use weak shock theory, which gives a simplification. We show that for small disturbances, the solutions of the simple wave equations can be continued after finite-time blow-up, by inserting shocks which satisfy the equal area rule as developed by Whitham (1974).

To establish that the weak shock hypothesis holds in our case, we show that a shock satisfying the full conditions developed by Needham & Hey (1991), is equivalent to inserting an equal area shock into a simple wave solution, up to the first nonlinear order in shock amplitude. We consider the case where there is a shock wave at $x = s(t)$, propagating into downstream conditions of uniform flow, in both the cases of shocks satisfying the conditions of Needham & Hey (1991), and the equal area rule of Whitham (1974). The shock wave families which satisfy the full conditions imposed by Needham & Hey (1991) are in fact the C_i-shock waves, $i = 1, 2, 3$, described in Zanré & Needham (1994). The rest of the upstream flow conditions for these shocks are denoted by

$$\xi = f(H), \quad v = g(H), \quad \dot{s} = \delta(H), \tag{6.1}$$

for the solutions involving the C_i-shock waves, $i = 1, 2, 3$, with $f(\cdot)$ and $g(\cdot)$ given in Zanré & Needham (1994), and where $\dot{s}$ is the shock speed. The upstream conditions for the equal area shocks, on the s_i-simple wave ($i = 1, 2, 3$), are

$$\xi = F(H), \quad v = G(H), \quad \dot{s} = \frac{\Lambda(H) - \Lambda(1)}{H - 1}, \tag{6.2}$$

with $F(\cdot)$ and $G(\cdot)$ given earlier and where again $\dot{s}$ is the shock speed, determined by writing the hyperbolic conservation laws (5.1) in the integral form

$$\frac{\mathrm{d}}{\mathrm{d}t}\int_{X_1}^{X_2} h\,\mathrm{d}x + [\Lambda_i(h)]_{X_1}^{X_2} = 0, \tag{6.3}$$

where

$$\Lambda_i(h) = \int_1^h \lambda_i(s)\,\mathrm{d}s \tag{6.4}$$

for $i = 1, 2, 3$, and then splitting the limits of integration so that to the left of the step discontinuity, $x_1 \leqslant x < s(t)$ and to the right of the discontinuity, $s(t) < x \leqslant x_2$. Expanding about $H = 1$, we find that to $O(H - 1)$, the shock speed in (6.2) is given by

$$\dot{s} = \lambda_i(1) + \tfrac{1}{2}(H - 1)\lambda_i'(1) \tag{6.5}$$

for $i = 1, 2, 3$. We consider the cases for each of the simple wave families in turn, showing consistency, up to first nonlinear order in shock amplitude, between the full shock conditions (6.1) and the weak shock conditions (6.2).

(*a*) *Weak shock consistency for the s_3-simple wave family*

In this case, we have for the upstream conditions (6.1) in the full C_3-shock (Needham & Hey 1991),

$$f(H) \sim \frac{-\varepsilon(H-1)(H(H+1))^{1/2}}{\sqrt{2F_0}H(1+[H(H+1)/(2F_0^2)]^{1/2})}\left\{2 + \frac{(H-1)(H+1)^{1/2}}{F_0\sqrt{2H}}\right\}, \tag{6.6}$$

$$g(H) \sim 1 + \frac{(H-1)H^{1/2}(H+1)^{1/2}}{\sqrt{2F_0}H}, \tag{6.7}$$

$$\delta(h) \sim 1 + \sqrt{H(H+1)}/(2F_0^2), \tag{6.8}$$

while the equal area shock (6.2) on the s_3-simple wave gives

$$F(H) \sim \frac{4\varepsilon}{9F_0}\left\{(2 - F_0)\log\left|\frac{F_0 - 2 + 3\sqrt{H}}{F_0 + 1}\right| + 6(1 - \sqrt{H})\right\}, \tag{6.9}$$

$$G(H) \sim 1 - \frac{2}{F_0} + \frac{\sqrt{H}}{F_0}, \tag{6.10}$$

$$\dot{s} \sim 1 + \frac{1}{F_0} + \frac{3}{2F_0}(H - 1), \tag{6.11}$$

from (3.28)–(3.30) and (6.5). Taking the weak shock limit, we substitute

$$H = 1 + \hat{H}, \quad \text{where} \quad \hat{H} \ll 1 \tag{6.12}$$

into (6.6)–(6.11), to find that the two sets of expressions are consistent to $O(\hat{H})$, which is readily verified.

(*b*) *Weak shock consistency for the s_2- and s_1-simple wave families*

To examine the consistency of the full shock conditions (6.1) with the weak shock conditions (6.2) we consider the (H, F_0)-plane for $H = 1 - \hat{H}$ with $0 < \hat{H} \ll 1$. It is then straightforward (although lengthy) to show that, up to $O(\hat{H})$, shocks of the C_2-class (as given in Needham & Hey 1991) are consistent with weak shocks inserted in s_2-simple waves, while shocks of the C_1-class (details in Needham & Hey 1991) are consistent with weak shocks inserted in the s_1-simple waves.

Thus we can now follow weak disturbances in the s_i-simple wave ($i = 1, 2, 3$) beyond breaking-time by inserting shocks into the multiple valued profiles which satisfy the Whitham equal area rule. We consider some specific examples.

(*c*) *Dredged channel*

Consider a dredged section of a riverbed; we have already seen in § 5 that if $F_0 < 1$ an $O(1)$ bedform develops and is transported downstream, being carried by the s_2-simple wave. Conversely, when $F_0 > 1$ the $O(1)$ bedform is carried upstream by the s_1-simple wave. Therefore, we apply weak shock theory to each of these situations in turn, again considering the depth height h, after which for the weak shock solution there is a simple linear transformation between h and the bedform ξ.

(i) $F_0 < 1$

At $t = 0$, we have a dredged section which is approximated by the initial condition of the top hat function,

$$h = \begin{cases} 1, & x \leqslant -1, \\ H, & -1 < x < 1, \quad H > 1, \\ 1, & x \geqslant 1, \end{cases} \tag{6.13}$$

and with h satisfying the hyperbolic conservation law (3.41), where

$$\lambda_2(h) \sim -2\varepsilon/(F_0^2 - h^3) \qquad (> 0).$$

In the weak shock limit, we write

$$\left.\begin{aligned} h &= 1 + \hat{H}, \quad 0 < \hat{H} \ll 1, \\ H &= 1 + \hat{H}_0, \quad 0 < \hat{H}_0 \ll 1, \end{aligned}\right\} \tag{6.14}$$

and substitute into the form for $\lambda_2(h)$, the initial condition (6.13) and the hyperbolic conservation law (3.41), to obtain at $t = 0$,

$$\hat{H} = \begin{cases} 0, & x \leqslant -1, \\ \hat{H}_0, & -1 < x < 1, \\ 0, & x \geqslant 1, \end{cases} \tag{6.15}$$

with $\hat{H}$ satisfying the hyperbolic conservation law

$$\frac{\partial \hat{H}}{\partial t} + \lambda_2(\hat{H}) \frac{\partial \hat{H}}{\partial x} = 0, \tag{6.16}$$

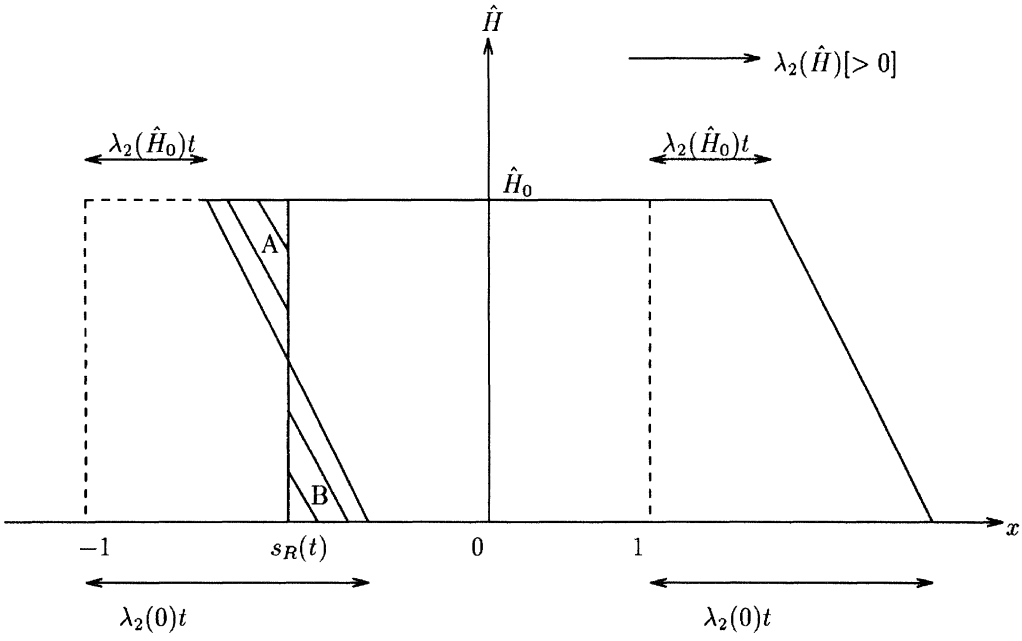

Figure 18. The $(\hat{H}, x)$ profiles in the channel dredging problem, $F_0 < 1$.

where $\lambda_2(\hat{H}) \sim \alpha + \beta\hat{H} > 0$ with $\alpha = 2\varepsilon/(1-F_0^2) > 0$ and $\beta = -6\varepsilon/(1-F_0^2)^2 < 0$. As $\hat{H}$ increases, $\lambda_2(\hat{H})$ decreases, resulting in an expansion at the downstream end and a shock at the rear. After some time $t > 0$, the initial profile has moved a distance $\lambda_2(0)t$ along $\hat{H} = 0$ and $\lambda_2(\hat{H}_0)t$ along $\hat{H} = \hat{H}_0$, from its initial position, as shown in figure 18. Since the solution has now become multivalued at the back, we follow Whitham (1974), and fit a shock at $x = s_R(t)$ such that two triangles A and B, of equal area, are formed. By simple geometry we know that the height of A and B are equal, and by using the equal area rule, namely

$$\text{area}(A) = \text{area}(B) \tag{6.17}$$

we find that

$$s_R(t) + 1 - \lambda_2(\hat{H}_0)t = \lambda_2(0)t - s_R(t) - 1.$$

Thus

$$s_R(t) = -1 + \tfrac{1}{2}[\lambda_2(0) + \lambda_2(\hat{H}_0)]t. \tag{6.18}$$

The expansion wave between $(1 + \lambda_2(\hat{H}_0)t, \hat{H}_0)$ and $(1 + \lambda_2(0)t, 0)$ can be found in the usual way, to give the expansion wave solution as

$$\hat{H}(x,t) \sim \begin{cases} \hat{H}_0, & s_R(t) \leqslant x \leqslant 1 + \lambda_2(\hat{H}_0)t, \\ \dfrac{\hat{H}_0(x - 1 - \lambda_2(0)t)}{[\lambda_2(\hat{H}_0) - \lambda_2(0)]t}, & 1 + \lambda_2(\hat{H}_0)t \leqslant x \leqslant 1 + \lambda_2(0)t, \\ 0, & x \geqslant 1 + \lambda_2(0)t, \end{cases} \tag{6.19}$$

with $s_R(t)$ given by (6.18). The height of the new profile remains the same, with a step discontinuity at $x = s_R(t)$, and the expansion wave (6.19) at the front. Eventually,

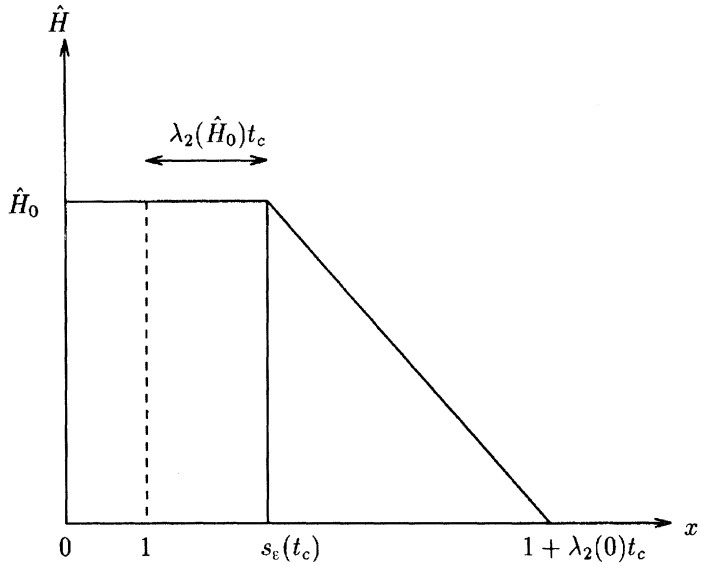

Figure 19. The $(\hat{H}, x)$ profile when the expansion and shock waves collide.

at some critical time $t = t_c$, the shock and expansion waves collide at $(s_\varepsilon(t_c), \hat{H}_0)$. Thus the profile at $t = t_c$ is as illustrated in figure 19. Along $\hat{H} = 0$, the profile has moved a distance $\lambda_2(0)t_c$, and along $\hat{H} = \hat{H}_0$ the distance moved is $\lambda_2(\hat{H}_0)t_c$, which is the position at which the shock is now situated, $s_\varepsilon(t_c)$. At $t = t_c$, we have

$$s_\varepsilon(t_c) = s_R(t_c) \tag{6.20}$$

giving, from (6.20), the critical time

$$t_c = \frac{4}{\lambda_2(0) - \lambda_2(\hat{H}_0)}, \tag{6.21}$$

and the shock position

$$s_\varepsilon(t_c) = \frac{\lambda_2(0) + 3\lambda_2(\hat{H}_0)}{\lambda_2(0) - \lambda_2(\hat{H}_0)}. \tag{6.22}$$

The expansion between $x = s_\varepsilon(t_c)$ and $1 + \lambda_2(0)t_c$ is now determined, giving the profile at $t = t_c$ as

$$\hat{H}(x, t_c) = \begin{cases} 0, & x \leqslant s_\varepsilon(t_c), \\ \dfrac{\hat{H}_0}{4}\left(\dfrac{(x-5)\lambda_2(0) - (x-1)\lambda_2(\hat{H}_0)}{\lambda_2(\hat{H}_0) - \lambda_2(0)}\right), & \\ & s_\varepsilon(t_c) < x < 1 + \lambda_2(0)t_c, \\ 0, & x \geqslant 1 + \lambda_2(0)t_c, \end{cases} \tag{6.23}$$

where $s_\varepsilon(t_c)$ is given by (6.22) and

$$1 + \lambda_2(0)t_c = (5\lambda_2(0) - \lambda_2(\hat{H}_0))/(\lambda_2(0) - \lambda_2(\hat{H}_0).$$

At time $t > t_c$, the profile at $t = t_c$ has expanded more at the front and shocked at the back, having moved $\lambda_2(0)(t-t_c)$ and $\lambda_2(\hat{H}_0)(t-t_c)$ along $\hat{H} = 0$ and $\hat{H} = \hat{H}_0$, respectively. Again, a shock must be fitted at position $x = s_1(t)$, creating two triangles which satisfy the equal area rule (6.17), as shown in figure 20. The shock line now forms the new profile, of a right angled triangle of height $\hat{H}_1$. From the conservation of area, the original triangle in figure 19 must have the same area as the double valued triangular profile in figure 20. By (6.17) it must also have the same area as the triangle of height $\hat{H}_1$. Equating the areas of the original profile at $t = t_c$, and the triangle of height $\hat{H}_1$, we find that

$$s_1(t) = 1 + \lambda_2(0)t - \frac{\hat{H}_0}{\hat{H}_1}[\lambda_2(0) - \lambda_2(\hat{H}_0)]t_c, \tag{6.24}$$

with t_c as given in (6.21). The expansion line between

$$(1 + \lambda_2(\hat{H}_0)t, \hat{H}_0) \quad \text{and} \quad (1 + \lambda_2(0)t, 0)$$

is

$$\hat{H} = \frac{\hat{H}_0(x - 1 - \lambda_2(0)t)}{(\lambda_2(\hat{H}_0) - \lambda_2(0))t}. \tag{6.25}$$

On substituting the condition $\hat{H} = \hat{H}_1$ at $x = s_1(t)$ along with the form of $s_1(t)$ from (6.24), into (6.25), we find that the height of the triangle has now reduced to

$$\hat{H}_1 = \hat{H}_0(t_c/t)^{1/2}, \tag{6.26}$$

and the new shock position is given by

$$s_1(t) = 1 + \lambda_2(0)t - (tt_c)^{1/2}[\lambda_2(0) - \lambda_2(\hat{H}_0)] \tag{6.27}$$

from (6.26) and (6.24). We observe that the shock height in (6.26) decays as $O(t^{-1/2})$, which is consistent with Lax (1957). On differentiating (6.27) with respect to t, we find that the shock speed is

$$\dot{s}_1(t) = \lambda_2(0) - \tfrac{1}{2}(t_c/t)^{1/2}[\lambda_2(0) - \lambda_2(\hat{H}_0)], \tag{6.28}$$

which tends to $\lambda_2(0)$ from below as $t \to \infty$.

Referring to the bedform, we observe that the dredged section propagates downstream with $O(\varepsilon)$ speed. A sediment bore forms at the rear and a sediment expansion wave at the front. The dredged section maintains its original depth until $t = t_c$, after which the sediment bore catches up with the rear of the sediment expansion wave. The depth of the dredged section thereafter diminishes, being of $O(t^{-1/2})$, having propagated a distance of $O(\varepsilon t)$ as $t \to \infty$.

(ii) $F_0 > 1$

Here, the initial conditions are as in (i) with h satisfying the hyperbolic conservation law (3.51). In the weak shock limit we substitute

$$\left.\begin{aligned} h &= 1 - \hat{H}, \quad 0 < \hat{H} \ll 1, \\ H &= 1 - \hat{H}_0, \quad 0 < \hat{H}_0 \ll 1, \end{aligned}\right\}, \tag{6.29}$$

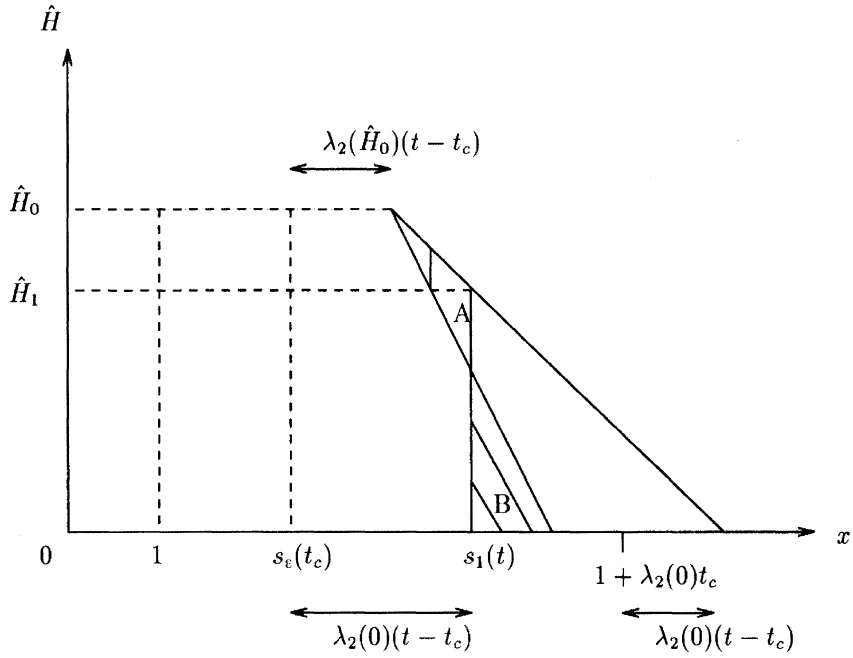

Figure 20. The $(\hat{H}, x)$ profiles for $t > t_c$, $F_0 < 1$.

into (3.51), (5.26) and the $O(\varepsilon)$ form for $\lambda_1(h)$, given in (3.52), to obtain the conservation law for $\hat{H}$,

$$\frac{\partial \hat{H}}{\partial t} + \lambda_1(\hat{H})\frac{\partial \hat{H}}{\partial x} = 0, \tag{6.30}$$

where $\lambda_1(\hat{H}) \sim \alpha - \beta\hat{H} < 0$, with $\alpha = 2\varepsilon/(1-F_0^2) < 0$ and $\beta = -6\varepsilon/(1-F_0^2)^2 < 0$. Thus $|\lambda_1(\hat{H})|$ is monotone decreasing with increasing $\hat{H}$. Also, initially, $\hat{H}$ satisfies the condition (6.15).

After finite time $t > 0$ we have the situation illustrated in figure 21, where there is a shock facing downstream and an expansion at the rear, with the profile moving upstream. As in (i), we fit the shock at the point $x = s_R(t)$, creating two triangles A and B, which satisfy the equal area rule (6.17). We then find, on applying (6.17), that

$$s_R(t) = 1 + \tfrac{1}{2}[\lambda_1(0) + \lambda_1(\hat{H}_0)]t. \tag{6.31}$$

We also readily establish that the expansion wave solution is given by

$$\hat{H}(x,t) \sim \begin{cases} 0, & x \leqslant -1 + \lambda_1(0)t, \\ \dfrac{\hat{H}_0(x+1-\lambda_1(0)t)}{[\lambda_1(\hat{H}_0) - \lambda_1(0)]t}, & -1 + \lambda_1(0)t < x < -1 + \lambda_1(\hat{H}_0)t, \\ \hat{H}_0, & -1 + \lambda_1(\hat{H}_0)t \leqslant x \leqslant s_R(t), \end{cases} \tag{6.32}$$

with $s_R(t)$ as given in (6.31). Eventually, at $t = t_c$, the shock wave will have caught up with the expansion wave at the point $x = s_\varepsilon(t_c)$, so that the profile is now that

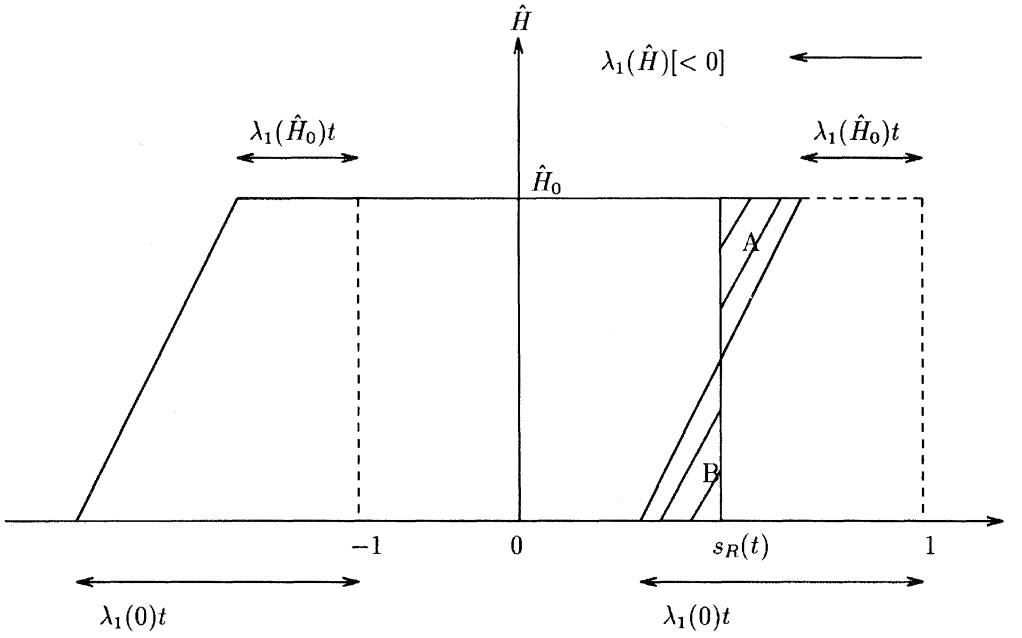

Figure 21. The $(\hat{H}, x)$ profiles in the channel dredging problem, $F_0 > 1$.

of a right-angled triangle of height $\hat{H}_0$. We find that the critical time is

$$t_c = \frac{4}{\lambda_1(\hat{H}_0) - \lambda_1(0)}, \tag{6.33}$$

giving the shock position as

$$s_\varepsilon(t_c) = \frac{\lambda_1(0) + 3\lambda_1(\hat{H}_0)}{\lambda_1(\hat{H}_0) - \lambda_1(0)}. \tag{6.34}$$

From the equation of the hypotenuse, the equation for $\hat{H}$ at $t = t_c$ is therefore

$$\hat{H}(x, t_c) = \begin{cases} 0, & x \leqslant -1 + \lambda_1(0)t_c, \\ \dfrac{\hat{H}_0}{4}\left(\dfrac{(x+1)\lambda_1(\hat{H}_0) - (x+5)\lambda_1(0)}{\lambda_1(\hat{H}_0) - \lambda_1(0)}\right), & \\ \qquad -1 + \lambda_1(0)t_c < x < s_\varepsilon(t_c), & \\ 0, & x \geqslant s_\varepsilon(t_c), \end{cases} \tag{6.35}$$

with $s_\varepsilon(t_c)$ given by (6.34). Using the same arguments as for $F_0 < 1$, we use the conservation of area rule to fit a shock of height $\hat{H}_1$ at $x = s_1(t)$, after some time $t > t_c$ shown in figure 22, to find the new shock position as

$$s_1(t) = -1 + \lambda_1(0)t - \frac{\hat{H}_0}{\hat{H}_1}[\lambda_1(0) - \lambda_1(\hat{H}_0)]t_c, \tag{6.36}$$

with t_c given by (6.33). We can again find the equation of the expansion wave between

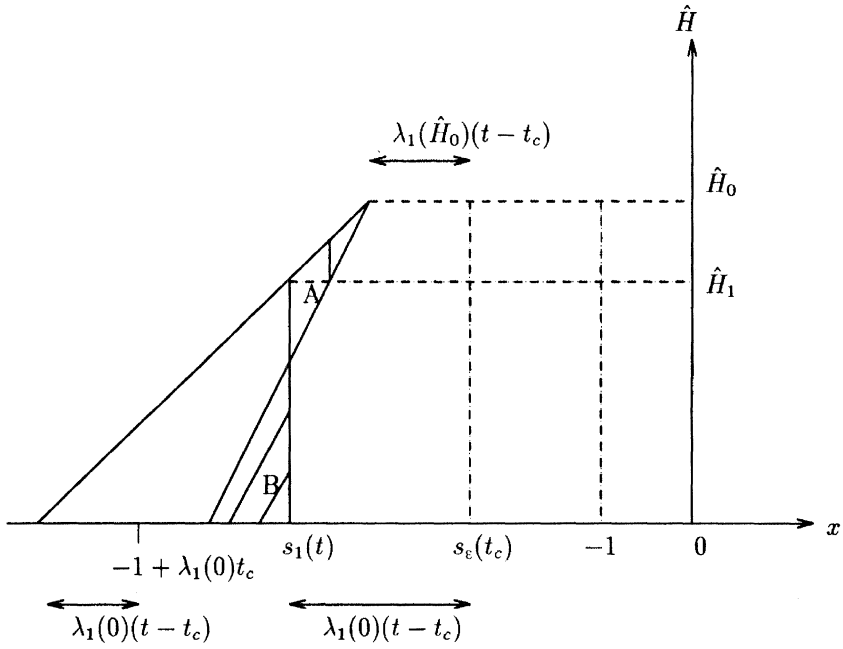

Figure 22. The $(\hat{H}, x)$ profiles for $t > t_c$, $F_0 > 1$.

$(-1+\lambda_1(0)t, 0)$ and $(-1+\lambda_1(\hat{H}_0)t, \hat{H}_0)$ and substitute $\hat{H} = \hat{H}_1$ into the resulting equation, with $x = s_1(t)$ given by (6.36). Thus, we find that the shock height again decays as $O(t^{-1/2})$, and is given by (6.26). The substitution of (6.26) into (6.36), leads to the shock speed

$$\dot{s}_1(t) = \lambda_1(0) - \tfrac{1}{2}(t_c/t)^{1/2}[\lambda_1(0) - \lambda_1(\hat{H}_0)]. \tag{6.37}$$

As $t \to \infty$, $\dot{s}_1 \to \lambda_1(0)$ from below.

Relating to the bedform, we observe that now the dredged section propagates upstream with $O(\varepsilon)$ speed. A sediment bore forms at the downstream edge and a sediment expansion wave at the upstream edge. The dredged section maintains its original depth until $t = t_c$, after which the sediment bore catches up with the rear of the sediment expansion wave. The depth thereafter diminishes as $O(t^{-1/2})$, having propagated over a distance of $O(\varepsilon t)$ as $t \to \infty$.

(*d*) *Transportation of a sediment slug*

Sediment slugs are localized humps of bed-load sediment which propagate through the bedform. This is very similar to the dredged channel problem of the previous section. Again, to propagate a significant bedform disturbance, we require the properties of the s_2-simple wave family, for $F_0 < 1$, and those of the s_1-simple wave family, for $F_0 > 1$. As before, we construct the analytic solution for the flow depth with there being a simple linear transformation to the bedform results.

(i) $F_0 < 1$

In this case we use the initial condition (5.26), $H < 1$ and h satisfying (3.41), with $\lambda_2(h)$ being the $O(\varepsilon)$ form of (3.38). Since $h < 1$, in the weak shock limit we substitute (6.29) for h and H, in the relevant equations, to give the initial condition (6.15), with

$\hat{H}_0 > 1$ and $\hat{H} \geqslant 1$ satisfying the conservation law (6.16). Here $\lambda_2(\hat{H}) \sim \alpha - \beta\hat{H} > 0$, where $\alpha = 2\varepsilon/(1 - F_0^2) > 0$ and $\beta = -6\varepsilon/(1 - F_0^2) < 0$. As $\hat{H}$ increases, $\lambda_2(\hat{H})$ also increases. Therefore we have a shock at the front and an upstream expansion wave, while the whole system is transported downstream. The analysis is then the same as the dredging problem for $F_0 > 1$, with the same results except that, instead of $\lambda_1(h)$, the characteristic wavespeed is now $\lambda_2(h)$.

Relating to the bedform, we see that the hump or slug in bedform propagates downstream with $O(\varepsilon)$ speed. A sediment bore forms at the front and a sediment expansion wave at the rear.

(ii) $F_0 > 1$

Here, h satisfies the partial differential equation (3.51), with the initial data (5.22), where $\lambda_1(h)$ is $O(\varepsilon)$ and given by (3.52). For weak shock conditions, we substitute for h and H from (6.13), to obtain the conservation law satisfied by $\hat{H}$ as (6.30), where $\lambda_1(\hat{H}) \sim \alpha + \beta\hat{H}(< 0)$ and $\alpha = 2\varepsilon/(1 - F_0^2) < 0$, $\beta = -6\varepsilon/(1 - F_0^2)^2 < 0$, and the initial condition is now (6.15), with $\hat{H}_0 > 0$. We observe that $|\lambda_1(\hat{H})|$ is monotonically increasing with increasing $\hat{H}$, and the system is carried upstream by the $\lambda_1(h)$-wave. By continuing the weak shock analysis we see that the situation is very similar to that for the dredged section when $F_0 < 1$, and the results are exactly the same with $\lambda_2(h)$ replaced by $\lambda_1(h)$. Regarding the bedform hump or slug, this propagates upstream with an $O(\varepsilon)$ speed. A sediment bore forms at the upstream face of the slug, with a sediment expansion wave at the downstream face.

(e) *Upstream sediment injection and starvation*

Here, we consider the downstream evolution in bedform which occurs when at a specific upstream control station, say at $x = x_{\mathrm{D}}$, there is either a prescribed increase or decrease in sediment flux from the uniform conditions. We consider the problem in the weak shock limit; that is for small increases and decreases in sediment flux.

(i) *Injection*

The generated bedform must propagate downstream, and must therefore be carried on the s_2-simple wave family, along the λ_2 characteristics. We can relate (via $q = v^2$ and (3.39), (3.43)) the upstream condition to an associated condition on h. On doing this we arrive at a signalling problem to be solved for h in $x > x_{\mathrm{D}}, t > 0$. Here, h satisfies the s_2-simple wave conservation law (3.41), subject to the initial and boundary conditions,

$$\left.\begin{aligned} h(x,0) &= 1, \quad x \geqslant x_{\mathrm{D}}, \\ h(x_{\mathrm{D}},t) &= H, \quad t > 0, \end{aligned}\right\} \tag{6.38}$$

where $q_{\mathrm{D}} = 1/H^2$ is the upstream prescribed sediment discharge. In this case $q_{\mathrm{D}} > 1$ and so $H < 1$. There are two cases to consider. When $F_0 > 1$, the associated bedform generated in $x > x_{\mathrm{D}}$, $t > 0$ is uniformly of $O(\varepsilon)$ and large scale bedforms are 'washed-out' (from (3.42)–(3.44) with $H \sim 1$). We do not pursue the details of this case any further.

However, when $F_0 < 1$, the bedforms which are generated are of $O(1)$ (from (3.38)–(3.40)) and we consider the details. Since $H < 1$, we substitute for h and H from

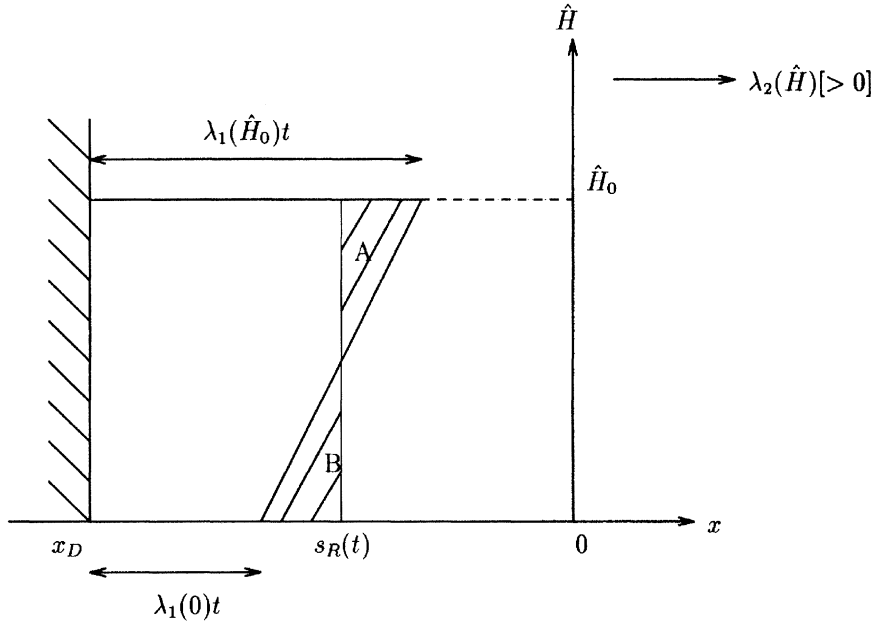

Figure 23. The $(\hat{H}, x)$ profiles for the injection problem, $F_0 < 1$.

(6.29), which gives the initial and boundary conditions as

$$\left.\begin{aligned} \hat{H}(x,0) &= 0, \quad x \geqslant x_{\mathrm{D}}, \\ \hat{H}(x_{\mathrm{D}},t) &= \hat{H}_0, \quad t > 0, \end{aligned}\right\} \tag{6.39}$$

with $\hat{H}_0 > 0$. In the weak shock limit ($\hat{H}_0 \ll 1$) $\hat{H}(x,t)$ now satisfies the hyperbolic conservation law (6.16), where $\lambda_2(\hat{H}) \sim \alpha - \beta\hat{H}(>0)$, with $\alpha = 2\varepsilon/(1-F_0^2) > 0$ and $\beta = -6\varepsilon/(1-F_0^2) < 0$. We see that $\lambda_2(\hat{H})$ is monotonically increasing with increasing $\hat{H}$. We have therefore, a shock moving downstream, as shown in figure 23. We insert a shock at position $x = s_R(t)$, and apply the equal area rule (6.17) to the two resulting triangles. We find that the shock position is given by

$$s_R(t) = x_{\mathrm{D}} + \tfrac{1}{2}[\lambda_2(0) + \lambda_2(\hat{H}_0)]t. \tag{6.40}$$

The solution is therefore

$$\hat{H}(x,t) = \begin{cases} \hat{H}, & x_{\mathrm{D}} \leqslant x < s_R(t), \\ 0, & x \geqslant s_R(t), \end{cases}$$

in $x \geqslant x_{\mathrm{D}}, t > 0$. The associated bedform, obtained from (3.40) thus generates a sediment bore from $x = x_{\mathrm{D}}$ which is located at $x = s_R(t)$ and propagates steadily downstream with speed of $O(\varepsilon)$.

(ii) *Starvation*

Again the generated bedform must propagate downstream, and is therefore carried as an s_2-simple wave. As in § 6 *e* (i), we again solve a signalling problem with initial

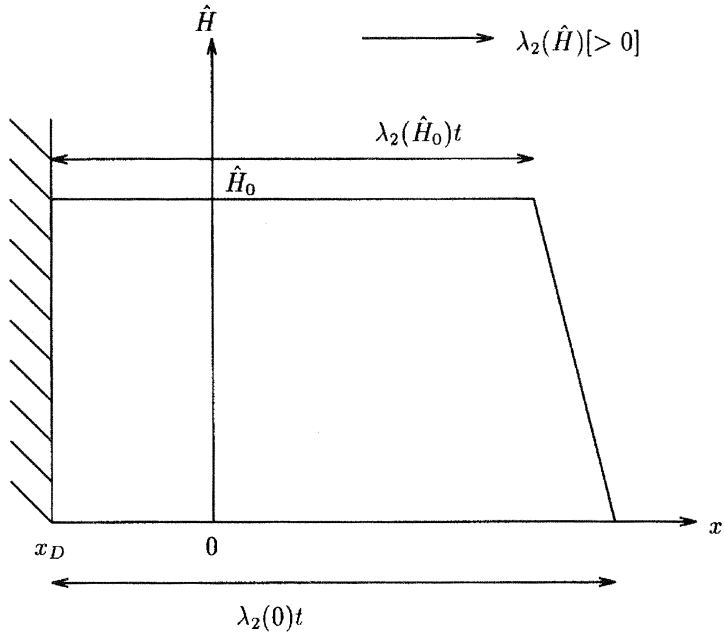

Figure 24. The $(\hat{H}, x)$ profiles for the starvation problem, $F_0 < 1$.

and boundary conditions given by (6.38), except that now, since $q(x_{\mathrm{D}}, t) < 1$, we require $H > 1$.

When $F_0 > 1$, the associated bedform, given by (3.44), is uniformly of $O(\varepsilon)$. We do not consider the case further.

For $F_0 < 1$ an $O(1)$ bedform is generated (via (3.40)). In the weak shock limit we substitute for h and H using (6.14) (as $H > 1$), which leads to the initial and boundary conditions (6.39) with $\hat{H}_0 > 0$, and $\hat{H}(x,t)$ now satisfying (6.16), where $\lambda_2(\hat{H})$ is given by $\lambda_2(\hat{H}) \sim \alpha + \beta\hat{H}(> 0)$, $\alpha = 2\varepsilon/(1 - F_0^2) > 0$ and $\beta = -6\varepsilon/(1 - F_0^2)^2 < 0$. In this case $\lambda_2(\hat{H})$ is monotone decreasing with increasing $\hat{H}$, and an expansion wave is generated, as shown in figure 24. It is readily established that the expansion is given by

$$\hat{H}(x,t) = \begin{cases} \hat{H}_0, & x_{\mathrm{D}} \leqslant x < 1 + \lambda_2(\hat{H}_0)t, \\ \dfrac{\hat{H}_0(x - 1 - \lambda_2(0)t)}{[\lambda_2(\hat{H}_0) - \lambda_2(0)]t}, & 1 + \lambda_2(\hat{H}_0)t \leqslant x < 1 + \lambda_2(0)t, \\ 0, & x \geqslant 1 + \lambda_2(0)t. \end{cases} \tag{6.41}$$

The associated bedform, from (3.39), generates a sediment expansion wave from $x = x_{\mathrm{D}}$, which accommodates the lowering in bed-level. This propagates downstream with $O(\varepsilon)$ speed.

(*f*) *Downstream sediment blocking and extraction*

Here we consider the upstream evolution in bedform which occurs when at a specific downstream control station, say at $x = x_{\mathrm{D}}$, there is either a blockage in sediment flux from uniform conditions, or there is sediment extraction. Again we consider the problem in the weak shock limit; that is for small rates of blockage or

extraction. Blockage corresponds to a reduction in sediment flux at $x = x_{\mathrm{D}}$, whereas extraction corresponds to an increase in sediment flux at $x = x_{\mathrm{D}}$.

(i) *Blocking*

The generated bedform must propagate upstream from $x = x_{\mathrm{D}}$, and must be carried on the s_1-simple wave family, along the λ_1-characteristics. We can relate the downstream condition on q to an associated condition on h, via $q = v^2$ and (3.46) and (3.49). We therefore arrive at a signalling problem to be solved for h in $x < x_{\mathrm{D}}$, $t > 0$. Here, h satisfies the s_1-simple wave family conservation law, (3.51), subject to the initial and boundary conditions,

$$\left.\begin{aligned} h(x,0) &= 1, \quad x \leqslant x_{\mathrm{D}}, \\ h(x_{\mathrm{D}},t) &= H, \quad t > 0, \end{aligned}\right\} \tag{6.42}$$

where $q_{\mathrm{D}} = 1/H^2$ is the downstream prescribed sediment flux. In this case $q_{\mathrm{D}} < 1$ and so $H > 1$.

There are two cases to consider. When $F_0 < 1$, the associated bedform generated in $x < x_{\mathrm{D}}$, $t > 0$ is uniformly of $O(\varepsilon)$ and large scale bedforms are 'washed-out' (from (3.48)–(3.50) with $H \sim 1$). We do not pursue the details of this case further.

However, when $F_0 > 1$, the bedforms which are generated are $O(1)$, from (3.52)–(3.54). Since $H > 1$, we substitute for h and H from (6.14), which gives the initial and boundary conditions as

$$\left.\begin{aligned} \hat{H}(x,0) &= 0, \quad x \leqslant x_{\mathrm{D}}, \\ \hat{H}(x_{\mathrm{D}},t) &= \hat{H}_0, \quad t > 0, \end{aligned}\right\} \tag{6.43}$$

with $\hat{H}_0 > 0$. In the weak shock limit $\hat{H}(x,t)$ now satisfies (6.30) with

$$\lambda_1(\hat{H}) \sim \alpha + \beta\hat{H} < 0,$$

with $\alpha = 2\varepsilon/(1-F_0^2) < 0$ and $\beta = -6\varepsilon/(1-F_0^2)^2 < 0$. We observe that as $\hat{H}$ increases, $|\lambda_1(\hat{H})|$ also increases. The system propagates upstream, with a shock forming, as seen in figure 25. We fit a shock at $x = s_R(t)$, such that the two triangular regions formed satisfy the equal area rule (6.17). We find that the shock position is given as

$$s_R(t) = x_{\mathrm{D}} + \tfrac{1}{2}[\lambda_1(0) + \lambda_1(\hat{H}_0)]t. \tag{6.44}$$

The solution is thus

$$\hat{H}(x,t) = \begin{cases} \hat{H}_0, & s_R(t) < x \leqslant x_{\mathrm{D}}, \\ 0, & x < s_R(t), \end{cases} \tag{6.45}$$

in $x \leqslant x_{\mathrm{D}}$, $t > 0$. The associated bedform, obtained from (3.54), thus generates an upstream propagating sediment bore from $x = x_{\mathrm{D}}$, which is located at $x = s_R(t)$ and propagates steadily upstream with speed of $O(\varepsilon)$.

(ii) *Extraction*

Again the generated bedform must propagate upstream, and is therefore carried as an s_1-simple wave. As in § 6 *f* (i), we solve a signalling problem given by (6.42) except that now, since $q(x_{\mathrm{D}},t) > 1$, we require $H < 1$.

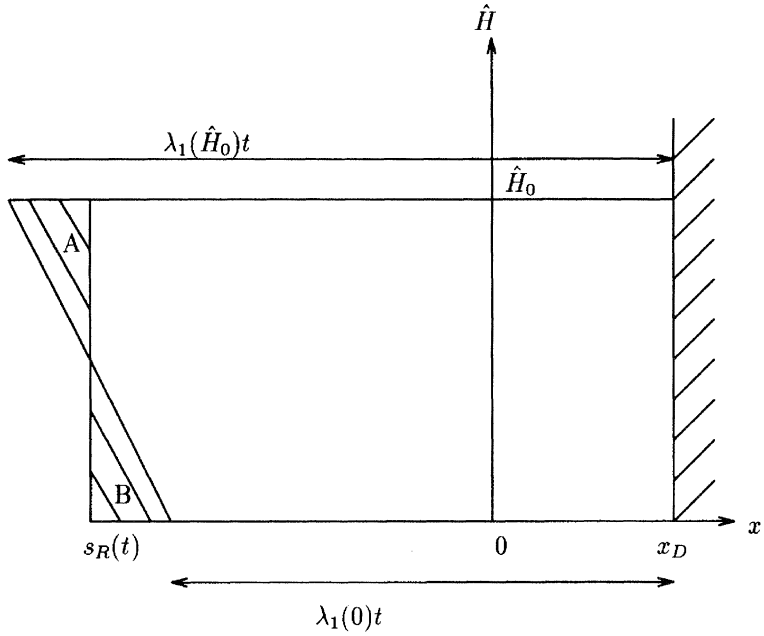

Figure 25. The $(\hat{H}, x)$ profiles for the sediment blocking problem, $F_0 > 1$.

When $F_0 < 1$, the associated bedform (given by (3.50)) is uniformly of $O(\varepsilon)$ and this case is not considered further.

For $F_0 > 1$, an $O(1)$ bedform is generated, via (3.54). In the weak shock limit we substitute for h and H from (6.29), with $H < 1$, which leads to the initial and boundary conditions (6.43) with $\hat{H}_0 > 0$, and $\hat{H}(x,t)$ now satisfying (6.30), where $\lambda_1(\hat{H}) \sim \alpha - \beta\hat{H} < 0$, $\alpha = 2\varepsilon/(1 - F_0^2) < 0$ and $\beta = -6\varepsilon/(1 - F_0^2)^2 < 0$. We observe that $|\lambda_1(\hat{H})|$ is monotonically decreasing with increasing $\hat{H}$, thus creating an expansion wave solution, as shown in figure 26. It is readily established that the solution is given by

$$\hat{H}(x,t) = \begin{cases} \hat{H}_0, & 1 + \lambda_1(\hat{H}_0)t < x \leqslant x_{\mathrm{D}}, \\ \dfrac{\hat{H}_0(x - 1 - \lambda_1(0)t)}{[\lambda_1(\hat{H}_0) - \lambda_1(0)]t}, & 1 + \lambda_1(0)t \leqslant x \leqslant 1 + \lambda_1(\hat{H}_0)t, \\ 0, & x < 1 + \lambda_1(0)t. \end{cases}$$

The associated bedform, obtained from (4.37), generates an upstream propagating sediment expansion wave which accommodates the lowering of the bed-level at $x = x_{\mathrm{D}}$. This propagates upstream with a speed of $O(\varepsilon)$.

7. Discussion

The nonlinear hydraulic equations of alluvial river dynamics have recently been considered by Needham & Hey (1991, I) and Zanré & Needham (1994, II). In II the equations, in differential form, were shown to form a third order strictly hyperbolic system. Thus, for general initial data, finite-time blow-up of classical solutions will often occur, this being pointwise in gradient. To continue solutions beyond this blow-

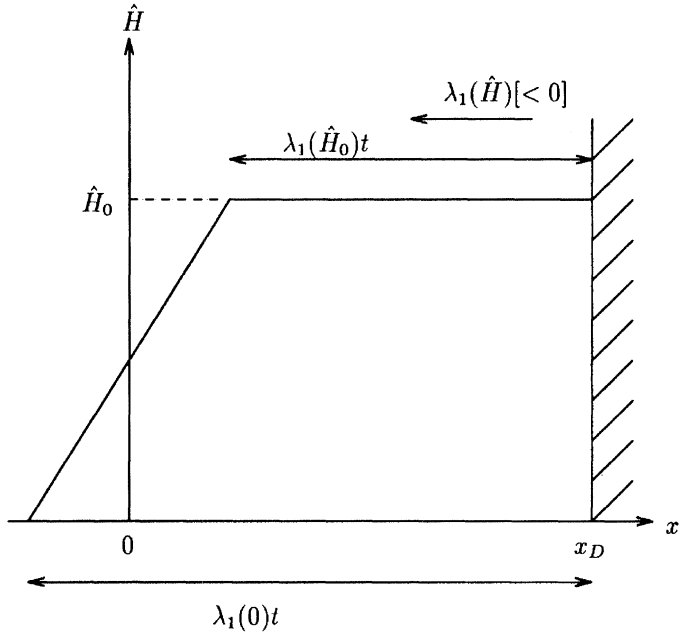

Figure 26. The $(\hat{H}, x)$ profiles for the sediment extraction problem, $F_0 > 1$.

up time, Needham & Hey returned to the primary integral conservation laws and augmented the system with a shock-depth function, I. This enabled solutions to be continued beyond the blow-up time through the insertion of appropriate shock waves. The possible shock waves which may then propagate in the system were studied in detail in I. It was found that there are three distinct shock-wave families, referred to as c_i-shocks $(i = 1, 2, 3)$, corresponding to characteristic intersection on the λ_i-characteristic families $(i = 1, 2, 3)$ respectively. The c_1-, c_2-shocks were shown to correspond to sediment bore propagation in alluvial rivers, a feature borne out by experimental observations, I. It was also shown in II that energy dissipating shocks are stable to smoothing perturbations.

In the present paper we have examined the three simple-wave families which can propagate in alluvial rivers. These have been identified as s_i-simple waves $(i = 1, 2, 3)$. In each simple wave family there is an associated expansion wave, the e_i-expansion wave $(i = 1, 2, 3)$, which are the counterparts to the c_i-shock waves $(i = 1, 2, 3)$. The details of each expansion wave have been derived, and it has been shown that the propagation of an expansion wave through an alluvial river requires a decrease in the upstream sediment transport rate. This is in accord with the results of I which established that the propagation of a shock wave through an alluvial river flow requires an increase in the upstream sediment transport rate. In particular it has been shown that the e_1-, e_2-expansion waves are responsible for the propagation of the observed sediment expansion waves through alluvial rivers. The long time evolution of general disturbances to alluvial flows can then be decomposed into the propagation and interaction of sediment bores (c_1-, c_2-shocks) and sediment expansion waves (e_1-, e_2-expansion waves).

More general simple waves associated with monotone and single hump bedforms have been considered, together with sediment injection and starvation problems.

These problems have been related to the generation of sediment expansion waves and sediment bores in alluvial flows.

Finally a weak shock theory has been developed for the system, and this has been applied to several situations of practical interest. These include channel dredging, transportation of sediment slugs, upstream sediment injection and starvation and downstream sediment blocking and extraction.

D.D.L.Z. thanks EPSRC for financial support through an Earmarked Research Studentship.

References

Bettes, R. & White, W. R. 1979 A one dimensional morphological river model. Hydraulics Research Station Report no. IT 194.

Cunge, J. A., Holly, F. M. & Verway, A. 1981 *Practical aspects of computational river hydraulics.* London: Pitman.

De Vries, M. 1973 *River bed variations, aggradation and degradation.* New Delhi: IAHR Seminar.

Engelund, F. & Hansen, E. 1967 *A monograph on sediment transport in alluvial streams.* Copenhagen: Teknisk.

Falconer, R. A. & Owens, P. H. 1984 *J. Inst. Water Engng Sci.* **38**, 528–534.

Gibson, A. H. 1934 *Hydraulics and its applications.* London: Constable.

Gill, M. A. 1983*a* *J. Hydraulic Res.* **21**, 355–367.

Gill, M. A. 1983*b* *J. Hydraulic Res.* **21**, 367–378.

Gill, M. A. 1987 *J. Hydraulic Res.* **25**, 537–549.

Krishnappan, B. G. 1985 *Can. J. Civ. Engng* **12**, 464–471.

Lax, P. D. 1972 *Am. Math. Mon.* **79**, 227–241.

Lax, P. D. 1973 *SIAM Regional Conf. Ser. in Appl. Math.* **11**, 1–48.

Mehta, P. J., Garde, R. J. & Ranga Raju, K. G. 1983 *2nd Symp. on River Sedimentation.* Water Resources and Electric Power Press.

Needham, D. J. 1990 *Geophys. Astrophys. Fluid Dynamics* **51**, 167–194.

Needham, D. J. 1988 *J. Appl. Math. Phys. (ZAMP)* **39**, 28–49.

Needham, D. J. & Hey, R. D. 1991 *Phil. Trans. R. Soc. Lond.* A **334**, 25–53.

Needham, D. J. & Hey, R. D. 1992 Dynamic modelling of bed waves. In *Dynamics of gravel bed rivers* (ed. P. Billi, R. D. Hey, C. R. Thorne & P. Tacconi). Chichester: Wiley.

Peter, W. 1981 Numerical modelling of the Alpine Rhine. Hydraulics Research Station Report no. IT 220.

Reynolds, A. J. 1965 *J. Fluid Mech.* **22**, 113–133.

Ribberink, J. A. & Van Der Sande, J. T. M. 1985 *J. Hydraulic Res.* **23**, 273–283.

Smoller, J. 1983 *Shock waves and reaction-diffusion equations.* New York: Springer.

Stoker, J. J. 1957 *Water waves.* New York: Wiley.

Whitham, G. B. 1974 *Linear and nonlinear waves.* New York: Wiley.

Zanré, D. D. L. & Needham, D. J. 1994 *Geophys. Astrophys. Fluid Dynamics* **76**, 193–222.

Received 8 August 1995; accepted 2 November 1995